Gelation and Gel Properties of Gellan Gum and Xyloglucan

Yoko Nitta

2005

Department of Food and Human Health Sciences
Graduate School of Human Life Science
Osaka City University

ジェランガムとキシログルカンの
ゲル化およびゲル特性

大阪市立大学大学院
生活科学研究科
食・健康科学講座

新田　陽子

2005 年

Contents

ABBREVIATIONS AND SYMBOLS

1. INTRODUCTION

Use of polysaccharides in foods 1

Objective and outline of this thesis 8

Overview of gellan gum 10

Overview of Tamarind seed xyloglucan 14

2. METHODS

Rheology 19

Rheological properties of polysaccharide solutions 30

Determination of gel point by rheology 31

Thermal analysis: Differential scanning calorimetry (DSC) 32

Conformational transition of polysaccharides 35

Sol-gel transition of polysaccharide 35

Circular dichroism (CD) 36

Conformational transition of polysaccharides 41

3. GELATION AND GEL PROPERTIES OF GELLAN GUM

The helix-coil transition of gellan in gels

Introduction 43

Experimental 43

Results and discussion 45

Conclusion 49

The sol-gel transition of gellan affected by thermal history

Introduction 50
Experimental 51
Results and discussion 52
Conclusion 59

4. THE EFFECT OF SURFACTANT, SALT, AND SUGAR ON GELATION AND GEL PROPERTIES OF GELLAN GUM

The effect of SDS on the gelation of gellan
Introduction 61
Experimental 62
Results and discussion 63
Conclusion 69

The effect of the immersion into salt solution on gel properties of gellan
Introduction 70
Experimental 71
Results and discussion 71
Conclusion 76

The effect of sugars on gel properties of gellan
Introduction 77
Experimental 77
Results and discussion 78
Conclusion 80
Appendix 80

5. GELATION OF XYLOGLUCAN BY ADDITION OF SMALL MOLECULES IN FOODS

Gelation of tamarind seed xyloglucan by addition of epigallocatechin gallate
Introduction 89
Experimental 91
Results and discussion 92

Conclusion 108

6. GELATION OF XYLOGLUCAN BY ADDITION OF MACROMOLECULES IN FOODS

Gelation of tamarind seed xyloglucan by mixing with gellan

Introduction 109

Experimental 110

Results and discussion 111

Conclusion 126

The effect of salts on the gelation of tamarind seed xyloglucan/gellan mixture

Introduction 127

Experimental 127

Results and discussion 128

Conclusion 134

REFERENCES 135

SUMMARY 145

CONCLUDING REMARKS 149

ACKNOWLEDGEMENTS 151

LIST OF PUBLICATION 153

Abbreviations and symbols

CD	circular dichroism
DSC	differential scanning calorimetry
EGCG	epigallocatechin gallate
KGM	konjac glucomannan
NMR	nuclear magnetic resonance
NOESY	nuclear Overhauser effect spectroscopy
Na-G	sodium salt form of gellan
SDS	sodium dodecyl sulfate
TSX	tamarind seed xyloglucan, tamarind xyloglucan
E	Young's modulus
Ea	activation energy
E′	storage Young's modulus
E″	loss Young's modulus
G	shear modulus
G*	complex shear modulus
G′	storage shear modulus
G″	loss shear modulus
M_n	number-average molecular weight
M_w	weight-average molecular weight
Tc	cloud point
Tg	gelation point
Tm	peak temperature, mid-point transition temperature
t	time
tanδ	mechanical loss tangent

γ	shear strain
γ_0	amplitude of shear strain
$\dot{\gamma}$	shear strain rate
ΔH	enthalpy change
Ψ	specific ellipticity
$[\Psi]_{202}$	specific ellipticity at 202nm
ε	strain
η	viscosity
θ	ellipticity
θ_{202}	ellipticity at 202nm
σ	stress
σ_0	amplitude of stress
ω	angular frequency

1
Introduction

USE OF POLYSACCHARIDES IN FOODS

Polysaccharides are widely used in food industry. They are used as a texture modifier to enhance or standardize the eating quality of a product by thickening and gelling, by stabilizing emulsion or suspensions, and by reducing the undesired defect of water release (syneresis) in some processed foods. Besides texture modifier, some of polysaccharides except starch are used as food supplement of a dietary fiber, the functional component that provides a health benefit.

Texture modifier

So many food polysaccharides are used as a texture modifier. The commercially important polysaccharides used as a texture modifier and their origin are given in Table1.1. Texture is defined by International Organization for Standardization (ISO) as ‘all the rheological and structural (geometrical and surface) attributes of a food product perceptible by means of mechanical, tactile and, where appropriate, visual and auditory receptors’. Since addition of most polysaccharide changes rheological properties, for example, increases the viscosity of a liquid, polysaccharides are used as a thickener to control texture and organoleptic characteristics (like ‘mouth feel’ and

Table 1.1 Source of commercially important polysaccharides

Botanical	*Trees*
	cellulose
	Tree gum exudates
	gum arabic, gum karaya, gum ghatti, gum tragacanth
	Plants
	starch, pectin, cellulose
	Seeds
	guar gum, locust bean gum, tara gum, tamarind gum
	Tubers
	konjac mannnan
Algal	*Red seaweeds*
	agar, carrageenan
	Brown seaweeds
	Alginate
Microbial	xanthan gum, curdlan, dextran, gellan gum, cellulose
Animal	Chitosan

(Williams and Phillips, 2000)

'body'). Polysaccharides are also used to control texture as stabilizer and emulsifier (Lapasin and Pricl, 1995). Many food products are emulsions; a mixture of two immiscible liquids in which one phase is dispersed throughout the other as small, isolated droplets. Polysaccharides can assist in obtaining a fine dispersion and in maintaining the homogenous mixture. Foams are related to emulsions, being a dispersion of gas (or gases) in a liquid (or solid), and polysaccharides can be conventionally used to modify the interfacial tension and obtain a stable, firm foam. Suspending agents are those substances that are used to uniformly disperse solid particles through a liquid phase, and the polysaccharides help in preventing particle setting. The principal use of polysaccharides is as thickener and stabilizer in Japanese food industry, and thus there are so many polysaccharides approved and used as thickener and stabilizer in Japan as listed in Table 1.2.

Polysaccharides are also used to modify texture of foods by preventing syneresis (Innden and Yokawa, 1999). Syneresis is a phenomenon in which water containing dissolved components is released from a gel network. In most cases, occurrence of syneresis is undesirable for gel-like food products. It can be prevented by incorporating ingredients into the gel that have water binding properties. Polysaccharides are commonly used to help retain water within the gel network.

Since some polysaccharides form thermoreversible or thermoirreversible gels at low concentrations (~1%), polysaccharides are added into foods as a gelling agent (Lapasin and Pricl, 1995; Innden and Yokawa, 1999). The gels resulting from different polysaccharides will present distinct structural forms and textures (from smooth to chewy) and thus polysaccharide gels are employed in a variety of food types. The principal gelling agents are listed in Table1.3.

Japan is a typical country where various types of polysaccharide gels are eaten, such as ‘kuzukiri’ (kuzu starch gel), ‘mizuyokan’ (red bean-agar jelly dessert), ‘konnyaku’ (konjac glucomannan gel), ‘natadecoco’ (fermentation-derived cellulose gel), jams (pectin gel) and dessert jellies. Japanese tends to be perceptive of subtle difference of texture among similar foods. Product developers are required to create food products with new texture. Addition of polysaccharide to food products is one way to create new texture.

In recent years, with increasing the interest about health, awareness of the link between health and texture is growing. Texture, in particular, plays an important role for many elder adults who are malnourished because of mental and/or oral problems. Texture modification of conventional foods is often appropriate for these problems and is necessary when dysphagia (chewing or swallowing problems) is present. Taking texture into consideration, the Ministry of Health and Welfare in Japan made a standard of functional foods for the elderly. For older adults diet, texture modification using polysaccharides is getting popular.

Table 1.2 Thickening and stabilizing agent approved in Japan. Only thickeners consisting of polysaccharides were listed.

Aeromonas gum
Agrobacterium succinoglycan
Alginic aid
Almond gum, Cedo gum
Aloe extract
Aloe vera extract
Arabino galactan
Artemisia sphaerocephala seed gum, *Artemisia* seed gum
Aureobasidium cultured solution
Azotobacter vinelandii gum
Carob bean gum, Locust bean gum
Carrageenan, semirefined carrageenan, processed eucheuma algae, processed red algae, purified carrageenan, refined carrageenan, powdered red algae
Cassia gum
Chitin
Chitosan
Curdlan
Demmar resin
Dextran
Elemi resin
Enterobacter gum
Enterobacter simanus gum
Enzymatically hydrolyzed guar gum
Erwinia mitsuensis gum
Fermentation-derived cellulose
Fukuronori extract
Furcellaran
Gellan gum
Glucosamine
Guar gum
Gum Arabic, Arabic gum, Acacia gum
Gum ghatti
Karaya gum
Kelp extract

The Director-general of Environmental Health Bureau Notice, No. 56 (published by the Ministry of Health and Welfare on May 23, 1996)

Table 1.2 Continued

Konjac extract
Gum ghatti
Karaya gum
Kelp extract
Konjac extract
Linseed gum, Linseed extract
Levan
Macrophomopsis gum
Mirofibrillated cellulose
Oligoglucosamine
Peach gum
Pectin
Psyllium seed gum
Pullulan
Rhamsan gum
Sclero gum, Scleroglucan
Seaweed cellulose
Sesbania gum
Soybean polysaccharides
Sweetpotato cellulose
Tamarind seed gum
Tara gum
Tororoaoi
Tragacanth gum
Triacanthos gum
Welan gum
Xanthan gum
Yeast cell wall

The Director-general of Environmental Health Bureau Notice, No. 56 (published by the Ministry of Health and Welfare on May 23, 1996)

Table 1.3 Main thermoreversible gelling polysaccharides

Agar
Gel formed on cooling. Molecules undergo a coil-helix transition followed by aggregation of helices
Kappa Carrageenan
Gel formed on cooling in the presence of salts notably potassium salts. Molecules undergo a coil-helix transition followed by aggregation of helices.
Iota Carrageenan
Gel formed on cooling in the presence of salts. Molecules undergo a coil-helix transition followed by aggregation of helices.
Low methoxyl (LM) pectin
Gel formed in the presence of divalent cations, notably calcium at low pH (3-4.5). Molecules crosslinked by the cations.
Gellan gum
Gels formed on cooling in the presence of salts. Molecules undergo a coil-helix transition followed by aggregation of helices.
Methyl cellulose and hydroxypropyl methyl cellulose
Gel formed on heating. Molecules associate on heating due to hydrophobic interaction of methyl groups.
Xanthan gum and locust bean gum or konjac mannan
Gels formed on cooling mixtures.

(Williams and Phillips, 2000)

Food supplement as dietary fiber

Nonstarch polysaccharides are known as dietary fiber. Starch is fully hydrolyzed to D-glucose by enzymes in the upper digestive tract whereas most of other polysaccharides eaten as normal components of everyday foods are not digested in human digestive tract, because no suitable enzymes are present in our gastrointestinal juices and the residence time at the acid pH of the stomach is too short to produce a significant hydrolysis product of the polysaccharide chain (Stephen, 1991). Polysaccharides that survive colon transit are extremely important from the physiological point of view (Katayama and Katayama, 1997). They improve intestinal

health by exerting a bulking action, with the result of slower nutrient uptake, which helps to normalize blood sugar levels (Katayama and Katayama, 1997). Also, their presence helps in maintaining low cholesterol levels (Marlett et al., 2002). These functions are important for health and thus ~25g intake of dietary fiber a day is recommended. In fact the average Japanese consumes only ~14g daily according to National Nutrition Survey in 2002. In order to increase the intake of dietary fiber, a powder of polysaccharides for adding into normal meal and food products containing higher amount of polysaccharides than common food products are being produced (Fig.1.1).

Figure 1.1 Examples of food products containing polysaccharide as dietary fiber. Left; a product of Kobayashi Pharmaceutical Co., Ltd. (Osaka, Japan), right; a product of Otsuka Pharmaceutical Co., Ltd (Tokyo, Japan). (ただしこれは特定の商品を推奨しているのではない)

THE OBJECTIVE AND OUTLINE OF THIS THESIS

Judging from great interest in the use of polysaccharide as a texture modifier, it is useful to propose an effective use of existing food polysaccharides as a texture modifier and create novel texture modifier with specific functionality from existing polysaccharides. Most of helix-forming polysaccharides such as agarose, carrageenan and gellan gum are used as gelling agent since these polysaccharides can form a gel at low concentrations. For using these polysaccharides as texture modifier effectively, clarifying gelation mechanism and characterizing gel properties are required. At the present stage they have not been clarified well.

In the case of the polysaccharide incapable of gelling by itself, although it is valuable for thickening agent or stabilizer, searching a gelling condition is important to enlarge possibilities as a texture modifier. Tamarind xyloglucan, obtained from purification of tamarind seed gum, does not form a gel unless much amount of tamarind xyloglucan is added.

In the present study, the gelation mechanism and gel properties of gellan gum and tamarind seed xyloglucan were investigated using rheological, differential scanning calorimetric, and circular dichrosim measurements. We regarded tamarind xyloglucan, a valuable thickener and/or stabilizer, as a representative of non-gelling polysaccharides and attempted to find novel gelling condition and specific interaction with food constituents.

In section 3 and 4 of chapter 1, gellan gum and tamarind gum are overviewed, respectively. In chapter 2, basic knowledge of the instruments of rheology, differential scanning calorimetry (DSC) and circular dichroism (CD) was presented and examples of rheological, DSC and CD behaviors of polysaccharide solutions were given. In chapter 3, the gelation and gel properties of gellan, in particular, about the helix-coil transition in gellan gels and the sol-gel transition affected by the thermal history were described. In chapter 4, the effects of surfactant, salt, and sugar on the

gelation and gel properties of gellan were presented. In chapter 5, the gelation of tamarind xyloglucan by addition of small molecules was given. We confirmed that tamarind xyloglucan forms a gel by addition of epigallocatechin gallate. Finally, in chapter 6, gelation of tamarind xyloglucan by addition of macromolecules was described. It was found that mixture of tamarind xyloglucan and gellan forms a gel under condition where individual polysaccharide does not form a gel.

OVERVIEW OF GELLAN GUM

Gellan gum is a microbial polysaccharide. Being a fermentation product, it can be produced on demand and with consistent quality. It is functional at very low use levels and is, therefore, very efficient in many applications. Gellan gum can provide a range of gel textures as opposed to a single characteristic texture. Consequently, it can be used to mimic the texture of existing gelling agent or to create new textures. In today's food industry, a tool to create new textures and hence permit the creation of new, differential food products would be highly desirable (Sanderson, 1990).

Source and production

Gellan gum is an extracellular polysaccharide produced by micro-organism *Sphingomonas elodea* (ATCC 31461) previously referred to as *Pseudomonas elodea*. The gum is formed by inoculating a carefully formulated fermentation medium with this organism. The medium consists of a carbon source such as glucose, a nitrogen source and a number of inorganic salts. The fermentation is allowed to proceed under sterile conditions with strict control of aeration, agitation, temperature and pH. When fermentation is complete, the viscous broth is pasteurized to kill the viable cells. Treatment of the pasteurized broth with alkali removes the acyl substituents on the gellan gum backbone. Following removal of the cellular debris, the gum is recovered by precipitation with alcohol. This produces the unsubstituted form of gellan gum with high degree of purity (Gibson and Sanderson, 1997).

Structure

The primary structure of gellan gum is composed of a linear tetrasaccharide repeat unit:→3)-β-D-Glcp-(1→4)-β-D-GlcpA-(1→4)-β-D-Glcp-(1→4)-α-L-Rhap-(1→ as reported by O'Neil et al., (1983) and Jannson et al., (1983). Figure 1.2 shows chemical structure of gellan gum. The polymer is produced with two acyl substituents

present on the 3-linked glucose, namely L-glyceryl, positioned at O(2) and acetyl at O(6). On average there is one glycerate per repeat unit and one acetate per every two repeats (Kuo et al., 1986). Generally we call deacylated gellan gum just gellan gum. The term 'gellan gum' in this thesis represents deacylated gellan gum.

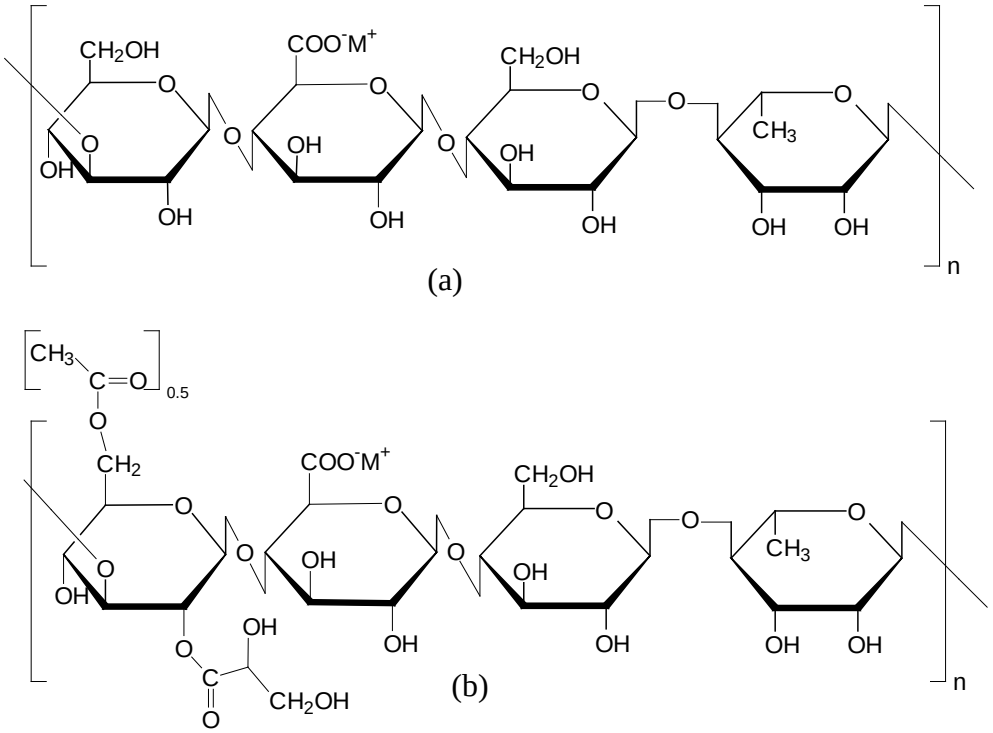

Figure 1.2 Chemical structure of (a) deacylated gellan gum and (b) native gellan gum.

Gelation and gel properties

Gellan gels in the presence of appropriate amount of cations are transparent, resistant to heat in the wide range of pH (Sworn, 2000). Brittle gellan gels have a good flavor release and microgel, which is assembly of particle of brittle gellan gels, was made for application to foods with new texture (Oomoto et al., 1999).

The mechanism whereby gellan gum forms gels in water is not fully understood. In order to understand gelation and gel properties of gellan gum further, the collaborative research group was organized in the research group of polymer gels affiliated to the

Society of Polymer Science, Japan, in 1989. The common deacylated gellan was used to study its properties with various techniques. The results of the collaborative studies were published in special issues of *Food Hydrocolloids* 7, 361-456 in 1993 (Nakamura et al., 1993; Ogawa, 1993; Okamoto et al., 1993; Watase and Nishinari, 1993), *Carbohydrate Polymers* 20, 75-207 in 1996 (Miyoshi et al., 1996a; Nishinari, 1996b; Ogawa, 1996), and *Progress in Colloid and Polymer Science*, 114, 1-131 in 1999 (Miyoshi and Nishinari, 1999a and 1999b; Ogawa, 1999; Takahashi et al., 1999). Light scattering (Takahashi et al., 1999) and osmotic pressure measurements (Ogawa, 1999) showed that gellan changes from two single chains to a double helix on cooling and changes from a double helix to two single chains on heating, i.e. helix-coil transition occurs thermoreversibly. Rheological measurements (Miyoshi and Nishinari, 1999b) showed that a gel formation followed the coil-to-helix transition on further cooling under appropriate conditions.

Regulatory status

Gellan gum has been given a ‘not specified’ Acceptable Daily Intake (ADI) by the Joint FAO/WHO Expert Committee on Food Additives (WHO Food Additive Series No. 28). In 1997, gellan gum is approved in 25 countries worldwide, including Japan, USA, Canada, Australia, South Africa, most of Southeast Asia and South America.

Uses and applications

Many application of low acyl gellan are a consequence of its characteristic properties, which are summarized in Table1.4. Based on some of these properties, the applications for gellan gum listed in Table1.5 were proposed. Gellan gum is used in low-calorie jams and jellies because in addition to providing good acid stability, clarity and flavor release, it can be easily incorporated to the manufacturing process used for these products.

Table 1.4 Key properties of gellan gum

Is easy to use
Has good inherent stability; also good stability in acidic products
Forms gels at extremely low use levels
Provides gels with excellent flavour release
Gels are exceptionally clear
Gels can be made which either melt or do not melt on heating
Gels are textually similar to those from agar and κ-carrageenan
Use levels are normally one-half to one-third those for agar and κ-carrageenan
A range of gel textures can be produced
Provides useful properties in combination with starches and gelatin

(Gibson and Sanderson, 1997)

Table 1.5 Proposed application areas for gellan gum

Potential application area	Typical products	Typical use level (%)
Water-based jellies	Dessert jellies, aspics	0.15-0.2
Jam and jellies	Low-calorie spreads, imitation jams, bakery fillings	0.12-0.3
Confectionery	Pastille-type confectionery, marshmallows	0.8-1.0
Fabricated foods	Fabricated fruit, vegetables or meats	0.2-0.3
Icings	Bakery icings, frostings	0.05-0.12
Dairy products	Milk desserts	0.1-0.2
Pie fillings	Fruit pie fillings	0.25-0.35

(Gibson and Sanderson, 1997)

OVERVIEW OF TAMARIND SEED XYLOGLUCAN

Xyloglucan is a major structural polysaccharide in the primary cell walls of higher plants. Tamarind xyloglucan is obtained from the endosperm of the seed of the tamarind tree, *Tamarindus indica*, a member of the evergreen family, that is one of the most important and common trees of Southeast Asia and widely indigenous to India, Bangladesh, Myanmar, Sri Lanka, and Malaysia. Tamarind xyloglucan was discovered during a search for new sizing materials. It came into commercial production in 1943 as a replacement for starch in cotton sizing used in Indian textile mills (Glicksman, 1986). Purified, refined tamarind xylogulcan is produced and permitted in Japan as a thickening, stabilizing, and gelling agent in the food industry.

Production

Tamarind seed flour and gum manufacture is similar to that for guar, locust bean gum, and other seed gums, entailing primarily the separation and grinding to a powder of the endosperm portion of the seed (Glicksman, 1986). The process begins by washing the seeds with water to free them from the attached pulp. The seeds are then heated to above 150ºC for at least 15min to make the seed coatings brittle and friable. The seeds are decorticated to leave the heavier, crushed endosperm, which is then ground to yield commercial tamarind seed powder or tamarind seed gum. This material which contains much insoluble matter can be further purified to give the pure tamarind polysaccharide gum.

Structure

Tamarind xyloglucan has a (1→4)-β-D-glucan backbone that is partially substituted at the O-6 position of its glucopyranosyl residues with α-D-xylopyranose (Gidley et al., 1991). Some of the xylose residues are β-D-galactosylated at O-2 (Gidley et al., 1991). Partial structure of tamarind xyloglucan is shown in Fig.1.3. The hydrolysis

products obtained from tamarind xyloglucan are a heptasaccharide A (Glc_4Xyl_3), two octasaccharides B_1 and B_2 (Glc_4Xyl_3Gal), and nonasaccharide C ($Glc_4Xyl_3Gal_2$) (structures III, IV, V, and VI, respectively in Fig.1.4) plus very small amounts of a saccharide of lower molecular weight originating from imperfections in the repeating structure of the xyloglucan..

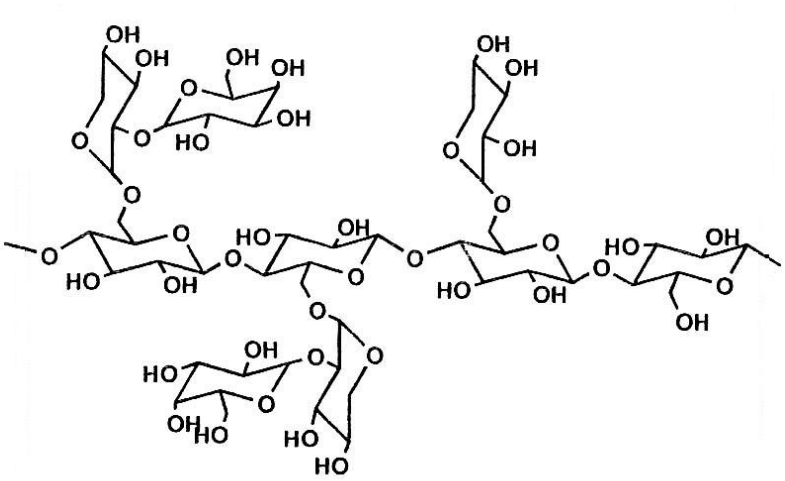

Figure 1.3 Partial structure of tamarind xyloglucan.

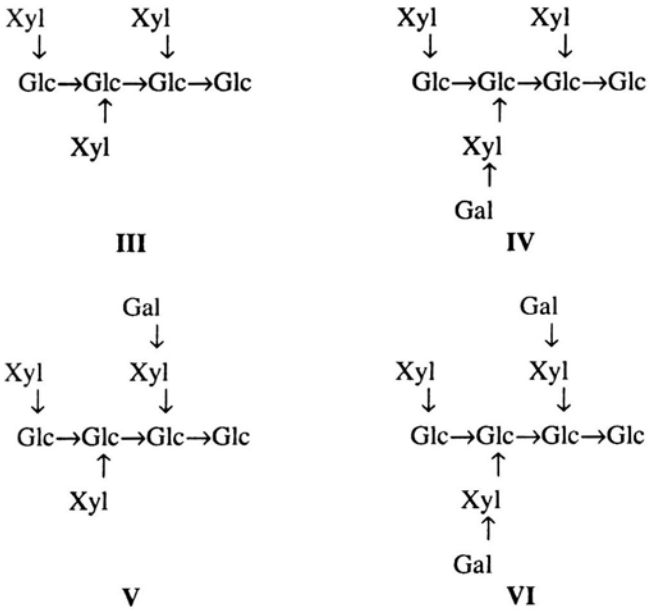

Figure 1.4 The unit structures of tamarind xyloglucan.

Regulatory status

Dainippon Pharmaceutical Co. conducted 2-year feeding toxicity tests on tamarind seed polysaccharides and reported the following results in 1978:

"Tamarind seed polysaccharide was incorporated at the level of 4, 8, 12% in a standard commercial diet and fed to male and female rats for 2 years. No significant changes were noted in the behaviour, mortality, body weight, food intake, biochemical analysis of urine and blood, hematological test, organ weight, and histopathological findings of rats receiving tamarind seed polysaccharide. In all groups, including control group, spontaneous diseases with aging, such as myocardial change, nephropathy, mammary tumor (in female), pituitary tumor, etc., were seen. Deaths of the animals in this study were mainly attributed to these spontaneous diseases."

Gelation by addition of sugar or alcohol and by enzymatic modification

Tamarind xyloglucan has gelling ability in the presence of sugar or alcohol (Nishinari et al., 2000). It forms a gel in the presence of 40-65% sugar over a wide pH range. This gel shows low water release. If alcohol (up to 20%) is added, the amount of sugar needed to form a gel can be substantially reduced. To form a gel, heating is required to dissolve polysaccharides and upon cooling to room temperature the gel will form. The freeze-thaw process makes tamarind xyloglucan-sugar gel harder and more elastic.

It has been reported that gelation occurred when about 50% of galactose were released from tamarind xyloglucan using β-galactosidase from a plant (Reid et al., 1988). Gelation also occurred by removing about 35% of the galactose residues from tamarind xyloglucan using fungal β-galactosidase (Shirakawa et al., 1998). This gel had the unique property of gel formation on heating and gel melting on further heating. Cooling the gel reverted to a sol. The phase transition between gel and sol was completely reversible. As the application of this thermoreversible enzyme-modified xyloglucan gel, use as a substained-release vehicle for the intraperitoneal

administration of mitomycin C was proposed.

Uses and application

Tamarind seed xyloglucan (TSX) has been used widely as a food additive in Japan. TSX is used as thickener, emulsion stabilizer, stabilizer of ice crystal, gelling agent, starch modifier, and fat replacer. The water holding capacity of TSX is so strong that a small amount of TSX prevents water release from carrageenan gel or agar gel. The practical uses of TSX are shown in Table 1.6.

Table 1.6 Food applications

Function	Effects	Subject foods
Thickener and stabilizer	Provides good viscosity free of pastyness and trailing threads Provides density and body Provides stable emulsification Suspends particles for stable dispersion Retains water	Sauces, batters, pickles, low-fat milk, coffee milk, dressings, mayonnaise-like seasonings, fruit juice beverages, shiruko, cocoa, seasoning solutions, seaweed tsukudani, enoki mushroom tsukudani
Gelling	Forms water release-free gel by synergism with sugar Forms gel by synergism with alcohol Forms gel resistant to freeze-thawing Offers water retention by gel	Fruit jellies, cocktail jellies, low-sugar jams, youkan, kuzu mochi, frozen jellies, kelp tsukudani
Ice crystal stabilization	Forms fine ice crystals Offers excellent shape retention Excellent acid resistance ensures stable overrun Thread-free viscosity offers good dissolution in the mouth	Ice creams, frozen dessert, glazing
Starch modification	Suppresses starch aging Confers heat resistance upon starch for protection Improves wheat flour product texture Confers mechanical strength upon starch for protection	Custard cream, flour pastes, gyoza sheets, curry, stew, noodles, rice cake, dango, Japanese traditional confectionery,

(Nishinari et al. 2000)

2
Methods

In this thesis, gelation and gel properties of gellan gum and xyloglucan were studied by rheological and DSC measurements. In order to understand the gelation at the molecular level, rheological and DSC results were compared with CD results.

2.1 RHEOLOGY

Rheology, a branch of mechanics, is the study of those properties of materials which determine their response to mechanical force (Ross-Murphy, 1994; Young, 1981). The word rheology was given in the 1920's to represent the science of the deformation and flow of matter. Many rheological studies have been carried out for food polysaccharide because rheological properties are an important factor for texture modification. Rheology deals with the material between purely elastic solid and purely viscous fluid. This category includes properties of most foods.

Elastic solid

The stress of a material, σ or τ, is defined as the force F acting per initial unit area A_0. This tends to produce a deformation, the strain (ε or γ), here defined as the ratio of the change in dimension relative to the original dimensions. The effect of tension

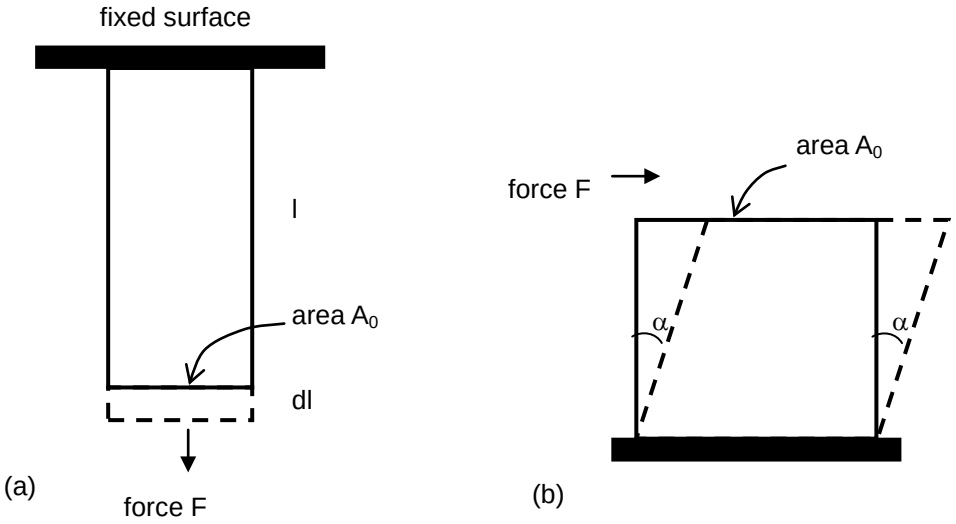

Figure 2.1 (a) Tensile stress and (b) shear stress applied to idealized geometries.

(tensile stress) on a rectangular block is illustrated in Fig. 2.1(a). The application of a shear stress to the sample (Fig. 2.1(b)) is regarded as a displacement gradient acting parallel to the fixed face. For a tensile deformation the strain is d*l*/*l*, whereas for shear stress tangent of the angle α gives the shear strain. For small strains tanα ≈ α. The Young's modulus or tensile modulus that describe the stiffness of the material is then given by

$$E = \frac{\sigma}{\varepsilon} = \frac{F/A_0}{dl/l}$$

(Since A will tend to change when the sample is deformed, the true stress is sometimes defined as F/A, the area at the given strain.)

Correspondingly, the shear modulus may be written as

$$G = \frac{\tau}{\gamma} = \frac{F/A_0}{\tan\alpha} \quad \text{and if} \quad \tan\alpha \cong \alpha \quad \text{then} \, G \cong \frac{F}{A_0\alpha}.$$

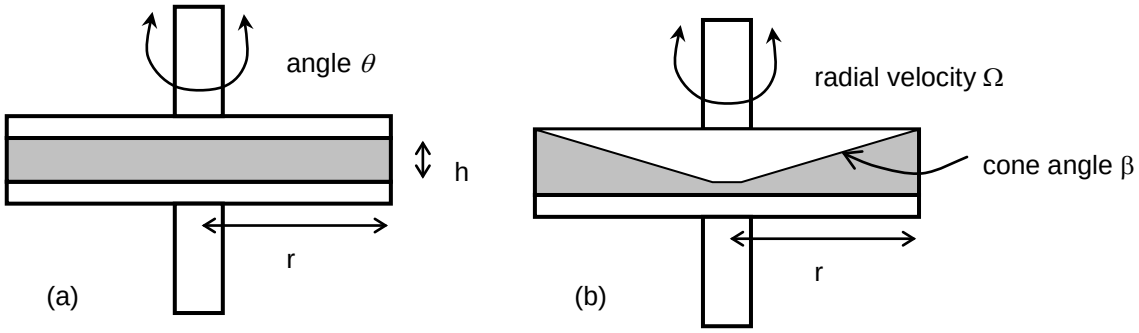

Figure 2.2 (a) Parallel plate geometry and (b) cone /plate geometry. The cone tip is truncated, and a gap corresponding to this truncation is set.

Since strain is dimensionless, the SI units of modulus are Nm^{-2} or Pa. One of problems in such a definition for shear modulus is that the measurement is rarely performed on a regular cube of material such as illustrated in Fig.2.1. In practice a much more useful 'geometry' is that of the parallel plate illustrated in Fig.2.2(a). The maximum strain (at the edge) is then equal to $\theta r/h$.

Viscous fluid

For liquids the stress depends on the rate of change of strain with time rather than the amount of deformation. In Fig. 2.3, the liquid is moving in the direction *x*. The *x*-components of the average velocities of molecules in different layers are represented by arrows of different lengths. The velocity gradient is in the *y* direction; that is, the *x*-component of the velocity *u* increases with increasing *y*. The molecules are also moving in the *y*- and *z*-directions. However, because there is no net flow in the *y*- and *z*-directions, the movement of the molecules in these directions is random. Many fluids, such as water and most gases, satisfy Newton's criterion and are known as Newtonian fluids. Newton's criterion is that, for straight, parallel and uniform flow, the shear stress, τ, between layers is proportional to the velocity gradient, du/dy, in the direction perpendicular to the layers, in other words, the relative motion of the layers.

$$\tau = \eta \frac{du}{dy} = \eta \frac{dx/dt}{dy} = \eta \frac{dx/dy}{dt} = \eta \frac{d\gamma}{dt} = \eta\dot{\gamma}$$

Here, the constant η is known as the coefficient of viscosity, viscosity, or dynamic viscosity which is resistance to flow of a liquid. η of Non-Newtonian fluids, in most cases, depend on the strain rate. The corresponding SI unit of viscosity is the Pas and the viscosity of water at 20ºC is almost exactly 10^{-3} Pas. A convenient steady-shear geometry is that of a cone and plate illustrated in Fig. 2.2(b). The shear rate in this design is constant across the gap, and is given by $\dot{\gamma} = \Omega/\beta$ where Ω is the radial velocity of rotation (rad s^{-1}) and β is the cone angle (rad). Corresponding to the shear viscosity, we can also define the extensional (elongational) viscosity ($\overline{\eta} = \sigma/\dot{\varepsilon}$).

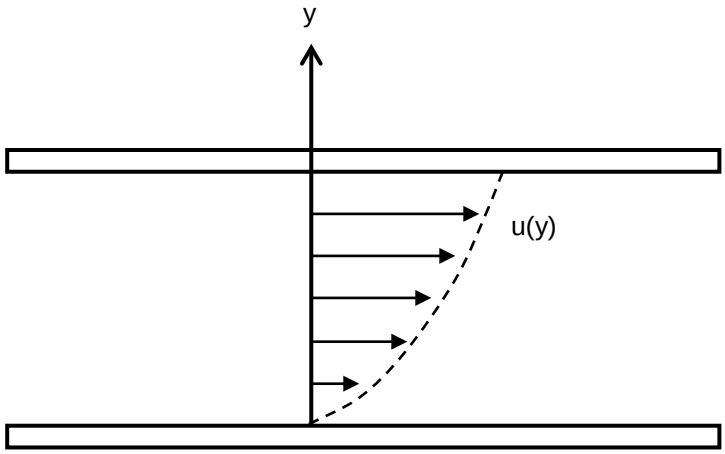

Figure 2.3 Velocity gradient produced in a fluid placed between a moving wall and a parallel stationary wall.

Viscoelastic material

The behavior of elastic solids such as metals and ceramics, at least at low strains, obeys Hooke's law and the stress is proportional to the strain and independent of

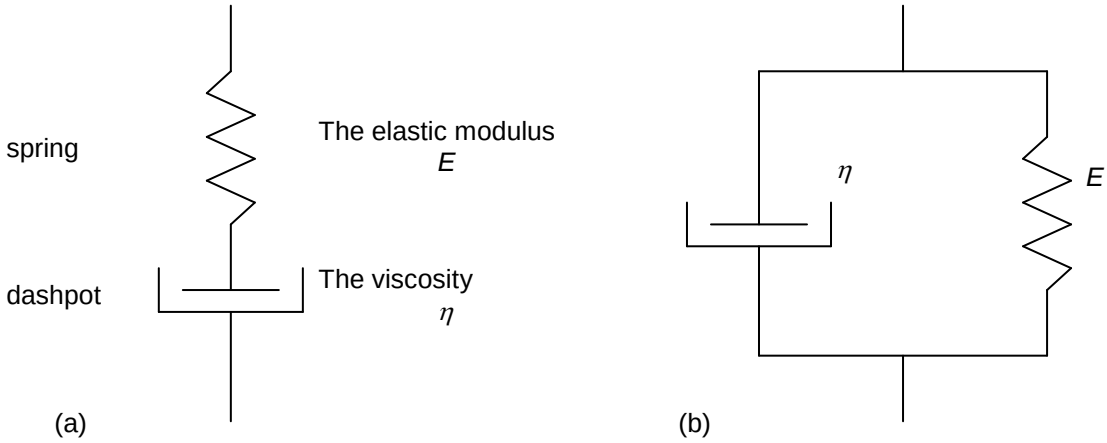

Figure 2.4 Mechanical model used to represent the viscoelastic behavior. (a) Maxwell model, (b) Voigt model.

loading time. On the other hand the mechanical behavior of liquids is completely time dependent. Their behavior at low rates of strain obeys Newton's law where the stress is proportional to the strain rate and independent of the strain. The behavior of most foods can be thought of as being somewhere between that of elastic solids and liquids. Foods are therefore termed viscoelastic as the display aspects of both viscous and elastic types of behavior.

Viscoelasticity of the material leads to the stress relaxation, decrease in stress in a material subjected to prolonged constant strain at a constant temperature and creep, a time dependent deformation of a material under load. During the stress relaxation the strain is held constant and the stress decays slowly with time whereas in an elastic solid it would remain constant. The Maxwell model is a simple model to predict the response of the materials during stress relaxation. It consists of a spring of modulus E which obeys Hooke's law and a dashpot of viscosity η which obeys Newton's law in series as shown in Fig. 2.4(a).

Under the action of an overall stress σ there will be an overall strain ε in the system

which is given by $\varepsilon = \varepsilon_1 + \varepsilon_2$, where ε_1 is the strain in the spring and ε_2 the strain in the dashpot. Since the elements are in series the stress will be identical in each one and so $\sigma_1 = \sigma_2 = \sigma$.

Hooke's law and Newton's law can be written as follows;

$$\frac{d\sigma}{dt} = E\frac{d\varepsilon_1}{dt}, \quad \sigma = \eta\frac{d\varepsilon_2}{dt} \tag{2.1}$$

for the spring and the dashpot, respectively. Differentiation of $\varepsilon = \varepsilon_1 + \varepsilon_2$ gives $d\varepsilon/dt = d\varepsilon_1/dt + d\varepsilon_2/dt$ and so for the Maxwell model

$$\frac{d\varepsilon}{dt} = \frac{1}{E}\frac{d\sigma}{dt} + \frac{\sigma}{\eta} \tag{2.2}$$

During stress relaxation a constant strain $\varepsilon = \varepsilon_0$ is imposed on the system and so $d\varepsilon/dt = 0$. Eq. (2.2) then comes $0 = (1/E)d\sigma/dt + \sigma/\eta$, and hence $d\sigma/\sigma = -(E/\eta)dt$. This can be integrated if as $t = 0$, $\sigma = \sigma_0$ and so

$$\sigma = \sigma_0 \exp(-\frac{Et}{\eta}) \tag{2.3}$$

where σ_0 is the initial stress. The term η/E is constant for a given Maxwell model and it is referred to as a 'relaxation time', τ_0. The Eq. (2.3) can then be written as

$$\sigma = \sigma_0 \exp(-t/\tau_0) \tag{2.4}$$

and it predicts an exponential decay of stress as shown in Fig. 2.5(a).

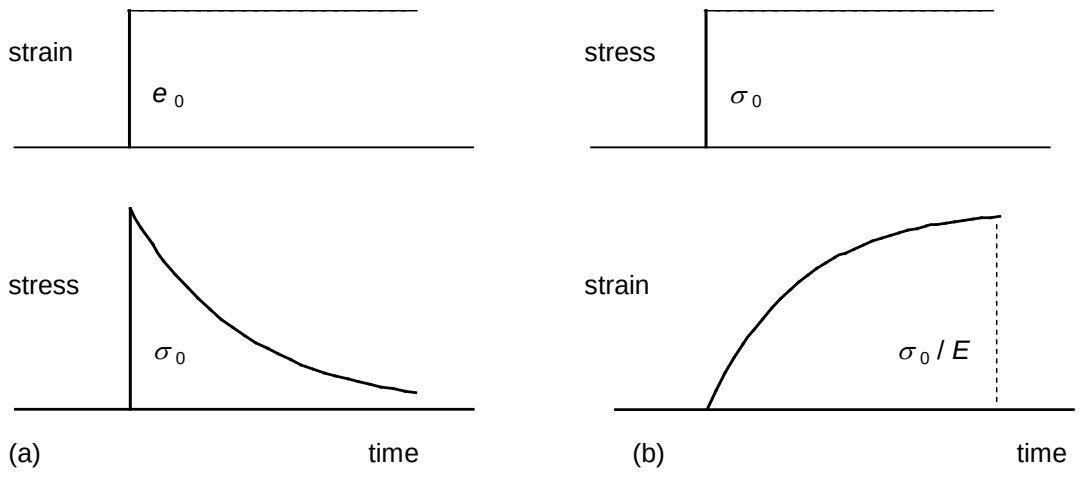

Figure 2.5 The behavior of the Maxwell and Voigt models during different types loading. (a) Stress relaxation, (b) Creep.

During creep loading a constant stress is applied to the specimen at t = 0 and the strain increases rapidly at first, slowing down over longer time periods. The behavior of a viscoelastic solid the strain stays constant with time. The Voigt model is useful in describing the behavior during creep where the stress is held constant at $\sigma = \sigma_0$. It consists of the same elements as are in the Maxwell model but in this case they are in parallel as shown in Fig. 2.4(b) rather than in series. The parallel arrangement of the spring and the dashpot means that the strain are uniform, $\varepsilon = \varepsilon_1 = \varepsilon_2$, and the stress in each component will add to make an overall stress of σ such that $\sigma = \sigma_1 + \sigma_2$. The individual stress σ_1 and σ_2 can be obtained as

$$\sigma_1 = E\varepsilon \quad \text{and} \quad \sigma_2 = \eta \frac{d\varepsilon}{dt} \tag{2.5}$$

for the spring and the dashpot respectively. Putting these expressions into $\sigma = \sigma_1 + \sigma_2$ and rearranging gives $d\varepsilon/dt = \sigma/\eta - E(\varepsilon/\eta)$. During creep the stress is constant at $\sigma = \sigma_0$. Then

$$\frac{d\varepsilon}{dt}+\frac{E\varepsilon}{\eta}=\frac{\sigma_0}{\eta} \tag{2.6}$$

The simple differential equation has the solution

$$\frac{d\varepsilon}{dt}=-\frac{\varepsilon-\sigma_0/E}{\eta/E}$$

$$\frac{d\varepsilon}{\varepsilon-\sigma_0/E}=-\frac{Edt}{\eta}$$

$$\ln|\varepsilon-\frac{\sigma_0}{E}|=-\frac{Et}{\eta}+C_1$$

$$\varepsilon-\frac{\sigma_0}{E}=C_2\exp(-\frac{Et}{\eta})$$

Since $\varepsilon = 0$ at $t = 0$, $C_2=-\frac{\sigma_0}{E}$. Hence

$$\varepsilon=\frac{\sigma_0}{E}\left[1-\exp\left(-\frac{Et}{\eta}\right)\right] \tag{2.7}$$

The constant ratio η / E can be replaced by τ_r, the retardation time and so the variation of strain with time for a Voigt model undergoing creep loading is given by

$$\varepsilon=\frac{\sigma_0}{E}\left[1-\exp\left(-\frac{t}{\tau_r}\right)\right] \tag{2.8}$$

This behavior is shown in Fig. 2.5(b) and it represents the correct form of behavior for a material undergoing creep.

Stress relaxation and creep represent static viscoelasticity. On the other hand, a

viscoelastic behavior obtained by oscillational measurements is called dynamic viscoelasticity. Dynamic oscillational measurements are useful for food analysis since it is possible to shorten the measuring time so that foods remain unchanged with time during measurement.

Fig. 2.6 shows a sinusoidal oscillation of strain applied to (a) purely elastic solid and (b) purely viscous fluid and the resultant stress. If the material is perfectly elastic, the resultant stress wave is exactly in phase with the strain wave. On the other hand, if the material is purely viscous fluid, the resultant stress wave is exactly $\pi/2$ out of phase with the imposed deformation. The stress wave of the viscoelastic material has a phase difference δ ($0<\delta<\pi/2$).

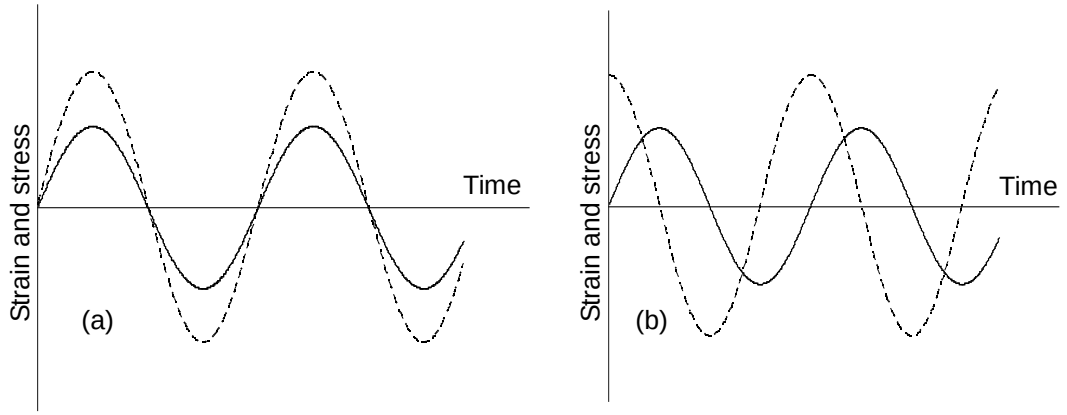

Figure 2.6 Sinusoidal oscillation of strain (solid line) and stress (dashed line) for (a) a purely elastic solid and (b) a purely viscous fluid.

Fig. 2.7 shows the relation between strain and stress when the sinusoidal shear oscillation was applied to the viscoelastic material with an angular frequency ω and a strain amplitude γ_0. Complex shear modulus G^* is defined as

$$G^* = \frac{\tau_0}{\gamma_0}\left(\cos\delta + i\sin\delta\right)$$

where τ_0 is a stress amplitude and $i^2 = -1$. The real and imaginary parts of G' and G'' of G^* ($G^* = G' + iG''$) are called storage shear modulus and loss shear modulus. The real and imaginary parts of complex Young's modulus E^* obtained by longitudinal oscillation are called storage Young's modulus E' and loss Young's modulus E''. G' and E' are proportional to the elastic energy stored in viscoelastic material in a period of oscillation, while G'' and E'' are proportional to the dissipated energy as heat in a period of oscillation. The ratio G''/G' or $E''/E' = \tan\delta$ is called mechanical loss tangent. The value of $\tan\delta$ tends to infinity for a purely viscous fluid, while it tends to zero for a purely elastic solid.

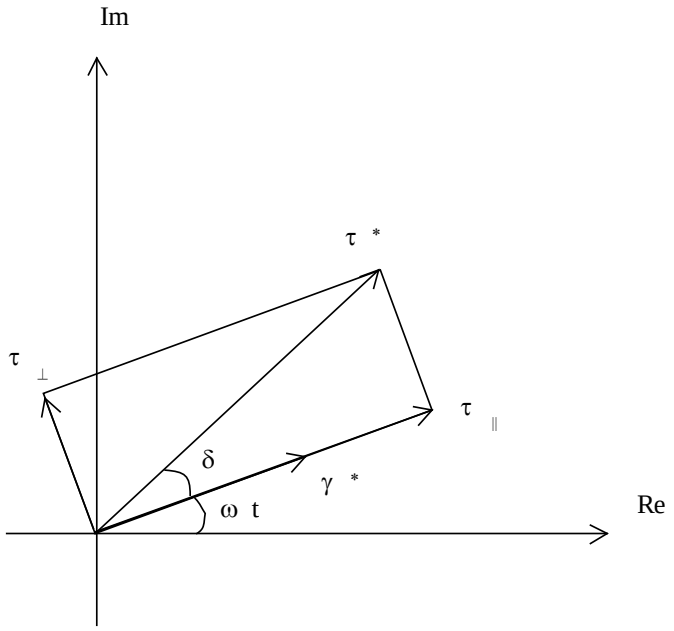

Figure 2.7 Strain vector γ^* and stress vector τ^* in complex plane. γ^* rotates with angular velocity ω and τ^* rotates with the same angular velocity but out of phase δ. $\tau_{\parallel} = \tau_0\cos\delta$ and $\tau_{\perp} = \tau_0\sin\delta$ are components of τ^* which are in-phase and out of phase to γ^* respectively.

Fig. 2.8 shows schematic diagram of the rheometer used in the present study. The

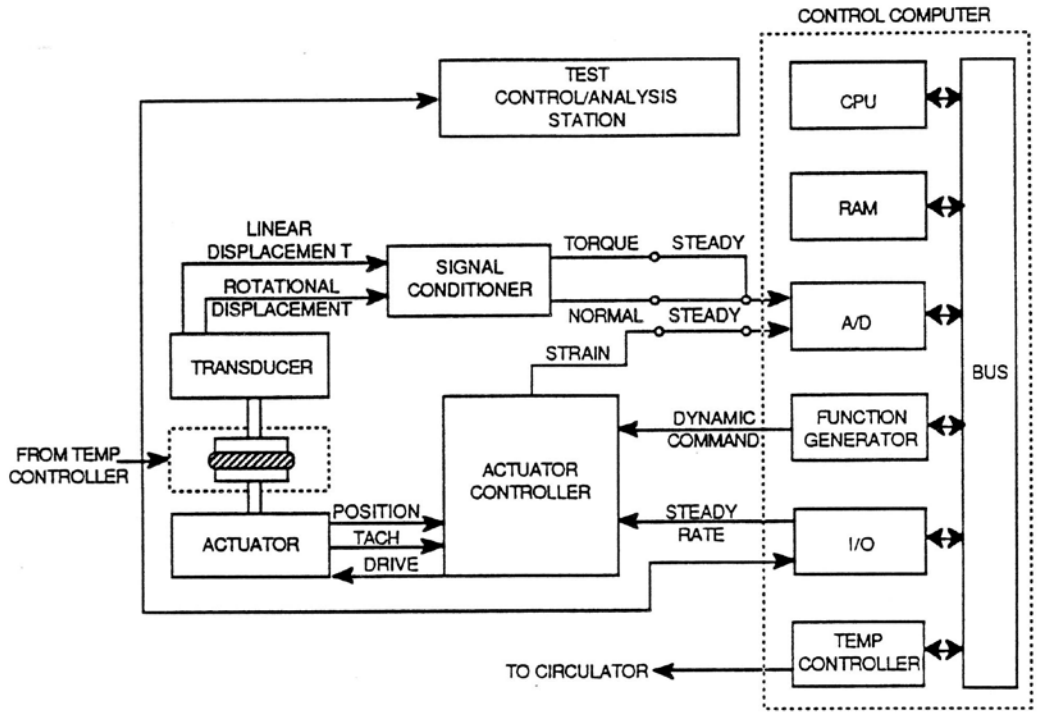

Figure 2.8 System block diagram of strain-controlled rheometer (from Owner's Manual of Rheometrics Fluids Spectrometer).

sample geometry is mounted between the instrument actuator that applies the test strain, and the transducer that senses the sample response. The sample to be tested is loaded into the test geometry appropriate to the sample and the test. Testing is controlled by the test control/analysis station, which is also used for data storage and analysis.

When preparations are complete, the test is started from the test control/analysis station. The test program passes instructions and parameter information to the instrument firmware for test control. As the test proceeds, the control computer receives coordinated signals from the actuator and transducer reflecting the sample responses to the applied strain. The control computer, in conjunction with circuitry in the test station, provides all necessary signal conditioning and digitizing for driving the actuator in the selected test pattern and for storing results in the control computer

memory. For reporting, the test control/analysis station can obtain results either in real time for on-line test monitoring, or after the test is completed for analysis/preparation.

2.1.1 Rheological properties of polysaccharide solutions

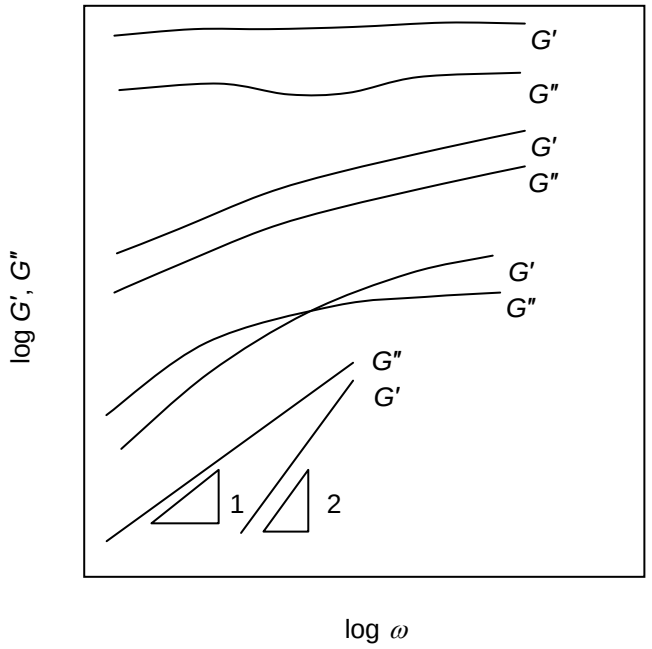

Figure 2.9 Examples of frequency dependence of G' and G'' for polysaccharide solutions.

Mechanical spectra (frequency dependence of storage and loss moduli) are often examined to investigate characteristics of a polysaccharide solution. Fig. 2.9 shows examples of frequency dependence of G' and G'' for polysaccharide solutions. A power law $G' \sim \omega^2$ and $G'' \sim \varpi$ is found in dilute solutions of polysaccharide at low frequencies. Another rheological behavior where G' and G'' cross at a certain frequency, below which G'' is higher than G', is found in semi-dilute solution. In elastic polysaccharide gels, G' is higher than G'' at all frequencies examined and both moduli show a plateau even at low frequencies. Some polysaccharide solutions show

a gel-like behavior in mechanical spectra but if subjected to a steady shear flow, they will apparently flow rather than fracture. In this case the behavior is called a “weak gel type”, where G' is higher than G'' at all frequencies examined and both moduli show only a slight frequency dependence.

2.1.2 Determination of gel point by rheology

For determining gelation point, Winter and Chambon (1986) proposed following equations;

$$G' \sim G'' \sim \omega^n \tag{2.9}$$

$$\tan\delta = \frac{G''}{G'} = \tan\left(\frac{n\pi}{2}\right) \tag{2.10}$$

According to these equations, at gelation point, G' and G'' show the same frequency dependence in wide range and the exponent n in equation (2.9), which can be obtained from the slope in the double logarithmic plot of G' and G'' as a function of frequency, agrees with n in equation (2.10), which can be obtained from tanδ. These were proposed for chemical gels first. It has been reported that many chemical gelation satisfies this criteria (Chambon and Winter, 1987; Koike et al., 1994; Takahashi et al., 1994). It was found that gelation of some physical gels also satisfied these equations (Te Nijenhuis and Winter, 1989; Hsu and Jamieson, 1993; Aoki et al., 1998; Hossain et al., 1997).

2.2 THERMAL ANALYSIS: DIFFERENTIAL SCANNING CALORIMETRY (DSC)

Differential scanning calorimetry (DSC) is one of the most widely used of all the thermal analysis techniques (Laye, 2002; Hatakeyama and Quinn, 1994). The concept underlying this technique is to obtain information on thermal changes in a sample by heating or cooling it alongside an inert reference.

In the case of heat flux type of differential scanning calorimeters, the instrument signal is derived from the temperature difference established when the sample and reference are heated in the same furnace. The temperature difference is measured by the temperature sensors – usually thermocouples arranged back-to-back. Fig. 2.10 shows the operating principle of heat flux type of the DSC calorimeters used in the present study.

The results from DSC experiments are displayed as a DSC curve in which the instrument signal is plotted against temperature – usually the sample temperature – or time as shown in Fig. 2.11. Analysis of the DSC curve is carried out using the instrument software. Tm is the peak maximum temperature. In the figure the peak represents an exothermic event (exotherm) and has been represented as a positive displacement (Laye, 2002). This is the usual convention for heat flux DSC. When confusion is likely to arise the direction of the exotherms/endotherms should be shown on the DSC curve.

Application of DSC is found widely in the general area of material science. DSC techniques give great contribution in the study of polymeric materials with thermal transitions such as crystallization, melting and glass transition. Crystallization and melting are thermal transitions that involve both a latent heat and a change in the heat capacity of the material whereas glass transition is a thermal transition that involves a change in heat capacity, but does not have a latent heat. Thermal transition involving a latent heat shows a DSC peak and the area of DSC peaks can be used to estimate the

enthalpy of transition, ΔH.

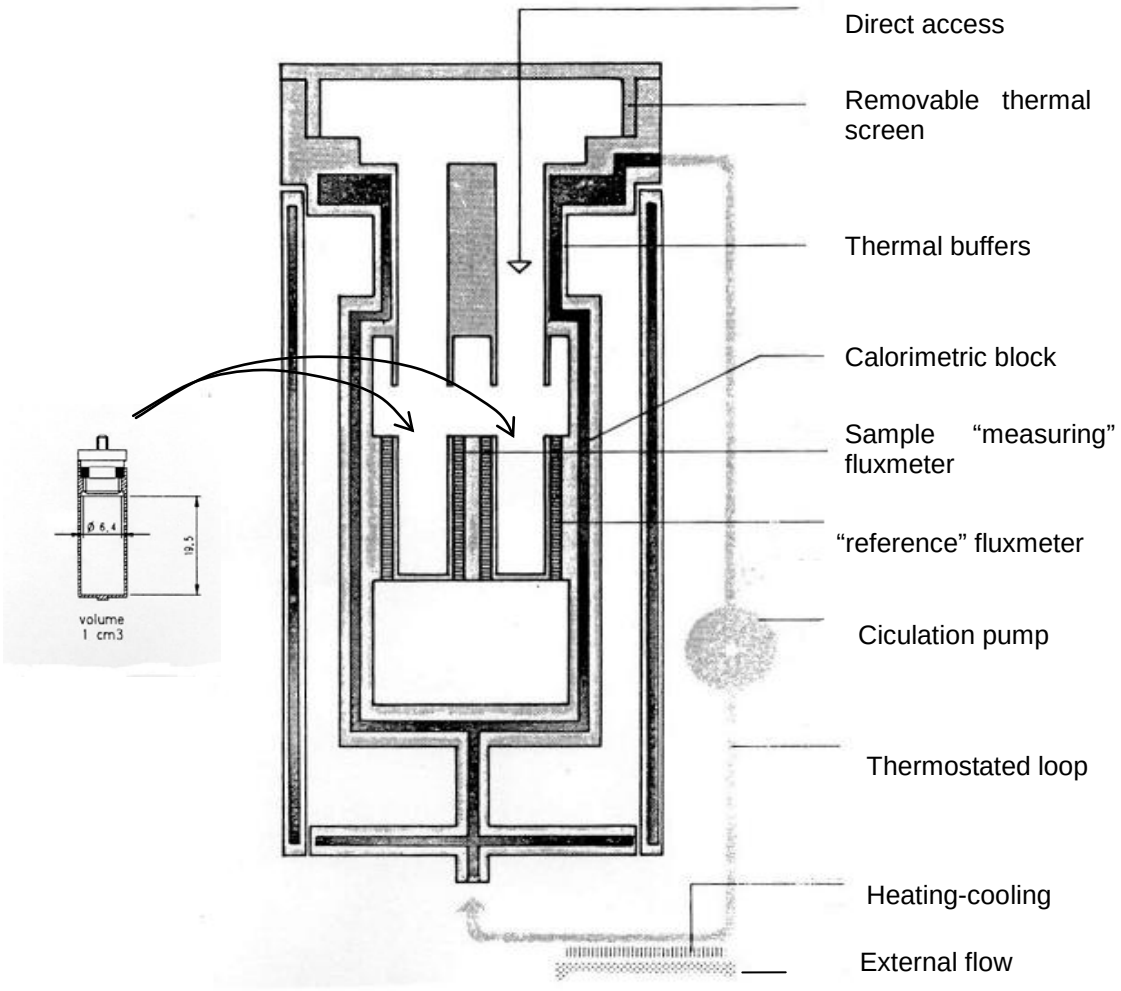

Figure 2.10 Operating principle of DSC (from Owner's manual of setaram micro DSC).

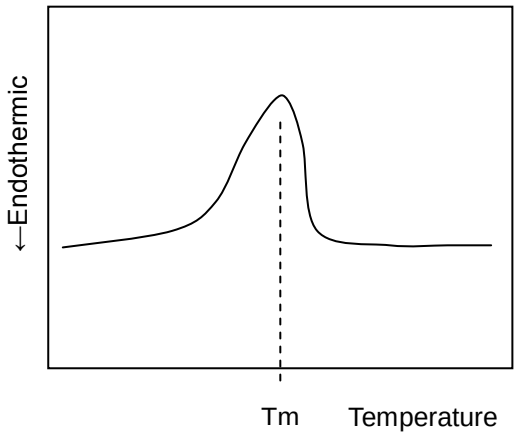

Figure 2.11 Schematic representation of a DSC curve.

ΔH is determined by software with the input of the times corresponding to the start and finish on the peak. The software may provide different options for constructing the base-line. The calculation is straightforward if the peak is reasonably sharp and the heat capacity of the product does not differ greatly from that of the initial sample. A straight line from start to finish of the peak is constructed to represent the base-line (Fig. 2.12). Some difficulty may occur in identifying the precise starting point of a peak, for example, when there is a marked change in heat capacity and the base-line no longer even approximates to a straight line (Laye, 2002). In that case, the construction of the base-line must reflect the changing heat capacity of the sample which in turn will depend on the proportion of the initial sample (reactant) and the product (Fig. 2.13).

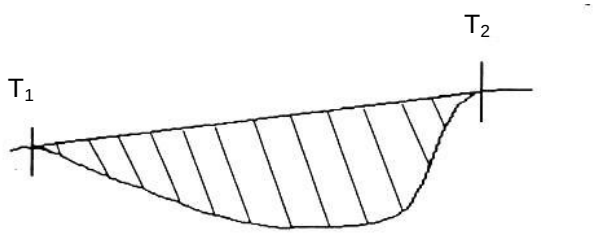

Figure 2.12 The base line of a straight line joining the points corresponding with the temperatures T1 and T2 chosen on the curves.

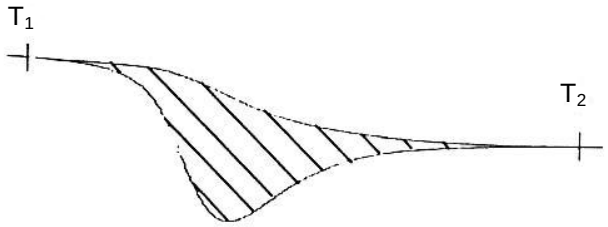

Figure 2.13 The base line obtained by taking account of the variation in specific heat before and after transformation.

2.2.1 Conformational transition of polysaccharides

It is generally recognized that an exothermic DSC peak appears when the system changes from the disordered state to ordered state whereas an endothermic DSC peak appears when the system changes from the ordered state to disordered state (Nishinari, 1997). When helix forming polysaccharides such as agarose, carrageenans and gellan taking disordered conformation in the solutions at higher temperatures are cooled, the polysaccharides change from disordered conformation to helical conformation at a certain temperature at which an exothermic DSC peak appears. Also, when the helix forming polysaccharides taking helical conformation at lower temperatures are heated, the polysaccharides change from helical conformation to disordered conformation at a certain temperature at which an endothermic DSC peak appears.

2.2.2 The sol-gel transition of polysaccharide

The sol-gel transition occurs by accompanying the conformational transition in some polysaccharides. The sol-to-gel transition follows the disorder-to-order transition whereas the gel-to-sol transition follows the order-to-disorder transition of the polysaccharides. Therefore DSC is applied to investigate the sol-gel transition of polysaccharides. Some polysaccharides show the sol-gel transition with thermal hysteresis where DSC peak temperature arising from gelation is lower than that arising from gel-melting. Agarose gel is a typical example for such sol-gel transition. The difference in peak temperatures is considered to be due to formation of aggregates of different polysaccharide chains during gelation (Clark and Ross-Murphy, 1987). Some polysaccharides show several peaks when gel melting and it is considered to be due to formation of aggregates with various thermal stabilities.

2.3 CIRCULAR DICHROISM (CD)

Circular Dichroism (CD) is observed when optically active matter absorbs left and right handed circularly polarized light slightly differently.

Electromagnetic radiation can be described by an electric-field vector that oscillates with a characteristic frequency in time and space. For unpolarized light, the electric vector may oscillate in any direction perpendicular to the direction of propagation. For a large number of photons in an unpolarized beam, all directions are equally

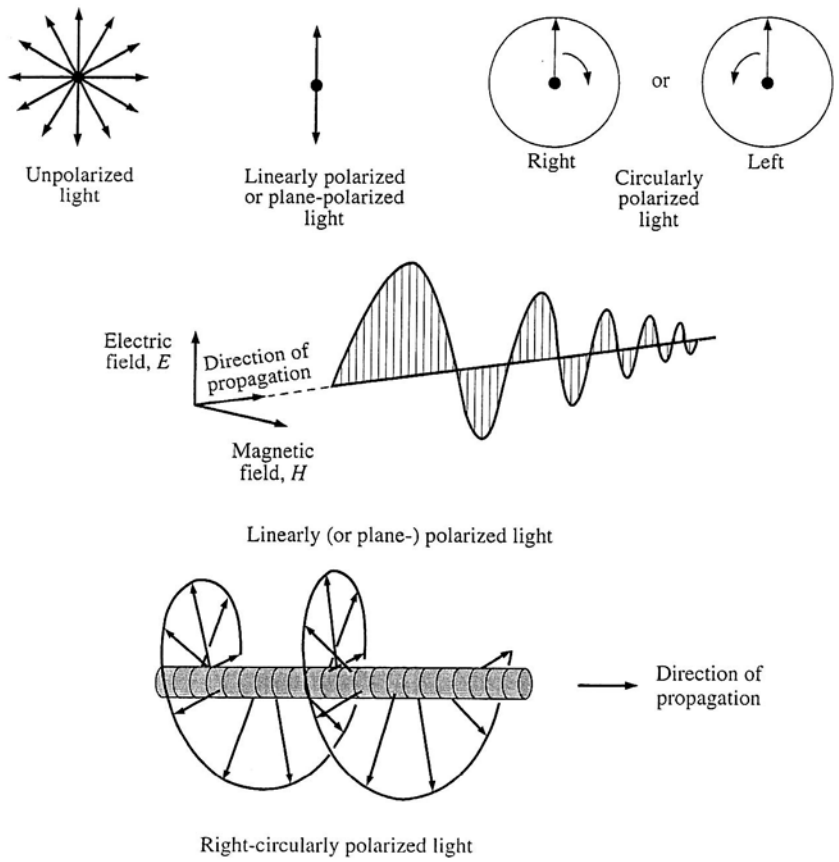

Figure 2.14 Different types of polarized light. At the top, the arrows represent the electric vector of the lights as seen by an observer moving with the light. The light is moving into the page. At the middle and bottom, the light is seen by a stationary observer (Tinoco et al., 2002).

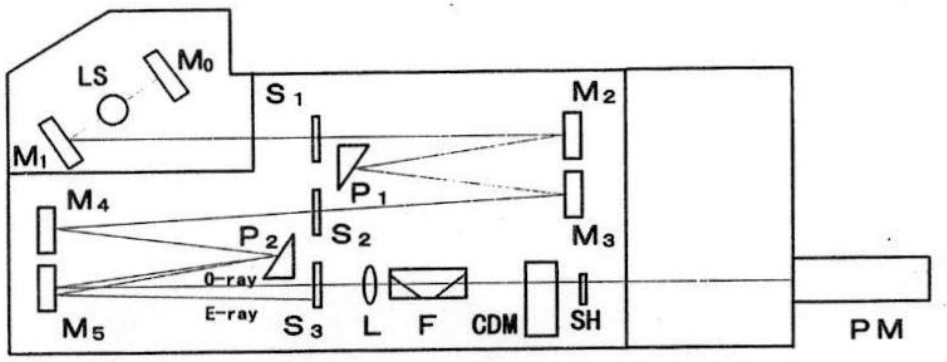

Figure 2.15 Layout of the CD spectrometer. LS: light source; M_1: elliptical mirror to focus radiation on the entrance slit (S_1) of the monochromator; M_0: spherical mirror to collect back-emitted radiation of the source; S_1, S_2, S_3: entrance, intermediate and exit slit of the double monochromator; $M_{2\text{-}4}$: spherical collimating mirrors of the monochromator; P_1, P_2: quartz prisms, used to disperse radiation and to generate a linearly polarized output; L: quartz lens to get a parallel beam through sample compartment; F: series of 45º quartz plates to clean further the polarization; CDM: photoelastic modulator, acting as an achromatic quarter wave plate generating left and right circularly polarized radiation at its oscillation frequency (50 kHz?); SH: mechanical shutter to remove, when needed, light on the sample; PM: photomultiplier tube detector.

represented. The electric vectors can be pictured as radiating spokes on a many-spoked wheel, as shown in Fig. 2.14. For plane-polarized light is shown in Fig.2.14 (top and middle). To an observer moving at the photon's velocity, the electric vector appears to be oscillating back and forth along a line. For this reason, plane-polarized light is also referred to as being linearly polarized. Circularly polarized light propagates so that the tip of its electric vector sweeps out a helix (Fig. 2.14 bottom); right-circularly polarized light produces a right-handed helix. To an observer moving with the photons, the electric vector appears to be moving in a circle, like the hands of a clock (Fig. 2.14 top). The convention is that for left-circularly polarized light the electric vector moves counterclockwise as the light moves away from the observer; for right-circularly polarized light, it moves clockwise.

Fig. 2.15 shows the layout of the CD spectrometer used in the present study. Circularly polarized light is generated by an optical modulator in this CD spectrometer.

Circular dichroism results from a differential absorption of left- and right-circularly polarized light by a sample that exhibits molecular asymmetry. A simple expression of the circular dichroism is given by

$$\Delta A = A_l - A_r$$

where A_l and A_r are the absorbances of the sample for pure left- and right-circularly polarized light, respectively. Circular dichroism is also expressed by molar circular dichroism.

$$\Delta\varepsilon = \varepsilon_l - \varepsilon_r = \frac{A_l - A_r}{dM}$$

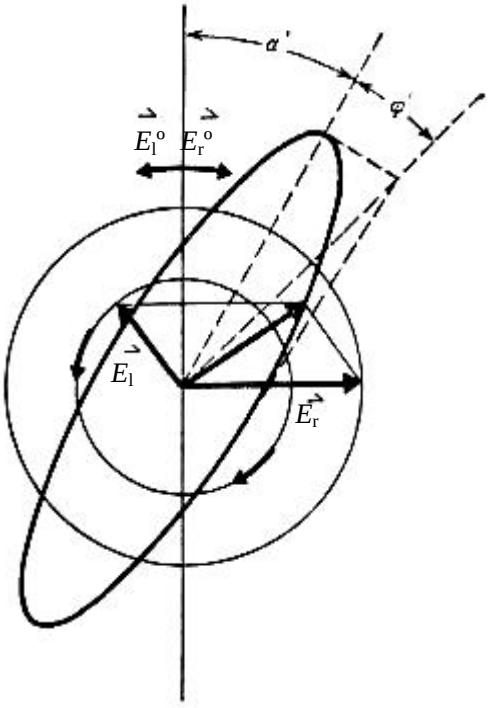

Figure 2.16 Ellipticity, φ', a measure of circular dichroism.

where ε_l and ε_r is the molar absorptivity (or molar extinction coefficient) of the sample for pure left- and right-circularly polarized light, respectively, d is the path length (cm) and M is concentration (mol L^{-1}).

When the right and left circularly polarized light passes through the optically active sample, the end of the electric vector traces out an ellipse with length of major and minor axes proportional to, respectively, the sum and difference of the transmitted intensities of the two components. The circular dichroism may be defined by the angle of ellipticity φ' (rad), whose tangent is equal to the ratio of the minor axis of the ellipse to the major axis.

$$\tan\varphi' = \frac{E_r - E_l}{E_r + E_l} \qquad (2.11)$$

where E_r and E_l are the amplitude of the electric vector of the right- and left-circularly polarized light. $E_r - E_l$ and $E_r + E_l$ are the values of the minor axis and the major axis of the ellipse, respectively, when the absorption of the left-handed circularly polarized light occurred much more than that of the right-handed one as shown in Fig. 2.16. E_r and E_l can be expressed by the intensity of the light. The intensity of the light I is expressed by $I_0 \exp(-kd)$ when the initial light intensity I_0 becomes I after it passes through the sample with the path length d (cm) and with the absorptivity coefficient k. Since the intensity is proportional to the square of the amplitude, E_r and E_l are expressed by

$$E_l \propto \sqrt{I} = \sqrt{I_0}\exp(-\frac{k_l d}{2}) \qquad E_r \propto \sqrt{I} = \sqrt{I_0}\exp(-\frac{k_r d}{2})$$

where k_l and k_r are the absorptivity coefficient of the sample for the left-handed and right-handed circularly polarized light, respectively. The ellipticity per cm, φ° (radcm^{-1}), corresponds to φ'/d and $\tan\varphi^\circ$ is given by

$$\tan\varphi^\circ = \frac{1-\exp(-\frac{k_l - k_r}{2})}{1+\exp(-\frac{k_l - k_r}{2})}$$

Since $k_l - k_r$ is quite small the tangent of the angle is approximately equal to the angle itself, $\tan\varphi^\circ \fallingdotseq \varphi^\circ$. (Expansion and ignoring the higher order terms give)

$$\varphi^{\circ} = \frac{k_l - k_r}{4} \tag{2.12}$$

The specific ellipticity, $[\varphi]$ (degdm^{-1}cm^{3}g^{-1}), and molar ellipticity, $[\theta]$ (10^{-2}degcm^{-1}M^{-1}), are defined using the ellipticity in degrees, φ (deg).

$$\varphi = \frac{180\varphi'}{\pi} \tag{2.13}$$

$$[\varphi] = \frac{\varphi}{c'd'} \tag{2.14}$$

$$[\theta] = \frac{\varphi}{dM} \times 10^2 \tag{2.15}$$

where c' is concentration (g cm^{-3}), d' is path length (dm), d is the path length (cm), and M is concentration (mol L^{-1}). In solutions the absorbance is generally defined for base 10 logarithms rather than natural logarithms. Thus ε (cm^{-1}M^{-1}), the molar absorptivity defined by $I = I_0 \times 10^{-\varepsilon dM}$ from Beer-Lambert law, is used rather than k. Since the relation between ε and k is given by $k = 2.3025\varepsilon M$, equation (2.15) is expressed by

$$[\theta] = \frac{180}{4\pi M}(k_l - k_r) \times 10^2 = \frac{180}{4\pi} \times 2.3025(\varepsilon_l - \varepsilon_r) \times 10^2 \approx 3298(\varepsilon_l - \varepsilon_r) \tag{2.16}$$

This relation correlates the ellipticity with the differential absorption, each of which, therefore, is used as a measure of circular dichroism.

Most biological molecules have molecular asymmetry or chirality. These molecules are not identical to their mirror image and interact differently with right- or left-handed circularly polarized light. Achiral molecules (i.e. those that are identical

to their own mirror-image) have no basis for differential interaction with right- or left-handed circularly polarized light, and therefore have no optical activity. Thus the chiroptical methods cannot be applied to synthetic polymers (or to any other man-made products, unless biological materials, such as enzymes, have been used at some stage of the preparation). Food biopolymers (proteins and polysaccharides), however, are built up from chiral monomers, and are therefore all optically active (Morris, 1994).

CD can be applied only to molecules that absorb in an experimentally accessible spectral region. The effective wavelength range on most modern commercial CD spectrophotometers is about 185-700nm. Of industrial polysaccharides currently allowed for food use, only alginate, pectin, xanthan and gellan, give significant CD at wavelength above about 185nm since all of these contain uronic acid residues which show strong CD (Morris, 1994).

2.2.3 Conformational transition of polysaccharides

The thermoreversible order-disorder transition of polysaccharides can be monitored by a change in optical rotation and it is accompanied by larger changes in circular dichroism. Xanthan gum exists in solutions in a regular, ordered chain conformation, which can be stabilized by salt and disrupted on heating. The conversion from the ordered form at lower temperature to the disordered coil form at higher temperature induces changes in CD spectra as shown in Fig. 2.17(a). Gellan gum also exhibits a thermally reversible conformational transition with an associated sharp change in optical rotation and CD spectra as shown in Fig. 2.17(b).

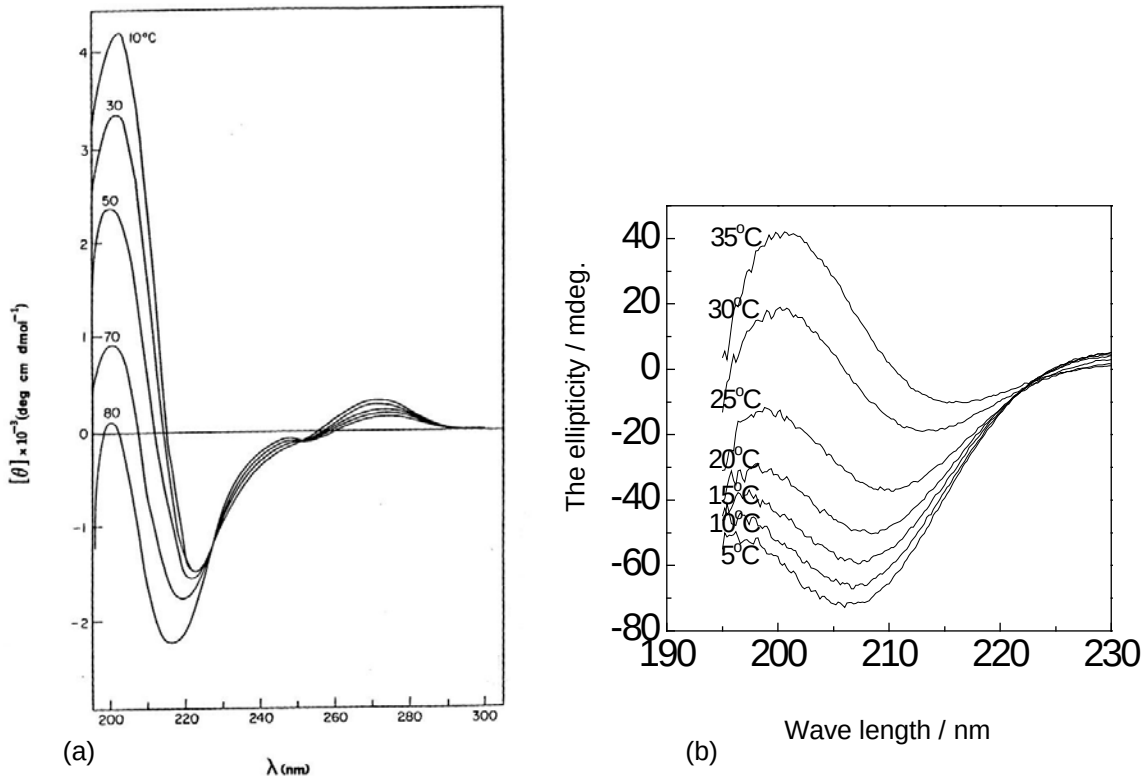

Figure 2.17 (a) CD changes accompanying the order-disorder transition of xanthan. Spectra were recorded at the temperatures shown in figure (Morris et al., 1977). (b) CD changes accompanying the order-disorder transition of 1.2% gellan. Path length; 2mm.

3

Gelation and gel properties of gellan gum

3.1 THE HELIX-COIL TRANSITION IN GELLAN GELS

3.1.1 Introduction

It is believed that, in a solution state, gellan gum molecules change from the disordered state (single chain) to the ordered state (double helix) with decreasing temperature and that, above a certain critical concentration, double helices form aggregates which play a role of junction zones (Robinson et al., 1991). It has been suggested that the gelation occurs when the helix content exceeds a threshold value above which the number of helical aggregates is sufficient to form a three dimensional network (Miyoshi et al., 1995).

In the present work, the temperature dependence of complex Young's modulus, specific ellipticity in CD were examined and DSC measurement was performed to get further insight into the gel-sol transition and helix-coil transition in gellan gum.

3.1.2 Experimental

Gellan gum was supplied by San-Ei-Gen FFI Ltd., Osaka, Japan. It is the first common sample in the collaborative research published in *Food Hydrocolloids*, **7**, 361-456 (1993). The metal contents in the sample are as follows: Na 1900μg/g, K

20800μg/g, Ca 5120μg/g and Mg 1460μg/g. The sample was not influenced by storage as for its molecular weight (Ogawa, 1996). The molecular weight was determined by converting it into the tetramethyl ammonium form using light scattering (Okamoto et al., 1993) and osmometry (Ogawa, 1993) as $M_w = 2.1 \times 10^5$ and $M_n = 0.5 \times 10^5$.

Gellan gum powder was swollen in distilled water and stirred overnight at 40°C. Then the solution was heated for 2 hours at 90°C. The solution was poured into teflon moulds (30mm height and 20mm diameter) and cooled at room temperature for more than 2 hours to obtain the samples for rheological measurements. The cylindrical gellan gels thus obtained were then kept at 5°C for 12 hours.

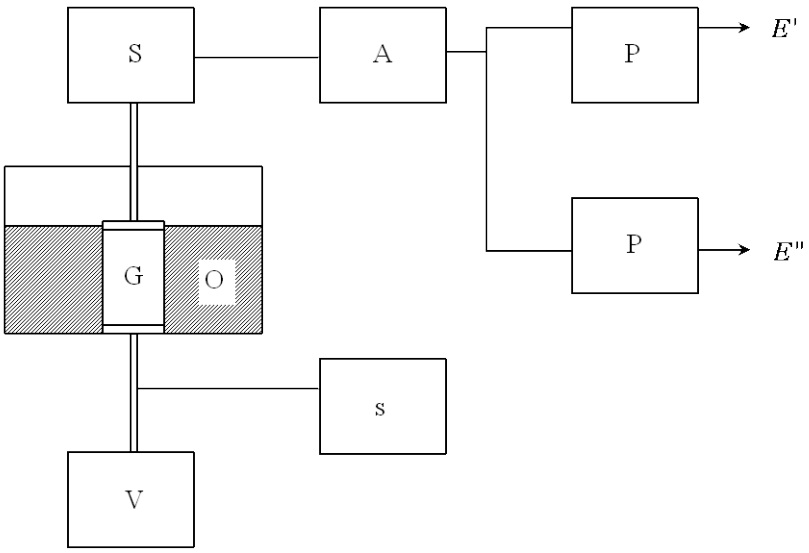

Figure 3.1 Schematic diagram of the apparatus for determining complex Young's modulus of gels (Rheolograph Gel, Toyo Seiki Seisakusho Ltd., Tokyo). G, cylindrical gel; O, silicone oil; V, vibrator; S, strain gauge for detection of stress, s, strain gauge for detection of strain; P, phase sensitive circuit.

The storage Young's modulus E' and the loss Young's modulus E'' were determined by the observation of longitudinal vibrations of cylindrically moulded gels. The

apparatus used (Nishinari et al., 1980) was a Rheolograph Gel (Toyo Seiki Seisakusyo Ltd, Tokyo). The temperature was raised from 10 to 55°C and then lowered from 55 to 10°C with an interval of 5°C. E' and E'' were measured in the equilibrium state. The typical time interval that required for equilibrium was 15 min.

The schematic representation of an apparatus for the determination of complex Young's modulus is shown in Fig. 3.1. The gel is immersed in silicone oil to prevent the evaporation of water and to control the temperature. The advantage of this method is that it is completely free from a notorious problem of slippage which affects quite often the viscoelastic measurement in shear oscillational mode (Richardson and Goycoolea, 1994; Zhang et al., 2001). The temperature was raised from 10℃ to 55℃ at an interval of 5℃. The temperature was kept at each temperature for 15 min. Then, the temperature was lowered from 55℃ to 10℃ at the same rate. Since it is well known that the storage modulus of a gel does not depend so much on the frequency (Nishinari, 1997; Te Nijenhuis, 1997; Clark and Ross-Murphy, 1987), the frequency is fixed as 3Hz and the amplitude was also fixed as 100 μm (strain 0.03) for this apparatus.

DSC measurements were carried out with a Setaram micro DSC-Ⅲ calorimeter, Caluire, France. The temperature was raised from 5°C to 55°C at 0.5°C/min and then lowered from 55°C to 10°C at the same rate.

CD measurements were carried out with a JASCO-820A spectropolarimeter. The specific ellipticity at 202nm $[\Psi]_{202}$ was measured in the temperature range from 5°C to 55°C at 0.5°C/min.

3.1.3 Results and discussion

Fig. 3.2 (a) shows the temperature dependence of the storage Young's modulus E', the loss Young's modulus E'', and mechanical loss tanδ for a 1.6% gellan gum gel, which was cylindrically moulded, observed at each temperature after being kept 15 min on heating. Both E' and E'' decreased with increasing temperature. Since E'' decreased

faster than E', tanδ decreased with increasing temperature. Gellan gels as well as other thermoreversible gels such as agarose, carrageenan and gelatin are believed to be formed by junction zones that are connected by chain molecules released out from junction zones. Junction zones are formed by aggregated helices. The widely accepted gelation mechanism of gellan is as follows: on cooling gellan aqueous solutions, the helices are formed from coiled molecules at a certain temperature. These helices aggregate on further cooling to form junction zones that play a role of knots of the three dimensional network. Gels are formed only if the polymer concentration is higher than the critical concentration, otherwise, even if helices are formed, they cannot percolate the whole space to form a gel. The gradual decrease in the storage Young's modulus E' and a steplike decrease in the loss Young's modulus E'' on heating shown in Fig. 3.2(a) are induced by the release of chain segments from junction zones as described in a reel-chain model (Nishinari et al., 1985).

Fig. 3.2(b) shows the temperature dependence of the specific ellipticity at 202 nm together with a heating DSC curve at 0.5℃/min. Both an endothermic peak in the heating DSC curve and the steep increase in the specific ellipticity suggest that helix to coil transition occurs at this temperature range.

Fig. 3.2(c) shows the temperature dependence of E', E'', and tanδ observed at each temperature after being kept 15 min on cooling. Fig. 3.2(d) shows the temperature dependence of the specific ellipticity at 202 nm together with a cooling DSC curve at 0.5 ºC/min. The exothermic peak in a cooling DSC curve is far sharper than a corresponding endothermic peak in a heating DSC curve, which may be induced by a mechanism like a supercooling as has been discussed in relation with a zipper model approach to the thermoreversible gel-sol transition (Nishinari et al., 1990). This is also true for the sharper change of elasticity and the specific ellipticity in the cooling process than in the heating process.

The loss Young's modulus E'' showed a step-like change at 30℃. The endothermic peak temperature in the heating DSC curve and the exothermic peak temperature in the

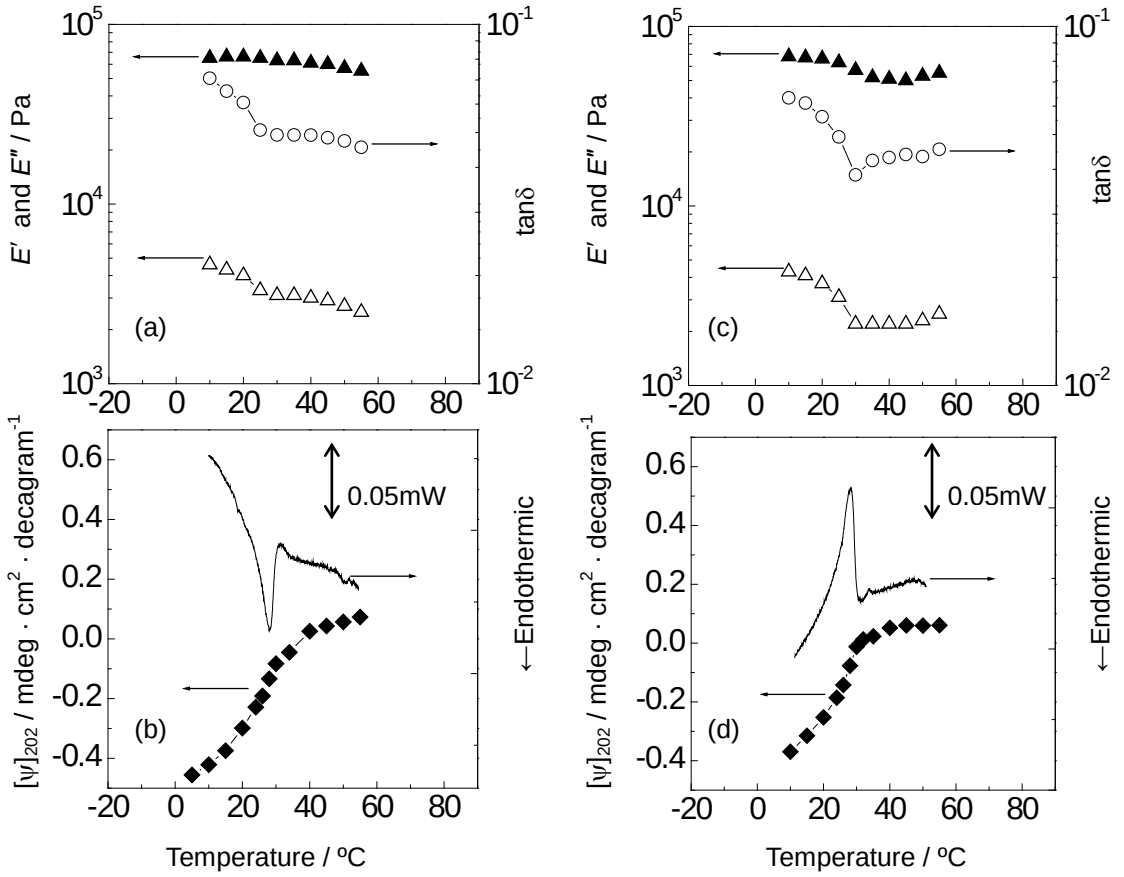

Figure 3.2　Temperature dependence of the storage modulus E' （▲）, the loss modulus E'' （△） and mechanical loss tanδ (○) on heating (a) and on subsequent cooling (c), the heating (b) and subsequent cooling (d) DSC curve (solid curve), and temperature dependence of the specific ellipticity at 202nm, $[\Psi]_{202}$, （◆）on heating (b) and subsequent cooling (d) for 1.6% (w/w) gellan gum gels. E' and E'' measurements were done after 15min equilibration at each temperature. Heating and cooling rates of DSC and CD measurements; 0.5ºC/min.

cooling DSC curve appeared at the midpoint transition temperature of the loss Young's modulus E'' and of the specific ellipticity.

It is generally believed in the gelation of polysaccharides such as agarose, carrageenan, gellan and also for gelatin that the helix formation is a prerequisite for the gel formation. It is generally accepted that helices are aggregated into a bundle which

acts as a knot of the three dimensional network. Therefore, on cooling of a solution of these polymers, coil conformers are transformed into helices, and then a gel is formed. In this process, however, not all the coils are transformed into helices and some molecular chains remain isolated, or dangling chains which are released from junction zones or from aggregated helices remain not to be incorporated into the network structure. Then, on further cooling, these dangling chains are reeled into junction zones as described in the reel-chain model.

From simple extension of a theory of rubber-elasticity, the increase in the elastic modulus should be attributed to the increase in the number of elastically active network chains. This should be induced by the increase in the number of junction zones or cross-linking region. Whether coiled chains are transformed into helices and reeled into junction zones or the newly created helices are cross-linked by weak molecular forces such as hydrogen bonds still remain to be clarified.

There should be two coil-to-helix transition temperatures; one is lower than the sol-to-gel transition temperature, and the other is higher than that. Although helix-coil transitions in polymer solutions have been studied extensively, a helix-coil transition in a gel state has never been reported. The sharp change in the elasticity and in the specific ellipticity and the DSC peaks shown in Fig. 2 should be attributed to the lower temperature helix-coil transition. In this process, some elastically non-active coiled chains may change into elastically active helical chains incorporated in network structure.

A gel consists of liquid and a network. The majority of water in agarose gel has been reported to be in a state of the so-called free water (Ablett et al., 1978). Therefore, the mobility of long chain molecules is not so restricted, and long chain molecules can execute not only macrobrownian motion as in a rubber state but also change their conformation such as in helix-coil transition.

Watase and Nishinari (1982) reported the increase in the elastic modulus of cylindrically moulded κ-carrageenan gels immersed in alkali salt solution with the lapse

of time. As is widely accepted, the gelation mechanism of κ-carrageenan is very similar to that of gellan as described above. Cations are believed to shield the electrostatic repulsion of sulfate groups in κ-carrageenan molecules, and then they promote the formation and aggregation of helices, which leads to the increase in elastically active network chains via the increase in junction zones. They examined the concentration change in gels that are immersed in salt solutions. The concentration was found to increase. Then, they estimated the elastic modulus taking into account of the concentration change based on the power law dependence of the elastic modulus on the concentration. Since the increase of the storage Young's modulus of gels was far larger than the calculated value by a method mentioned above, they concluded that the change in the elastic modulus should be rather attributed to the structural change of network in the gel and not to the concentration change of the gel. They suggested that the structural change such as the strengthening of the network structure in a gel can occur even after the gel is formed. In the light of the experimental results described in the present paper, the rheological change found in 1982 should have the same origin as described in the present work.

3.1.4 Conclusion

The temperature dependence of the loss Young's modulus E'' for a 1.6% potassium type gellan gum gel which was cylindrically moulded showed a step-like change at 30ºC. The endothermic peak temperature in the heating DSC curve and the exothermic peak temperature in the cooling DSC curve appeared at the midpoint transition temperatures of the loss Young's modulus E'' and of the specific ellipticity at 202nm in circular dichroism. It is concluded that the helix-coil transition occurs at this temperature, while the cylindrical gel keeps the shape. This is the first clear experimental evidence for the helix-coil transition in an elastic gel, as far as the authors are aware.

3.2 THE SOL-GEL TRANSITION OF GELLAN AFFECTED BY THERMAL HISTORY

3.2.1 Introduction

Thermal history is one of factors to influence the gelation of gellan and , therefore, the properties of gellan gels. Effect of thermal history on properties of gellan gels, gelatin gels and agarose gels was studied previously. The three gels are similar in terms of thermo-reversibility and network formed by helices. The elastic modulus of gellan gels formed at a constant temperature reached a plateau value after a certain time and the plateau values decreased with decreasing temperature, in which the reason was not described (Nakamura et al., 1993). The elastic modulus of gelatin gels increased with time not reaching an equilibrium value even after 100hrs (Te Nijenhuis, 1981). The thermal stability of gelatin gels increased with increasing storage time at the temperature which is a little higher than gelation temperature (Michon et al., 1997). For agarose gels the effect of the storage temperature near the gelation temperature on rheological and structural properties has been studied and it was found to differ from the behaviour of gelatin gels. Formation of agarose network developed more slowly at higher storage temperatures and the elastic modulus of thus-formed gel became smaller (Aymard et al., 2001). Contrary to this result, Mohammed et al. (1998) reported that agarose gels showed larger elastic modulus and were more thermally stabilized by cooling more slowly.

The effect of cooling rate, storage temperature and storage time on gel properties of such polymers remain ambiguous nevertheless it is expected that thermal history gives universal effects among these polymers since their gels are the same from viewpoint of cold-setting thermoreversible gels being composed of helices. In the present study, the effect of thermal history on the gelation behaviour of gellan were studied using longitudinal and shear oscillation measurements.

3.2.2 Experimental

Gellan gum was the same as that used in Chapter 3.1.

Gellan gum powder was swollen in distilled water and stirred at 40°C overnight. The 1.6% (w/w) gellan dispersion prepared in this way was heated at 80°C for 2 hours and at 90°C for 10 minutes and then cooled at various cooling rates to obtain gels.

The storage and loss Young's moduli, E' and E'', were determined by the observation of longitudinal vibrations of cylindrically moulded gels. The apparatus used was a Rheolograph Gel (Toyo Seiki Seisakusyo Ltd., Japan). A teflon mould was used to obtain a gel cooled gradually to a certain temperature. A stainless steel mould was used to obtain a gel cooled at a constant cooling rate. Fig. 3.3 shows the programmed temperature-time course of the circulator on cooling and the experimental temperature-time course of samples in the stainless steel mould which was detected by a thermo-couple. The sample could be cooled at a rate of 1°C/min or 0.5°C/min almost precisely. When a hot solution was poured into the stainless steel mould which was kept in circulating water at 25°C, detected temperature of the sample was 70°C at first and then decreased to 25°C within 3min. In this case, the cooling rate was regarded as ~15°C/min. A cylindrical gel thus formed, 10mm diameter, 15mm length, was fixed in the rheological apparatus. Silicone oil was filled around the sample to control the temperature and to avoid the evaporation of water. The frequency and the amplitude were 3Hz and 100μm, respectively.

The storage and loss shear moduli, G' and G'', as a function of temperature were measured by a Rheostress (Haake, Germany). The 1.6% (w/w) gellan sample was poured into geometry at 70°C and then immediately covered with silicone oil to prevent the evaporation of water. The temperature was controlled by the HAAKE circulator DC30-K10 (Haake, Germany). The applied frequency and strain were 3Hz and 0.5-1% which is within a linear viscoelastic regime, respectively.

The falling ball test was performed to determine a temperature at which the stainless steel ball on the gels falls steeply into the gels on heating. The displacement of the

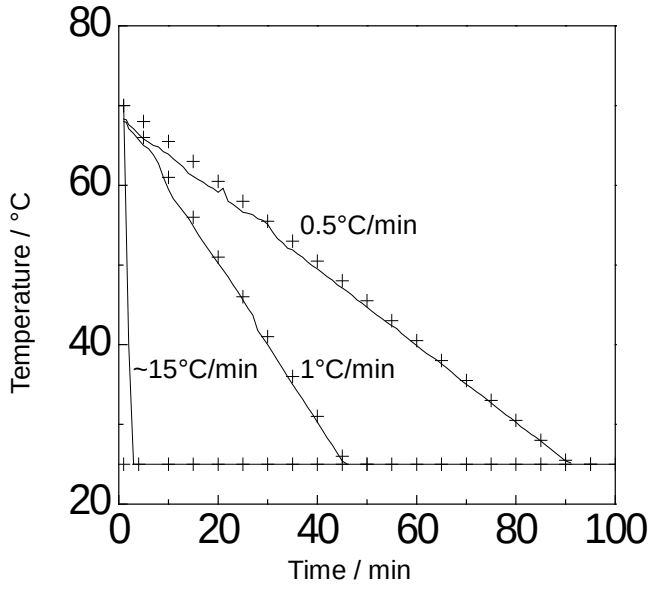

Figure 3.3 Temeprature of a circulator (+) and a sample (solid line) in cooling process from 70 to 25°C at various cooling rates.

ball on the gel was observed by a sliding microscope. A stainless steel ball (2mm diameter, 330μg) was set at the center of a bottom of a stainless steel mould and the solution was poured into the mould and cooled at different rates. The gel with the ball was taken out and put into a glass tube (diameter 11mm) so that the ball was at the top of the gel. The surface of the gel was covered with silicone oil to prevent the evaporation. The temperature was raised at a rate of ~0.8°C/min.

3.2.3 Results and discussion

Fig.3.4 shows temperature dependence of the storage Young's modulus E' of 1.6 wt % K-gellan gels formed at various cooling conditions. With decreasing storage temperature for gelation the elastic modulus of resultant gel decreased remarkably. K-gellan formed a gel by keeping at 40°C for 20hrs. E' of the gels kept at 5°C for 20hrs before measurements was about 100000 Pa at 25°C. Gel formation also occurred by keeping at 25°C for 3hrs. E' of the gels kept at 5°C for 20hrs before

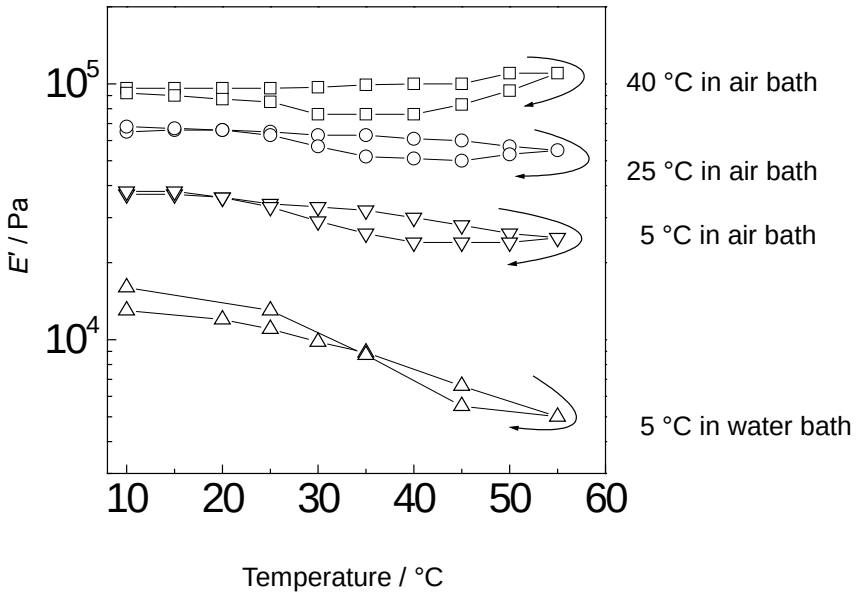

Figure 3.4 Temperature dependence of the storage Young's modulus *E′* of 1.6 wt % K-gellan gels formed at various cooling conditions. *E′* was measured at each temperature after being kept 15min on heating and on subsequent cooling at 3Hz.

measurements was about 70000 Pa at 25°C. When the storage temperature for gelation was 5°C, *E′* of the gels was about 30000 Pa at 25°C. Thermal stability of gels was also influenced by thermal history. *E′* of gels formed at storage temperature of 40°C increased slightly with increasing temperature in the temperature range from 10 to 55°C whereas *E′* of gels formed at storage temperature below 25°C decreased gradually with increasing temperature. This indicates that gels became stronger against heat with increasing storage temperature for gelation.

E′ of K-gellan gels obtained by being kept in water bath at 5°C was smaller than that of gels formed in air bath at 5°C. This indicates that cooling condition influenced strongly the elastic modulus of K-gellan gels. Fig.3.5 shows time dependence at 25°C of *E′* of 1.6 wt % K-gellan gels obtained at various cooling rates. *E′* decreased remarkably with increasing cooling rate. *E′* of gellan gels obtained at 0.5°C/min and 1°C/min was about 34000 Pa and about 24000 Pa, respectively. When the gellan sol

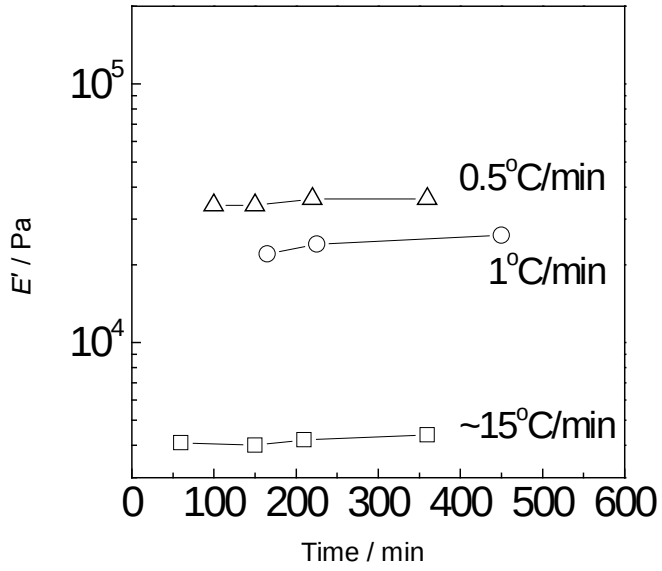

Figure 3.5 Time dependence of *E′* of 1.6 wt % K-gellan gels formed at various cooling rates. Freqency; 3Hz, temperature; 25°C.

was cooled rapidly (~15°C/min) *E′* of the resultant gel became about 4000 Pa at 25°C.

Fig. 3.6 shows the displacements of the ball on the gels as a function of temperature. The temperature at which the ball fell steeply was regarded as a gel-melting temperature Tm. Tm of the gel obtained at ~15°C/min, 1°C/min, and 0.5°C/min was 81.1°C, 87.6°C, and 96.6°C, respectively. Tm shifted to higher temperatures with decreasing cooling rate, indicating that the gel became heat resistant with decreasing cooling rate. From Fig.2-4, we confirmed that K-gellan gel formation is under kinetic control as observed for agarose gels and gelatin gels.

Fig. 3.7 shows temperature dependence of *E′* of 1.6 wt % K-gellan gels obtained at various cooling rates. Whether gels were further cooled to 5°C or not, *E′* of gels obtained at the same cooling rate was almost the same in the temperature range from 25 to 80°C. Time dependence of *E′* in Fig.3.5 showed that *E′* of each gel did not change with time dramatically once gel formation occurred above 25°C. In addition, heating the gels to ~60°C did not affect the elastic modulus of gels so much as shown

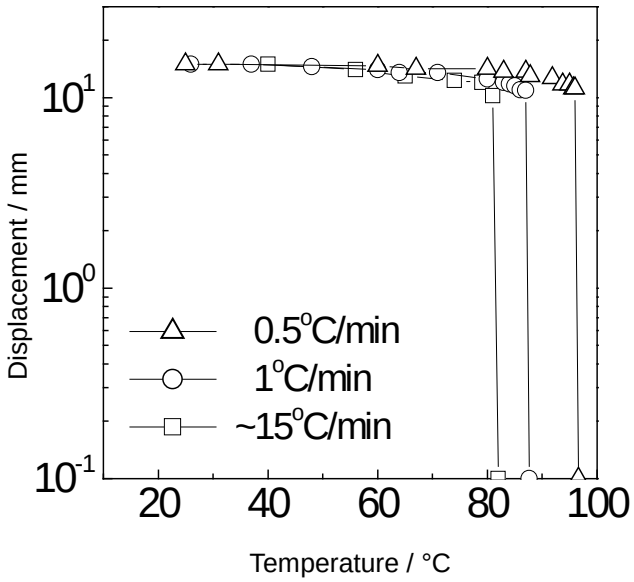

Figure 3.6 Results of falling ball tests of 1.6 wt % K-gellan gels formed at various cooling rates.

in Fig.3.4. From these results two thermal histories can be distinguished on the K-gellan. The one is thermal history during gelation which influences network formation strongly and the other is thermal history after gelation which is not significant for network of K-gellan.

To investigate effect of thermal history during gelation on the elastic modulus of gellan, shear oscillation measurement was carried out. Although shear deformation will be strongly influenced by slippage (Richardson and Goycoolea, 1994; Chronakis et al., 1996; Zhang et al., 2001), combination longitudinal and shear oscillation measurements may be useful to obtain further insight of effect of thermal history on gellan gels. It is necessary to check whether slippage cause serious damage to study a sol-gel transition of gellan before investigating the effect of thermal history on the elastic modulus of gellan gels.

Fig.3.8 shows temperature dependence of the storage shear modulus G' of 1.6 wt % gellan at cooling rate of 0.5°C/min. 1/3 E' of the gels formed at the same thermal

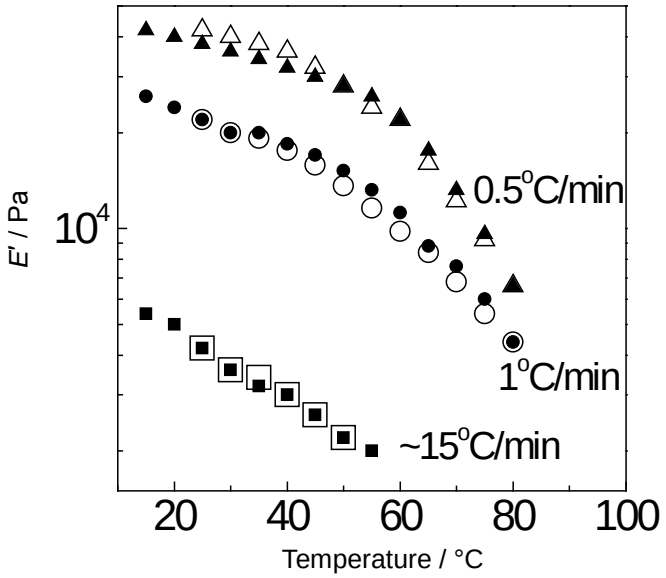

Figure 3.7 Temperature dependence on heating of E' of 1.6 wt % K-gellan gels formed at various cooling rates and then kept at 25°C (open) or kept at 5°C (closed) at 3Hz.

history was also shown for comparison. G' obtained in a serrated geometry and 1/3 E' showed almost the same temperature dependence on heating. The temperature at which G' decreased steeply was almost the same as Tm determined by falling ball test. G' obtained in the serrated geometry became almost 1/3 E' of gellan gels if thermal history of the gels was the same. G' obtained in smooth geometry was smaller than G' in serrated geometry. It was suggested that smaller values of the shear modulus were due to slippage as suggested in konjac glucomannan gelation (Zhang et al., 2001). The steep decrease of G' was observed around 45°C on heating in smooth geometry whereas such dramatic change was not observed in longitudinal oscillation tests and falling ball tests. This suggests that the slippage influences not only values of G' but also thermal behaviour for K-gellan gels. In the present study, to minimize the influence of slippage, the effect of thermal history during gelation on the elastic modulus of gellan was investigated using serrated geometry.

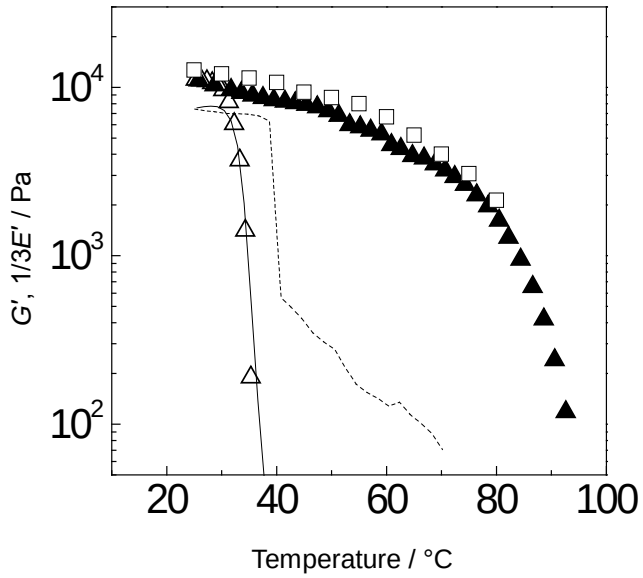

Figure 3.8 Temeprature dependence of the storage shear modulus G' of 1.6 wt % K-gellan on cooling (△; serrated geometry, solid line; smooth geometry) to 25°C and on subsequent heating (▲; serrated geometry, dashed line; smooth geometry) at 0.5°C/min and at 3Hz. 1/3 E' (□) of 1.6 wt % K-gellan gels formed at 0.5°C/min was also shown.

Fig. 3.9 shows time dependence of G' and G'' at various temperatures for gelation of 1.6 wt % K-gellan. Gelation proceeded at different rate where slower gel formation led to higher elastic modulus if the storage time was sufficient long. When the sample was cooled to 30°C at 0.5°C/min, gelation occurred around 35°C and G' at 30°C became almost constant in 5min. When the sample was cooled to 35°C at 0.5°C/min, gelation occurred at 35°C and proceeded with time. G' exceeded 10500 Pa, the plateau value obtained at 30°C, after 25min. The plateau value, about 20000Pa, was obtained at 35°C after about 400min. When the sample was kept at 40°C by cooling at 0.5°C/min gelation did not occur for ~10min first and then gelation occurred. G' increased more slowly with time and became larger than 10500Pa after 325min and continued to increase even after 2000min. G' was 23000Pa at 2000min.

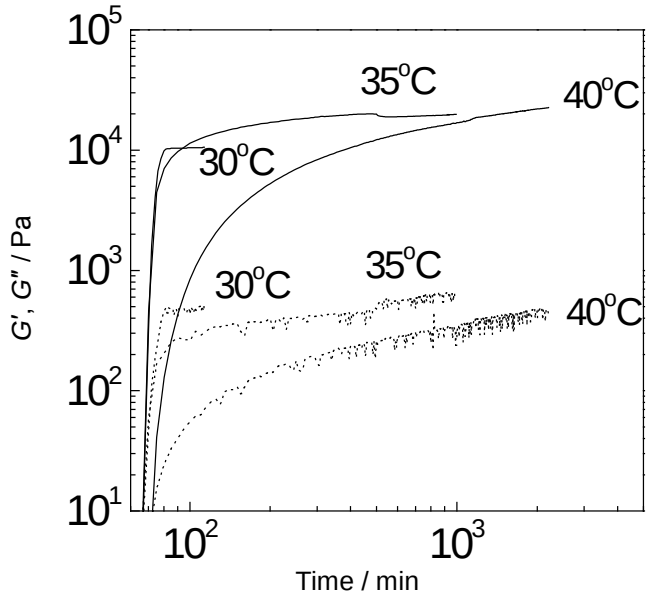

Figure 3.9 Time dependence of G' (solid line) and the loss shear modulus G'' (dotted line) of 1.6 wt % K-gellan which was cooled from 70 to 30, 35, 40°C at 0.5°C/min and kept at each temperature.

The falling ball test was performed for gels kept at 40°C or 35°C for 900min. Tm of the gellan gels kept at 40°C and 35°C, G' of which were 20000Pa and 17000Pa, respectively, was higher than 100°C. A lot of bubbles were observed in the gels above 100°C and we could not determine the temperature at which the ball fell from the top of the gels. As shown in Fig. 3.8, Tm of the gellan gels cooled to 30°C was ~95°C, indicating that gels formed at higher temperatures could show higher gel-melting temperature. This tendency did not conflict with that expected from results in Fig. 3.4.

It is believed that gel formation of K-gellan accompanies helix formation and aggregation of helices. When helix formation occurred at higher temperatures the helix length and degree of aggregation will be longer and larger since the energy to keep ordered structure would be higher at higher temperatures. The longer helix formation and/or larger aggregation should induce more thermally-stable network. As a result, gel melting temperature shifted to higher temperatures with increasing

storage temperatures as observed for gelatin gels. Higher Tm of gels formed at lower cooling rate might be interpreted in a similar manner since apparent gelation temperature shifts to higher temperature with decreasing cooling rate (data not shown). Agarose gels also showed higher thermal stability when the gels were formed at lower cooling rates.

In addition to temperature effects, kinetic effects should be taken into consideration on the properties of K-gellan gels. Lower E' and Tm of gels formed at higher cooling rate suggest that kinetic trapping might occur in helix formation and/or aggregation between helices by network formation. The network with a certain elastic modulus will prevent further ordered structure formation by restricting movement of gellan chains. Rapid gelation induces rapid network formation with a certain elastic modulus, which will prevent further ordered structure formation. Slow gelation induces a gradual network formation and will allow gellan to form further helices and aggregates in process of the network formation. Consequently the elastic modulus and Tm of gels formed at slower gelation rate became higher since the number and degree of helices and aggregates increased.

3.2.4 Conclusion

Effect of thermal history on the properties of K-gellan gels was investigated using dynamic viscoelastic measurements. K-gellan gel formation was controlled by kinetics of gelation as observed in gelation of agarose and gelatin. Higher values of the elastic modulus and the gel-melting temperature of gels induced by storage at higher temperatures or by lower cooling rates were thought to be due to longer helix formation and less kinetic trapping of helix formation and/or aggregation between helices by network formation.

Slippage effect was recognized by comparing the Young's modulus and the shear modulus of gellan gels formed at the same thermal histories. Gels inducing slippage might show not only lower shear modulus but also lower gel-melting temperature than

actual ones in shear rheological measurements.

4

The effect of surfactant, salt, and sugar on gelation and gel properties of gellan gum

4.1 THE EFFECT OF SDS ON THE GELATION OF GELLAN

4.1.1 Introduction

It has been considered that gel formation of most of helix-forming polysaccharides is induced by helix formation and aggregation between helices. The sol-gel transition of anionic polysaccharides, for instance κ-carrageenan and gellan, has been studied well in the presence of cations since cations promote their helix formation and aggregation strongly. When both helix formation and aggregation were promoted simultaneously, it is difficult to understand the role of helices and aggregates in the gels. Converting κ-carrageenan or gellan to tetramethylammonium (TMA) salts is a conventional method to minimize aggregation and study a helix-coil transition, in which bulky TMA ions do not allow the helices to aggregate (Robinson et al., 1980; Gunning and Morris, 1990). Another method to prevent aggregation of helices of κ-carrageenan is the addition of iodide ions. Grasdalen and Smidsröd (1981) reported that the gel formation of κ-carrageenan was prevented strongly by the addition of iodide ions whereas helix formation was promoted and hence it was concluded that iodide ions prevent aggregation between helices. Adding NaI to κ-carrageenan prevented the aggregation of helices and developed the interpretation of the role of helices and aggregates of

helices (Viebke et al., 1994; Ikeda and Nishinari, 2001; Ikeda et al., 2001).

As was done for κ-carrageenan, it is desirable to prepare a system in which helices exist without aggregates for elucidating gelation mechanism of gellan. If the additives have a large volume or they show some specific interaction with gellan, some of them could inhibit the aggregation of gellan molecules.

Sodium dodecyl sulfate (SDS) is a widely used surfactant and has a large anion. It is expected that the large anions minimize aggregation between helices. SDS forms micelles above the critical micelle concentration (~8mM) and this also might influence aggregation between helices. In addition, investigating viscoelastic properties of gellan in the presence of SDS is important not only as a study of polymer-surfactant interaction but also for applying gellan to cosmetic and pharmaceutical industries. In the present study, effect of SDS on the sol-gel transition of gellan was investigated using circular dichroism (CD), differential scanning calorimetry (DSC) and dynamic viscoelastic measurements.

4.1.2 Experimental

Gellan of potassium salt form (K-gellan) was the same as that used in Chapter 3.

The gellan powder was dispersed in distilled water and was stirred at 40°C overnight. The dispersion was heated at 80°C for 1hr and 90°C for 10min before an appropriate amount of SDS was added and then poured into instruments at 70°C.

SDS of reagent grade was purchased from Sigma Aldrich Japan Ltd. (Japan).

Rheostress1 was kindly lent to us by Haake Ltd. (Germany) and used to measure the storage and loss shear modulus G' and G''. A double gap cylinder was used and a serrated cylinder was used only when fatal artifacts were observed probably due to slippage (Zhang et al., 2001).

Jasco-820 spectropolarimeter of Nihon Bunko Ltd. (Japan) was used to measure the ellipticity at 202nm using a cell, the path length of which was 0.2cm.

4.1.3 Results and discussion

Fig. 4.1 shows temperature dependence of the ellipticity at 202nm, θ_{202}, obtained in CD measurements for the gellan with or without added SDS. θ_{202} decreased steeply at a characteristic temperature on cooling, which reflects coil-to-helix transition of gellan (Crescenzi et al., 1986; Matsukawa et al.,1999).

T_m, the temperature at the maximum of $d\theta_{202}/dT$ (data not shown), shifted to higher temperatures by addition of SDS, suggesting that helices were more thermally stabilized by addition of SDS. This tendency was observed in DSC cooling curves in which helix formation can be detected as an exothermic peak. Fig. 4.1 (b) shows cooling DSC curves of the gellan with or without SDS. The broad exothermic peak was observed around 35°C for the gellan sample in the absence of SDS. The broadness of the peak was due to containing various cations in the present sample (Watase and Nishinari, 1993). By addition of SDS the single sharp peak appeared and shifted to higher temperatures. T_m obtained in CD measurements agreed well with DSC peak temperatures. DSC results also suggested that helices were stabilized thermally by addition of SDS. Sharp peak was observed and DSC peaks shifted to higher temperatures previously by addition of salts such as NaCl (Miyoshi and Nishinari, 1999), suggesting that effect of SDS on helix formation is similar to that of salts, i.e. cations promoted helix formation by shielding electrostatic repulsion between anionic polysaccharides.

Fig. 4.2 shows temperature dependence of the shear storage modulus G' of 1.6% (w/w) K-gellan solutions and 1.6% (w/w) K-gellan with SDS. Since addition of SDS above 0.2mol·kg^{-1} caused phase separation measurements were performed below 0.2mol·kg^{-1} SDS. Gellan sample at this concentration formed strong gels with high elastic modulus. G' increased rapidly around 35°C on cooling and became 11000 Pa at 20°C. This indicates that gelation occurred around 35°C. On subsequent heating G' decreased gradually first and then decreased rapidly around 90°C, indicating that gel melting might occur around 90°C. This large thermal hysteresis on cooling and on

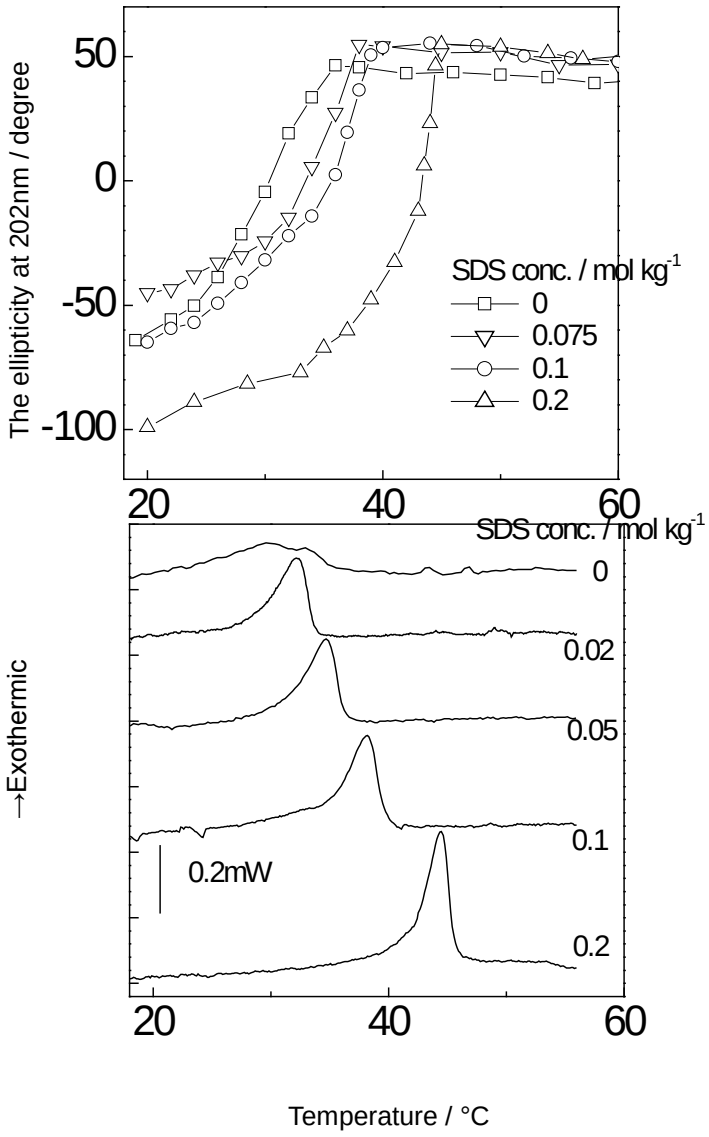

Figure 4.1(a) Temperaure dependence of the ellipticity at 202nm θ_{202} and (b) DSC curves on cooling of 1.6% (w/w) K-gellan with or without added SDS.

heating is a characteristic feature of true gels like agarose gels and it is considered that this thermal hysteresis was due to thermally stabilized network by aggregation between helices (Clark and Ross-Murphy, 1987). By addition of SDS up to certain amount a strong gel changed to a weak gel. By addition of relatively small amount of SDS G' decreased remarkably and the degree of thermal hysteresis was lowered as shown in Fig. 4.2 (a). In the presence of 0.02mol·kg^{-1}SDS, G' became the order of 10 Pa and the thermal hysteresis was negligible. This suggests that three-dimensional network

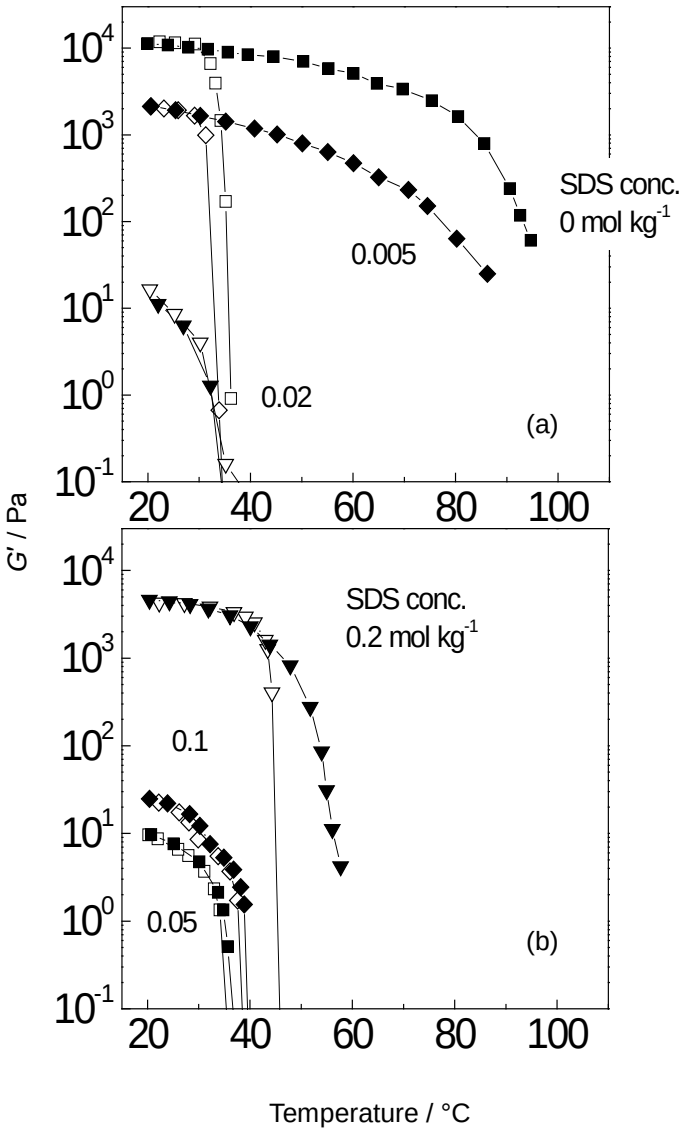

Figure 4.2 (a) (b) Temperature dependence of *G′* of 1.6% (w/w) K-gellan with or without added SDS on cooling (open) and on subsequent heating (closed) at 0.5°C/min. Frequency; 1rad/s, strain; 0.5%.

formation and aggregation between helices were prevented by addition of 0.02mol·kg^{-1}SDS. The small *G′* and negligible thermal hysteresis were obtained by addition of 0.02mol·kg^{-1}, 0.05mol·kg^{-1}, and 0.1mol·kg^{-1}SDS in the present study.

In the presence of relatively large amount of SDS as shown in Fig. 4.2 (b), *G′* increased with increasing concentration of SDS and strong gel was obtained in the presence of 0.2mol·kg^{-1} SDS. *G′* became 4500 Pa at 20°C and thermal hysteresis was

observed. This suggests that a large amount of SDS induced network formation and aggregation between helices. As shown in Fig. 4.1, DSC and CD results suggested that SDS stabilized helices of K-gellan thermally. If SDS stabilizes gellan helices, it is understandable for SDS to promote gel formation and aggregation. However, the value of G' and the degree of thermal hysteresis of gellan gels with SDS, at any SDS concentration, was lower than those of the gellan gels in the absence of SDS. Thus the viscoelastic behaviour of K-gellan in the presence of SDS could not be interpreted without involving effect of anions in SDS. This indicates that the anionic surfactant affects gel formation of the anionic polysaccharide.

Frequency dependence of G' and G'' showed that the gellan gels changed to weak gel and viscoelastic fluid by addition of 0.02-0.1mol·kg^{-1}SDS as shown in Fig. 4.3. G' and G'' of the gellan sample without SDS and with 0.01mol·kg^{-1} SDS showed "true gel" type behaviour in which G' and G'' were almost independent of frequency and G' was 10 times larger than G''. G' and G'' of the gellan sample with 0.02mol·kg^{-1} SDS showed "weak gel" type behaviour in which G' and G'' slightly depend on frequency keeping $G' > G''$ in the frequency range observed. G' and G'' of the gellan sample with 0.05mol·kg^{-1} SDS showed "semi-dilute solution" type behaviour in which $G' < G''$ at lower frequencies and $G' > G''$ at higher frequencies. G' and G'' of the gellan sample with 0.1mol·kg^{-1} and 0.2mol·kg^{-1} SDS showed "weak gel" type behaviour and "true gel" type behaviour, respectively. When "weak gel" or "semi-dilute solution" type behaviour was observed, the thermal hysteresis on cooling and on heating was not observed. These tendencies were recognized in κ-carrageenan and NaI systems in which I^- prevents gel formation by preventing aggregation between helices. κ-carrageenan/NaI system formed network that flowed by applying large deformation. In addition, after large deformation this system showed gel like behaviour again.

Fig. 4.4 shows G' and G'' of the gellan sample with 0.1mol·kg^{-1} SDS as a function of strain at 20°C. At small deformation G' was larger than G'' and frequency dependence of G' and G'' showed a "weak gel" type behaviour. After large deformation

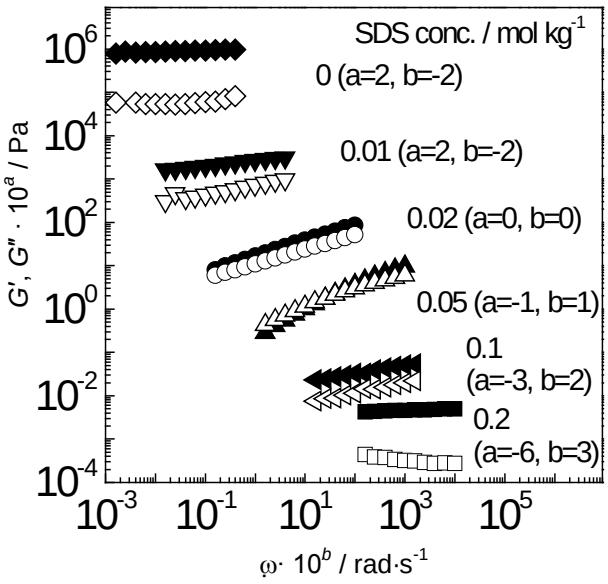

Figure 4.3 Frequency dependence of G' (closed) and G'' (open) of 1.6% (w/w) K-gellan with or without SDS at 20°C. The data are shifted along the vertical and horizontal axes by shift factor a and b, respectively, to avoid overlapping. Strain; 0.5%.

measurements the same experiment was repeated. A similar tendency, $G' > G''$ at a small deformation range, was observed in the second- and the third-run. As suggested previously for non-aggregated helices of κ-carrageenan in the presence of NaI, the network of K-gellan with 0.1mol·kg^{-1} SDS is not permanent but capable of flowing (Ikeda and Nishinari, 2001). This indicates that this K-gellan network in the presence of SDS is similar to that of κ-carrageenan in the presence of NaI.

As suggested in the case of κ-carrageenan/NaI, SDS might prevent gel formation of K-gellan by preventing aggregation since it did not prevent helix formation judging from CD and DSC results. This effect can be achieved if bulky anions in SDS exist around gellan helices by some interactions (e.g. hydrophobic interaction) and do not allow gellan helices to aggregate. However excessive amount of SDS induced strong gel with thermal hysteresis which was not observed in κ-carrageenan/NaI. It is known

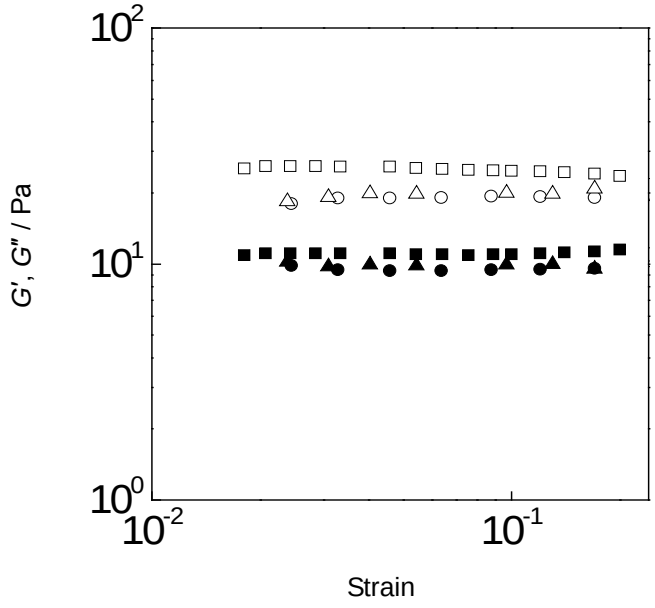

Figure 4.4 *G′* (open) and *G″* (closed) as a function of strain of 1.6% (w/w) the K-gellan gels in 0.1mol/kg SDS at 20°C. The first (square), the second (triangle) and the third (circle) run were shown. Frequency; 1rad/s.

that addition of cations and sugars promotes gel formation of gellan up to certain amount and excessive amount of cations and sugars decreased the elastic modulus (Moritaka et al., 1991; Sworn, 2000). The mechanism of gel formation in the presence of excessive amount of such substances has not been understood well. It is considered that “over conversion” of gellan occurs (Sworn, 2000). It should be further studied using gellan of sodium salt form that shows single sharp peak in DSC curves so that we can neglect effects of other cations in gellan except for Na^+.

In summary, it was found that SDS, anionic surfactant, affects properties of K-gellan, anionic polysaccharide, strongly. Helix formation of K-gellan was promoted by addtion of SDS, probably due to cations in SDS whereas gel formation of K-gellan was prevented by addition of SDS, which could not be explained without involving effect of anions in SDS. Viscoelastic fluids and weak gels of K-gellan induced by addition of SDS showed similar behaviour against thermal history and large deformation to those of κ carrageenan induced by addition of NaI in which NaI prevents aggregation between

helices and promotes helix formation of κ carrageenan.

4.1.4 Conclusion

Effect of sodium dodecyl sulfate (SDS) on the sol-gel transition of potassium type gellan (K-gellan) was investigated by circular dichroism (CD), differential scanning calorimetry (DSC) and dynamic viscoelastic measurements. CD and DSC results showed that SDS stabilized helices thermally as observed in the case of addition of salts to gellan. The addition of SDS lowered the storage modulus of the gellan gels and thermal hysteresis became less pronounced, which was not observed in gellan in the presence of salts. It was suggested that gel formation of K-gellan was prevented by anions in SDS, i.e. the anionic surfactant affects properties of the anionic polysaccharide.

4.2 THE EFFECT OF THE IMMERSION INTO SALT SOLUTION ON GEL PROPERTIES OF GELLAN

4.2.1 Introduction

In Chapter 3 it was shown that helix-coil transition occurred in gellan gels while the cylindrical gel keeps the shape, which was monitored from rheological, DSC and CD measurements. Since transition of all of helices into coil should induce gel melting, it was considered that gellan helices can change into coils partially.

κ–carrageenan, a helix-forming anionic polysaccharide like gellan, also showed similar behaviour in κ–carrageenan gels. Watase and Nishinari reported the increase in the elastic modulus of cylindrically moulded κ-carrageenan gels immersed in alkali salt solution with the lapse of time in 1982. Cations are believed to shield the electrostatic repulsion of sulfate groups in κ-carrageenan molecules, and then they promote the formation and aggregation of helices, which leads to the increase in rigidity of network. They examined the concentration change in gels that are immersed in salt solutions. The concentration was found to increase. Then, they estimated the elastic modulus taking into account of the concentration change based on the power law dependence of the elastic modulus on the concentration. Since the increase of the storage Young's modulus of gels was far larger than the calculated value by a method mentioned above, they concluded that the change in the elastic modulus should be rather attributed to the structural change of network in the gel, not just to the concentration change of the gel. They suggested that the structural change such as the strengthening of the network structure in a gel can occur even after the gel is formed.

It is expected that gellan gels is also influenced by the immersion into salt solutions and that conformational change in gellan gels occurs by the immersion. In food processing, the immersion of gels into salt solution is common processing especially in Japan. It is worth to understand the effect of the immersion into salt solution on the

gel properties not only from scientific point of view but also from industrial point of view. In the present study, gel properties of gellan immersed in salt solutions were investigated.

4.2.2 Experimental

Gellan gum used in the present study was the potassium form deacylated gellan gum, the same as that used in Chapter 3.

Gellan gum was swollen in distilled water at 40℃ for 20 hours and then heated at 90℃ for 1 hour to dissolve completely. Hot solutions were poured into teflon cylindrical (20mm diameter, 30mm height) moulds, and then the temperature was lowered to a room temperature and then kept at 5℃ for 20 hours.

The complex Young's modulus of a cylindrically moulded gel was determined by the observation of longitudinal vibrations, from the amplitude ratio and the phase difference of the stress and strain using Rheolograph Gel (Toyo Seiki Seisakusho Ltd., Tokyo). The gel is immersed in salt solution at 25℃. The frequency is fixed as 3Hz and the amplitude was also fixed as 100 μm (strain 0.03) for this apparatus.

The specific ellipticity in CD was measured by JASCO-820A spectropolarimeter (Jasco, Tokyo).

The falling ball test was performed to determine a temperature at which the stainless steel ball on the gels falls steeply into the gels on heating as described in Chapter 3.2.

4.2.3 Results and discussion

Fig. 4.5 shows time dependence of the storage Young's modulus E' of 1.5% gellan gels with or without the immersion into NaCl solutions. E' kept constant with time when the gel was not immersed in NaCl solutions. When the gel was immersed in 0.01 and 0.1 NaCl solutions, E' increased with time during immersion and reached a saturated value at a certain time. At 1M NaCl solutions E' increased rapidly and

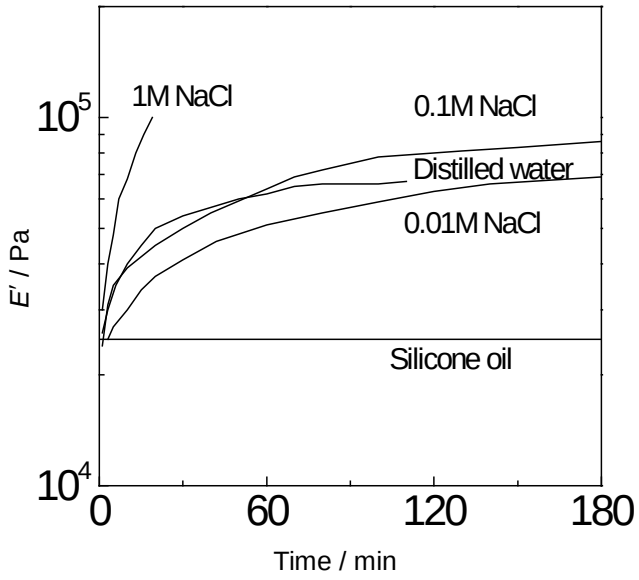

Figure 4.5 Time dependence of the storage Young's modulus E' of 1.5% gellan gels with or without the immersion into NaCl solutions. Temperature, 25°C. Frequency, 3Hz.

reached higher value than the limited value of the instrument and thus a saturated value was not observed. E' increased at all NaCl concentrations measured as observed for κ-carrageenan gels (Watase and Nishinari, 1982). Interestingly, E' also increased by immersion into distilled water.

Immersion might change gellan concentration in gels by changing amount of water in gels. Generally increase of gellan concentration increases the elastic modulus of gels. In order to check whether the increase of E' was due to an increase of gellan concentration in gels, the volume of gels was measured before and after immersion into NaCl solutions. Table 4.1 shows the changes in volume of 1.5% gellan gels before and after immersion of NaCl solutions. After immersion for 120min, the volume increased rather than decreased at 0.01 and 0.1M NaCl solutions, indicating that gellan concentration decreased. At 1M NaCl solution, although the increase of E' during the immersion was most remarkable, the change in volume of gellan gels was negligible. This indicated that change in volume had little effect on the increase of E'

Table 4.1 Changes in volume of 1.5% gellan gels before and after immersion into NaCl solutions.

	0M NaCl	0.01M NaCl	0.1M NaCl	1M NaCl
0min	10ml	10ml	10ml	10ml
120min	13ml	12ml	11ml	10ml

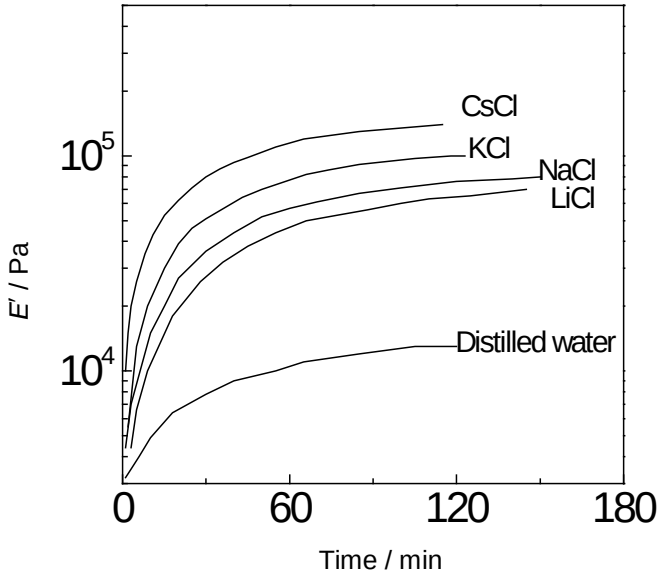

Figure 4.6 Time dependence of E' of 1% gellan gels immersed into 1M salt solutions. E' of 1% gellan gels immersed into distilled water was also shown. Temperature, 25ºC. Frequency, 3Hz.

induced by the immersion in 1M NaCl in the present study and it was suggested that the enhancement of rigidity of gel network during immersion was due to structural change of gellan rather than concentration change of gellan.

In other cases, especially in the immersion in distilled water, change in volume was not negligible. However, the volume increased by the immersion, indicating that gellan concentration of gel decreased by the immersion. The increase of E' by the

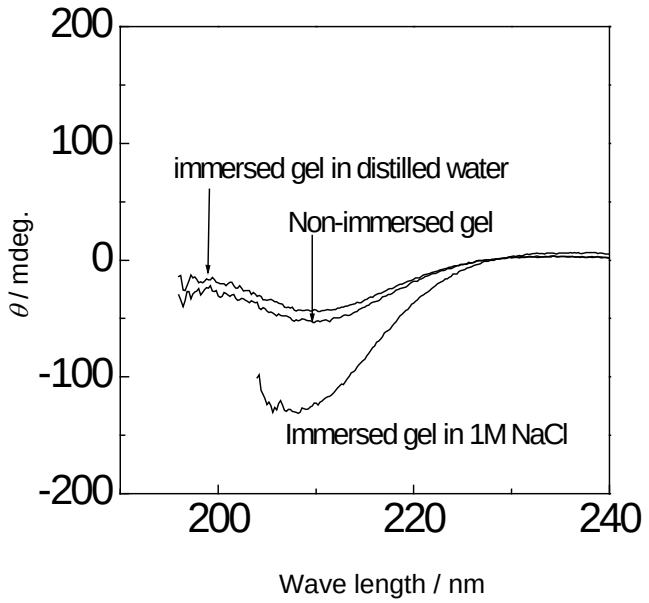

Figure 4.7 Circular dichroism (CD) spectra of the ellipticity θ of 1% gellan gels before and after 10min immersion into 1M NaCl solutions. Temperature, 25ºC.

swelling might be also due to structural change of gellan in gels.

Fig. 4.6 shows time dependence of E' of 1% gellan gels immersed into various salt solutions. At any salt solutions E' increased with time during immersion and reached a saturated value after a certain time. The saturated value increased in order of CsCl, KCl, NaCl, and LiCl. This was the same order of effectiveness for helix formationand aggregation of helices in gellan solutions. Gel formation was also enhanced in order of CsCl, KCl, NaCl, and LiCl. The role of cations on the gelation was considered as the enhancement of the helix formation of gellan by shielding electrostatic repulsion. We think that, in the case of the present study, cation in salt solution enhanced the helix formation of gellan in gels and increased the elastic modulus.

The helix formation of gellan can be investigated by circular dichroism (CD). Fig. 4.7 shows CD spectra of 1% gellan gels before and after immersion into 1M NaCl solution. It is known that helix formation of gellan decreases the ellipticity around

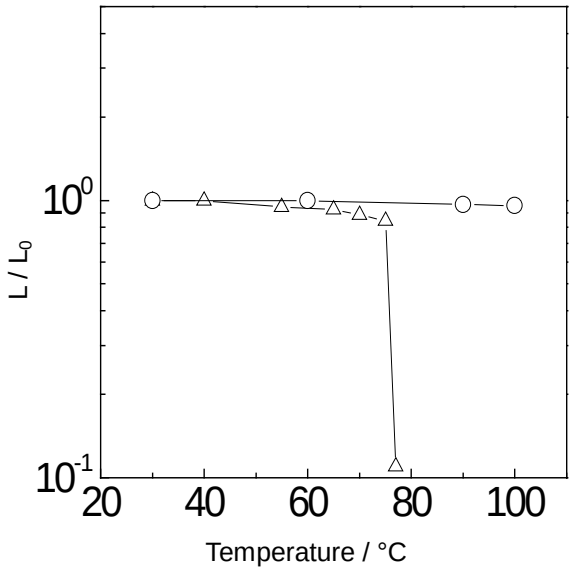

Figure 4.8 Results of falling ball tests of 1 wt % K-gellan gels before (triangle) and after (circle) immersion into 1M NaCl solutions. L; the displacement of the stainless steel ball, L_0; the initial displacement of the stainless steel ball.

200nm toward the negative value (Crescenzi et al., 1986). Since gellan gel has already a certain amount of helices, the ellipticity around 200nm was already negative values before immersion. After immersion the ellipticity around 200nm decreased, indicating that the amount of helices increased. Immersion in distilled water did not change the shape of spectra. CD results showed that further helix formation occurred in gellan gels by the immersion in NaCl solutions.

The results above indicate that the helix formation in a gel can occur even after the gel is formed. Similar behavior was observed in a previous study by changing temperature of gellan gels. It was concluded that helix-coil transition can occur in gellan gels (Nishinari et al., 2000). This implied that gellan exists at both disordered chains and helices in gels. In respond to environmental change, a certain amount of disordered chains may change into helices and vise versa maintaining gel shape.

Although gel structure has not been understood well in detail, it is believed that

lateral aggregation of gellan helices is prerequisite for strong gel network. Combining CD results, the increase in E' by immersion into salt solution can be interpreted as follows; cation in salt solution penetrated into gellan gels and induced transition of some disordered parts of gellan chains into helices. These helices reinforced gel network by aggregating laterally.

Lateral aggregation enhances thermal stability of gel network. Fig. 4.8 shows the result of a falling ball test of 1% gellan gels with or without immersion of NaCl solutions. The gel was immersed in 1M NaCl for 10 min. The gel melting temperature, T_m, which was determined as the temperature at which a stainless ball fell into gels, was around 80 ºC for non-immersed gellan gels whereas T_m could not be determined for immersed gellan gels because of high thermal stability resulting in the support of the gel shape even at higher than 100 ºC where a lot of bubbles existed in the gels. This supported that immersion into NaCl solution induced further lateral aggregation of gellan helices.

4.2.4 Conclusion

Further helix formation occurred in gellan gels by immersion of gels into salt solutions. This induced the increment of the rigidity and thermal stability of gellan gels. Further helix formation may enhance lateral aggregation of gellan helices, resulting in the increase of the elastic modulus and the gel melting temperature.

4.3 THE EFFECT OF SUGARS ON GEL PROPERTIES OF GELLAN

4.3.1 Introduction

Large deformation properties are important for foods since mastication and swallowing, two indispensable processes during eating, generally induce large deformation. As far as solid-like foods are concerned, fracture behavior has been studied to characterize large deformation properties of such foods. Recently, Bot et al. (1996a, 1996b) applied the BST equation (Blatz et al., 1974) to the fracture behavior of gelatin gels and they succeeded in fitting a stress-strain curve using parameter *n* which reflects the elastic properties of the system. Nagano et al. also used the BST equation to analyze the fracture behavior of egg (Nagano and Nishinari, 2001), and soybean (Nagano et al., 2003) protein gels. This equation has not been applied to polysaccharide gels yet although it is worth to estimate the parameter *n* of polysaccharide gels. The aim of this study is to apply the BST equation to the stress-strain curve of polysaccharide gels, especially to gellan gum gels.

4.3.2 Experimental

Gellan gum (lot. 6258A), the same sample in Chapter 3, was dispersed into distilled water under stirring and heated to obtain the homogenous solution. The solution was poured to a teflon mould and cooled to obtain cylindrical gels (20mm diameter, 20mm length). For gellan gels containing sugar, sucrose was added into the hot gellan solutions. Compression test was carried out using a Rheoner RE-3305 (Yamaden Co. Ltd.) with a compression speed of 0.5mm/s at room temperature.

In the simple compression of an incompressibile material, a unit cube deforms to a block with edges $1/\lambda^2$ in the direction of compression and λ in the perpendicular directions ($\lambda>1$) where λ is the stretch ratio, the measure for deformation.

The compression data were analyzed using the BST equation for simple compression.

$$\sigma_t = \frac{2E}{3n}(\lambda^n - \lambda^{-2n}) \tag{4.1}$$

Here σ_t and E is the true stress and the Young's modulus, respectively. n is the elasticity parameter which characterizes the non-linear elastic behavior at large deformations. Incompressibility is assumed in this equation. The true stress was calculated as follows;

$$\sigma_t = \frac{F}{A_0}(1 - \frac{\Delta L}{L_0}) \tag{4.2}$$

Where F is the force, L_0 is the initial length of the sample, ΔL is the change in length and A_0 is the initial sample area. The stretch ratio λ was calculated as follows;

$$1 - \frac{1}{\lambda^2} = \frac{\Delta L}{L_0} \tag{4.3}$$

$$\lambda = \sqrt{\frac{L_0}{L_0 - \Delta L}} \tag{4.4}$$

4.3.3 Results and discussion

The BST equation is the phenomenological equation for characterizing rubber-like materials. Since deformation of ideal rubber satisfies Eq. (4.1) with n = 2, this parameter can be regarded as a measure of the deviation from ideal behavior (McEvoy et al., 1985; Treloar, 1958).

Figure 4.9 shows stress-strain curves of gellan gum gels with or without sucrose. Stress-strain curves of gellan gum gels could not be fitted by this equation. This suggests that the network structure of gellan is far from rubber-like structure. On the other hand, we succeeded in fitting stress-strain data of gellan gum gels containing

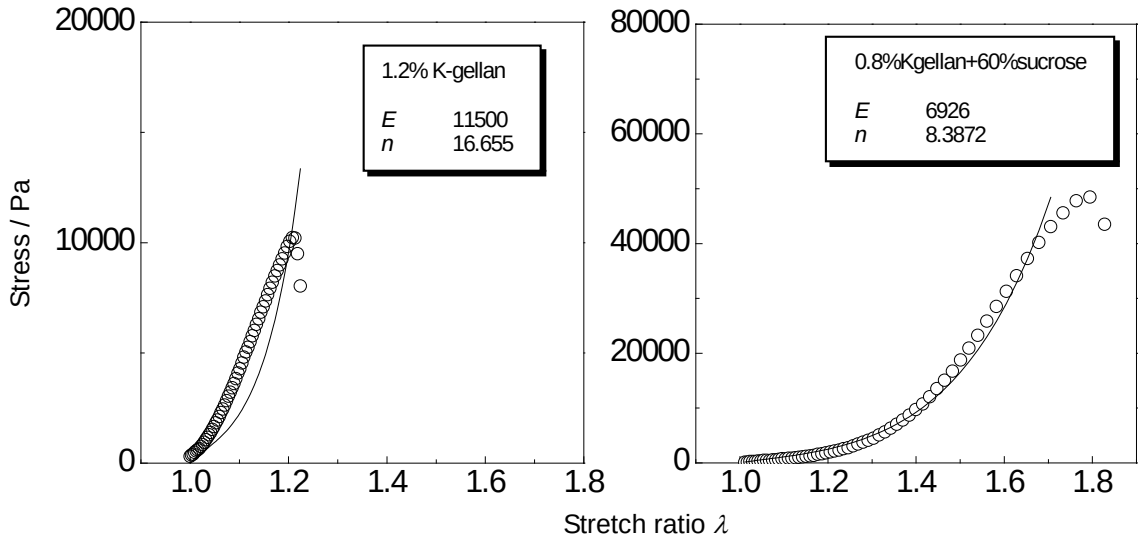

Figure 4.9 Stress-strain curves (circle) of gellan gum gels with or without sucrose and the corresponding fitting curves (solid line) obtained from Eq. (4.1).

much amount of sugar. The network structure might turn to be rubber-like by addition of high amount of sugar.

The value of *n* was in the range from 2 to 6 for gelatin gels at different gelatin concentration, aging time, aging temperature, pH, NaCl and $CaCl_2$ concentrations, whey protein concentration, the amount of pre-shearing and strain rate (Bot et al., 1996b). Nagano and Nishinari (2003) studied *n* of egg white gels by changing egg white concentration, heating time, heating temperature and compression speed. They reported that *n* ranged from 3 to 6. Nagano et al. (2003) also estimated *n* of soybean curd (tofu) in the range from 5 to 7. The value of *n* was larger than 8 for gellan gels in the presence of high amount sugar. This indicates that the deformation behavior of gellan gels in this study deviates from ideal behavior more widely than that of gelatin gels, egg white gels, and soybean curd.

4.3.4 Conclusion

The BST equation was applied to analyze fracture behaviors of gellan gum gels. The equation failed in fitting stress-strain curves of gellan gum gels. However it was possible to apply this equation to non-linear elastic behavior of gellan gum gels containing high amount of sugar. This supports that the network of gellan has a rubber-like character in the presence of high amount of sugar.

Appendix 1

Ideal rubber

The ideal rubber consists of the randomly-jointed polymer chain. The chain has n segments of equal length a. Let us consider the one dimensional arrangement of the chain. The direction of any segments is entirely random and bears no relation to the direction of any other link in the chain. Let n_+ be a number of a segment to the right and n_- be a number of a segment to the left. The end-to-end distance x for the chains is

$$x = (n_+ - n_-)a \tag{A.1}$$

The term

$$P = \frac{n!}{n_+!n_-!}\left(\frac{1}{2}\right)^n \tag{A.2}$$

gives probability that n_+ segments are to the right and n_- segments are to the left.

Since $n_+ + n_- = n$, n_+ and n_- are written as

$$n_+ = \frac{na + x}{2a}, \quad n_- = \frac{na - x}{2a} \tag{A.3}$$

P can be regarded as a function of x.

For large n, P can be approximated by continuous function of x and we may use Stirling's approximation

$$\ln n! = n\ln n - n + o(n) \qquad \text{(A.4)}$$

$$\lim_{n\to\infty} o(n)/n = 0$$

Using this formula, we get $\ln P = n\ln n - n_+ \ln n_+ - n_- \ln n_- - n\ln 2$.

From Eq. (A.3),

$$\ln n_\pm = \ln\frac{n}{2}\frac{na \pm x}{na} = \ln\frac{n}{2} + \ln\left(1 \pm \frac{x}{na}\right) \qquad \text{(A.5)}$$

$x/na \ll 1$ and expansion ($\ln(1\pm x) = \pm x - x^2/2 \pm x^3/3 - \cdots$) gives

$$\ln n_\pm = \ln\frac{n}{2} \pm \frac{x}{na} - \frac{1}{2}\left(\frac{x}{na}\right)^2 \pm \cdots \qquad \text{(A.6)}$$

We assume that the higher term in Eq. (A.6) can be neglected. Hence

$$n_+ \ln n_+ + n_- \ln n_- = (n_+ + n_-)\ln n - (n_+ + n_-)\ln 2 + (n_+ - n_-)\frac{x}{na} - (n_+ + n_-)\frac{x^2}{2n^2a^2}$$

$$= n\ln n - n\ln 2 + \frac{x}{a}\frac{x}{na} - n\frac{x^2}{2n^2a^2}$$

$$= n\ln n - n\ln 2 + \frac{x^2}{2na^2} \qquad \text{(A.7)}$$

$$\ln P = n\ln n - (n_+ \ln n_+ + n_- \ln n_-) - n\ln 2$$

$$= -\frac{x^2}{2na^2} = \ln e^{-\frac{x^2}{2na^2}} \qquad \text{(A.8)}$$

From Eq. (A.8) we obtain

$$P = Ae^{\frac{-x^2}{2na^2}} \quad (A = 1) \qquad \text{(A.9)}$$

Since we used the simple form of Stirling's approximation (Eq. (A.4)), $A = 1$. Instead, if we use more accurate form of Stirling's approximation, $A \neq 1$. Normalization gives $A = 1/\sqrt{2n\pi a^2}$ (see Appendix2). Then we find the standard form of the Gaussian distribution

$$p(x) = \frac{1}{\sqrt{2n\pi a^2}} e^{\frac{-x^2}{2na^2}} \qquad \text{(A.10)}$$

which satisfies

$$\int_{-\infty}^{\infty} p(x)dx = 1 \tag{A.11}$$

where $p(x)$ is probability density. The maximum of $p(x)$ is obtained at $x=0$ and $p(x)$ decreases steeply with increasing x.

The mean value of x is

$$\bar{x} = \int x p(x)dx = 0 \tag{A.12}$$

The mean square value of x is

$$\overline{x^2} = \int x^2 p(x)dx = na^2 \qquad \text{(see Appendix 2)} \tag{A.13}$$

This indicates that the average size of the end-to-end distance of a chain is proportional to the square-root of the number of segments. $\sqrt{\overline{x^2}} = \sqrt{n}a$ is far smaller than $x_{\max} = na$.

For the three dimensional arrangement of polymer chain, $p(x, y, z)dxdydz$ gives the probability that the components of the vector $\vec{r}(x, y, z)$ representing the end-to-end distance for the chain lie within the intervals x to $x+dx$, y to $y+dy$, and z to $z+dz$, respectively. We assume that the propability that the chain has a particular component of length in the x direction is completely independent of its components of length in the y and z directions. If $x \ll na$, $y \ll na$, and $z \ll na$, using the number of a segment $n/3$ for each direction,

$$p(x, y, z)dxdydz = \frac{\sqrt{3}}{\sqrt{2n\pi a^2}} e^{\frac{-3x^2}{2na^2}} dx \times \frac{\sqrt{3}}{\sqrt{2n\pi a^2}} e^{\frac{-3x^2}{2na^2}} dy \times \frac{\sqrt{3}}{\sqrt{2n\pi a^2}} e^{\frac{-3x^2}{2na^2}} dz$$

$$= \left(\frac{3}{2\pi na^2}\right)^{3/2} e^{-\frac{3\left(x^2+y^2+z^2\right)}{2na^2}} dxdydz \tag{A.14}$$

Since $r^2 = x^2+y^2+z^2$,

$$p(r) = \left(\frac{3}{2\pi na^2}\right)^{3/2} e^{-\frac{3r^2}{2na^2}} \tag{A.15}$$

A factor of $4\pi r^2 dr$ is needed to consider a differensial spherical surface. The

three-dimensional probability is

$$P(r)dr = 4\pi r^2 \left(\frac{3}{2\pi na^2}\right)^{3/2} e^{-\frac{3r^2}{2na^2}} dr \qquad \text{(A.16)}$$

The mean value of *r* is

$$\bar{r} = \int_0^\infty rP(r)dr = 0 \qquad \text{(A.17)}$$

The mean square value of *r* is

$$\overline{r^2} = \int_0^\infty r^2 P(r)dr = na^2 \qquad \text{(see Appendix 2)} \qquad \text{(A.18)}$$

This indicates that the average size of the end-to-end distance of a chain in the three dimensions, as well as that in the one dimension, is proportional to the square-root of the number of segments.

The ideal rubber is based on the following assumption.

1) The junction points between chains move on deformation as if they were embedded in an elastic continuum. As a result the components of length of each chain change in the same ratio as the corresponding dimensions of the bulk rubber.
2) The network contains *N* chains per unit volume, a chain being defined as the segment of molecule between successive points of cross-linkage.
3) The mean-square end-to-end distance for the whole assembly of chains in the unstrained state is the same as for a corresponding set of free chains, and is given by the Ep. (A.18)
4) There is no change of volume on deformation.
5) The entropy of the network is the sum of the entropies of the individual chains, the latter being given by

$$s = k \ln p(r) = const - \frac{3kr^2}{2na^2} \qquad \text{(A.19)}$$

where *k* is Boltzmann constant.

Appendix 2

Gauss integral

The basic Gaussian function has the form

$$G(x) = \exp(-\lambda x^2) \tag{A.20}$$

Let

$$I_0 = \int_{-\infty}^{\infty} e^{-\lambda x^2} dx = \int_{-\infty}^{\infty} e^{-\lambda y^2} dy \tag{A.21}$$

$$I_0{}^2 = \int_{-\infty}^{\infty} dx \int_{-\infty}^{\infty} dy e^{-\lambda(x^2+y^2)} \tag{A.23}$$

The integration extends over the entire two-dimensional *xy*-plane and it is easier to perform in polar coordinates *r* and θ where

$$x = r\cos\theta, \quad y = r\sin\theta, \quad dxdy = rdrd\theta \tag{A.24}$$

Thus with care in fixing the limits of integration

$$I_0{}^2 = \int_0^{\infty} dr \int_0^{2\pi} d\theta r e^{-\lambda r^2} = 2\pi \int_0^{\infty} r e^{-\lambda r^2} dr \tag{A.25}$$

Using $r^2 = X$, $2rdr = dX$

$$I_0{}^2 = \pi \int_0^{\infty} e^{-\lambda X} dX = \pi \left[-\frac{e^{-X}}{\lambda} \right]_0^{\infty} = \frac{\pi}{\lambda} \tag{A.26}$$

The required integral is therefore

$$I_0 = \sqrt{\frac{\pi}{\lambda}} \tag{A.27}$$

The basic integral can be used to evaluate more complicated integrals such as $I_2 = \int_{-\infty}^{\infty} x^2 e^{-\lambda x^2} dx$. This can be integrated by parts but it is easier to use the differential property

$$I_2 = -\frac{d}{d\lambda}\int_{-\infty}^{\infty} e^{-\lambda x^2} dx = -\frac{d}{d\lambda}\left(\frac{\pi}{\lambda}\right)^{\frac{1}{2}} = \frac{\sqrt{\pi}}{2\sqrt{\lambda^3}} \qquad \text{(A.28)}$$

Similarly

$$I_4 = \int_{-\infty}^{\infty} x^4 e^{-\lambda x^2} dx = -\frac{d}{d\lambda} I_2 = \frac{3\sqrt{\pi}}{4\sqrt{\lambda^5}} \qquad \text{(A.29)}$$

and so on.

The integral of Eq. (A.9) must be 1 for normalization.

$$\int_{-\infty}^{\infty} p(x)dx = A\int_{-\infty}^{\infty} e^{\frac{-x^2}{2na^2}} dx = 1 \qquad \text{(A.30)}$$

from Eq.(A.27)

$$A\sqrt{2n\pi a^2} = 1 \qquad \text{(A.31)}$$

Therefore

$$A = \frac{1}{\sqrt{2n\pi a^2}} \qquad \text{(A.32)}$$

The mean square value of *x* in Appendix 1 can be obtained using Eq. (A.28).

$$\int x^2 p(x)dx = \int x^2 \frac{1}{\sqrt{2n\pi a^2}} e^{\frac{-x^2}{2na^2}} dx = \frac{1}{\sqrt{2n\pi a^2}} na^2\sqrt{2n\pi a^2} = na^2$$

The mean square value of *r* in Appendix 1 can be obtained using Eq. (A.29).

$$\int_0^{\infty} r^2 P(r)dr = \int_0^{\infty} 4\pi r^4 \left(\frac{3}{2\pi na^2}\right)^{3/2} e^{-\frac{3r^2}{2na^2}} dr = 4\pi\left(\frac{3}{2\pi na^2}\right)^{3/2} \frac{3\sqrt{\pi}}{8}\left(\frac{2na^2}{3}\right)^{5/2} = na^2$$

Appendix 3

Calculation of mean values of the randomly jointed chain

The mean square value of x of the randomly jointed chain can be obtained without the calculation of $p(x)$. Let p be the probability of a segment to the right and q be the probability of a segment to the left. When we said that the direction of each segment was "random", we implied that $p = q = 1/2$. The sum of the probabilities of all possible outcomes of n segments can be represented in the form of $(q+p)^n$. The sum can be expanded by the binomial theorem:

$$Z = (q+p)^n = q^n + nq^{n-1}p + \cdots + \frac{n!}{n_+!(n-n_+)!}q^{n-n_+}p^{n_+} + \cdots + p^n \tag{A.33}$$

The mean square value of n_+ is given by

$$\overline{n_+^{\,2}} = \sum_{n_+=0}^{n} n_+^{\,2}\frac{n!}{n_+!(n-n_+)!}q^{n-n_+}p^{n_+}$$

$$= 0\cdot q^n + 1\cdot nq^{n-1}p + \cdots + n_+^{\,2}\cdot\frac{n!}{n_+!(n-n_+)!}q^{n-n_+}p^{n_+} + \cdots + n^2p^n \tag{A.34}$$

$$\frac{\partial Z}{\partial p} = nq^{n-1} + 2\frac{n(n-1)}{2!}q^{n-2}p + \cdots + n_+\frac{n!}{n_+!(n-n_+)!}q^{n-n_+}p^{n_+-1} + \cdots + np^{n-1} \tag{A.35}$$

$$p\left(\frac{\partial Z}{\partial p}\right) = nq^{n-1}p + 2\frac{n(n-1)}{2!}q^{n-2}p^2 + \cdots + n_+\frac{n!}{n_+!(n-n_+)!}q^{n-n_+}p^{n_+} + \cdots + np^n \tag{A.36}$$

$$\frac{\partial}{\partial p}\left[p\left(\frac{\partial Z}{\partial p}\right)\right] = nq^{n-1} + 2^2\frac{n(n-1)}{2!}q^{n-2}p + \cdots + n_+^{\,2}\frac{n!}{n_+!(n-n_+)!}q^{n-n_+}p^{n_+-1} + \cdots + n^2p^{n-1} \tag{A.37}$$

Comparing Eqs. (A.34) and (A.37), we note that multiplying the right side of (A.37) by p gives the right side of (A.34). Therefore

$$\overline{n_+^{\,2}} = p\left\{\frac{\partial}{\partial p}\left[p\left(\frac{\partial Z}{\partial p}\right)\right]\right\}$$

$$p\frac{\partial Z}{\partial p} = p\frac{\partial (q+p)^n}{\partial p} = np(q+p)^{n-1}$$

$$p\left\{\frac{\partial}{\partial p}\left[p\left(\frac{\partial Z}{\partial p}\right)\right]\right\} = np\left[p(n-1)+1\right]$$

For $p = 1/2$,

$$\overline{n_+^{\,2}} = p\left\{\frac{\partial}{\partial p}\left[p\left(\frac{\partial Z}{\partial p}\right)\right]\right\} = \frac{n}{2}\left(\frac{n-1}{2}+1\right) = \frac{n(n+1)}{4} \qquad \text{(A.38)}$$

The mean square value of x is

$$\overline{x^2} = \overline{(2n_+ - n)^2}a^2$$
$$\overline{(2n_+ - n)^2} = 4\overline{n_+^{\,2}} - 4\overline{n_+}n + n^2$$

$\overline{n_+} = n/2$ for a randomly jointed chain; thus

$$\overline{(2n_+ - n)^2} = 4\overline{n_+^{\,2}} - n^2$$

From Eq.(A.38) we obtain that

$$\overline{(2n_+ - n)^2} = 4\overline{n_+^{\,2}} - n^2 = n(n+1) - n^2 = n$$

Therefore the mean square value of x is

$$\overline{x^2} = na^2$$

5

Gelation and gel properties of xyloglucan by addition of small molecules in foods

5.1 GELATION OF TAMARIND SEED XYLOGLUCAN BY ADDITION OF EPIGALLO CATECHIN GALLATE

5.1.1 Introduction

For texture modifier, gelling ability is important for food polysaccharides. It has been reported that TSX forms a gel in the presence of large amount of sugar or alcohol (Nishinari et al., 2000; Glicksman, 1986; Yuguchi, 2002; Yamanaka, 2000). It has also been reported that TSX interacts with polyphenols or dyes to form a gel (Wood, 1980; Yuguchi, 2002).

Polyphenols are receiving more and more attention because of their beneficial functions to human bodies. It is becoming popular to design food products containing polyphenols as a functional food. Epigallocatechin gallate (EGCG) as shown in Fig. 5.1 is one of polyphenols which is found in green teas. EGCG is the most abundant among flavanols such as epicatechin, epicatechin gallate, and epigallocatechin in the tealeaves (Namiki et al., 1991). In addition, EGCG is known as a catechin derivative which shows strong biochemical and physiological activities (Kennedy et al., 1998).

Polymer-polyphenol interaction has been studied to control the quality of foods and beverages since this interaction induces haze formation and precipitation (Siebert et al.,

1996). Precipitation of protein in the presence of polyphenols is considered to be due to binding between proteins and polyphenols, which influences flavors of foods and beverages consequently. Luck et al. (1994) reported that the presence of polysaccharides changed the degree of precipitation of protein by polyphenols and thus might influence flavors. The binding between corn starch and catechin derivatives has been suggested by Muramoto et al. (1999) from colorimetric analysis and UV spectra.

The study on the interaction of TSX and EGCG is expected to be helpful for understanding properties of TSX, development of new types of food products, and preventing and/or controlling the haze formation and the flavor change of final products. In the present study, dynamic viscoelastic measurements and DSC were performed for TSX in the absence/presence of EGCG and 2D NOESY was carried out to complement the discussion about the possible interaction of TSX and EGCG predicted from rheological and DSC data.

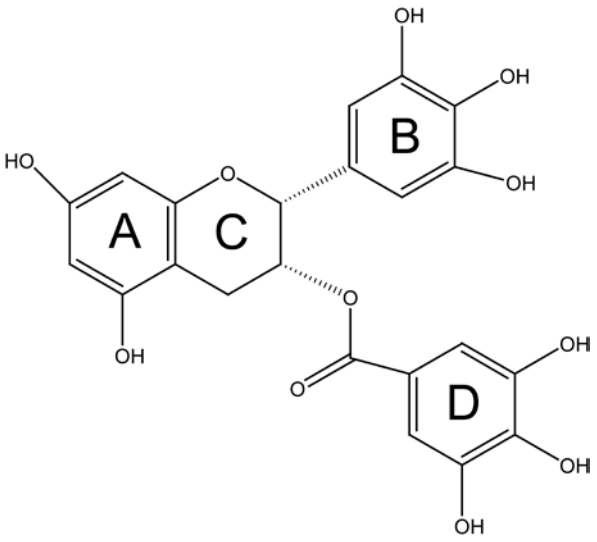

Figure 5.1 Chemical structure of Epigallocatechin gallate

5.1.2 Experimental

Tamarind seed xyloglucan (TSX) was supplied from Dainippon Pharmaceutical Co. Ltd., Japan and was purified as follows: TSX was dispersed in distilled water with a concentration of 0.5 wt % and the dispersion was centrifuged at ~1000g and then filtered to remove insoluble substances. TSX was obtained as precipitate by addition of acetone. The intrinsic viscosity of the purified TSX was determined at 25±0.02°C as 6.65±0.05 dL/g using an Ubbelohde-type viscometer (Kaburagi Scientific Instruments Ltd., Japan) from extrapolation to infinite dilution in both Huggins and Kraemer plots. The content of the nitrogen in the TSX was estimated using 240C Elemental Analyzer (Perkin Elmer Life and Analytical Sciences Ltd., USA) and was found too small to be detected. A detectable limit was 0.3 %, from which crude protein content (N×6.25) was calculated as less than 2 % in TSX (Meyer, 1960). EGCG of 99% purity (E-4143 product number) extracted from green tea of a reagent grade was purchased from Sigma Aldrich Japan Ltd and was used without further purification. Since EGCG solution changed the color during storage suggesting that the compound might change (Wang et al., 2000; Chen et al., 2001), the rheological and DSC experiments for TSX with EGCG were performed immediately after mixing TSX and EGCG in distilled water and heating at 80°C for 1h.

Dynamic viscoelasticity was studied by a strain-controlled rheometer, ARES (Rheometrics Ltd., USA) with a transducer, the sensitivity limit of which was 0.004 g·m. The sample solution was poured onto a parallel plate geometry (diameter of the plate = 25 mm) at 50°C and then immediately covered with silicone oil to prevent the evaporation of water. Strain dependence of the storage and loss shear moduli, G' and G'', was examined to determine a linear viscoelastic regime. Programmed software, Rheometric Scientific's RSI orchestrator TTS software, was used for the time-temperature superposition of G' and G''. Multi-wave was applied to obtain G' and G'' at various frequencies during the sol-gel transition for the TSX with EGCG. 1 rad/s was chosen as a fundamental frequency in multi-wave mode measurements with

duration time less than 10 seconds and thus temperature change during one multiwave measurement is expected to be almost negligible at cooling and heating rates of 0.5°C/min. The temperature was controlled by a refrigerated circulator FS18-MV (Julabo Ltd., Germany).

DSC was performed using a micro DSC-III calorimeter, Setaram Ltd., France. Approximately 800mg of the sample solution and the equal amount of distilled water as a reference were hermetically sealed into each DSC pan. Cooling and heating DSC curves were recorded in the temperature range from 2 to 60°C at 0.5°C/min.

The phase change in TSX solution in the presence of EGCG was observed visually. The cloud point T_c where the solution began to cloud was determined by visual observation. Temperature of the sample was controlled by a thermo-bath and was determined by a thermo-couple. The uncertainty of Tc was estimated to be ±1°C.

^{1}H 1D spectra and ^{1}H-^{1}H NOESY spectra were recorded with a Varian Unity plus operating at 499.865MHz. Mixtures of 0.5 wt% TSX with 0.2 wt% EGCG in 99.9 % D_2O were sealed in NMR tubes after heating and stirring at 80°C for 1h. Sodium 2,2-dimethyl-2-silapentane-5-sulfonate (DSS) was also added as the inner standard.

5.1.3 Results and discussion

Rheological properties of TSX solutions

TSX solutions kept sol state in the concentration range from 1 to 10 wt % and temperature range from 10 to 50 °C. The storage and loss shear moduli, G' and G'', of TSX solutions showed dilute and semi-dilute solution type behaviors in these conditions. The dilute solution type behavior was defined as follows; G'' was larger than G' in the frequency range from 0.1 to 100 and the semi-dilute solution type behavior was as follows; G'' was larger than G' at lower frequencies while G' was larger than G'' at higher frequencies. It was possible to apply time-temperature superposition with a horizontal shift along the frequency axis and a slight vertical shift along the modulus axis. This suggests that there was no significant change in TSX with temperature and

temperature mainly affected the time scale of the relaxation in the experimental temperature range. Table 5.1 shows horizontal and vertical shift factors a_T and b_T of TSX solution for the time-temperature superposition. Table 5.2 shows the apparent activation energy Ea of TSX solutions obtained from the following equation:

$$\ln a_T = Ea/RT + \text{const.}$$

where R is the gas constant. Ea was almost a constant value (about 30 kJ/mol) at various concentrations. It was reported that Ea did not depend on guar gum concentration (Wientjes et al., 2000) whereas Ea depended on concentration of κ-carrageenan in the κ-carrageenan/NaI system (Chronakis et al., 2000). Time-temperature superposition was applied to the κ-carrageenan/NaI system at helical conformation of κ-carrageenan. Since TSX does not take a helical conformation in the solution and TSX resembles galactomannans in solution properties, it is reasonable that Ea of TSX chains showed similar tendency to that of guar gum.

G′ and *G″* of TSX solutions at various concentrations could be superimposed by applying appropriate horizontal and vertical shift factors a_C and b_C for a master curve with time scale over six decades. Figure 5.2 shows the master curve of *G′* and *G″* of TSX solutions in the concentration range from 1 to 10 wt%. The master curve showed 'solution-like' behaviour. Shift factors a_C and b_C used to obtain the master curve were shown in Table 5.3. a_C was well described by a power law of $a_C \sim c^{2.77}$. b_C also showed a scaling law ($b_C \sim c^{-1.58}$). The value of the exponent of a_C was closer to that of concentrated solutions of flexible polystyrene molecules (Baumgärtel and Willenbacher, 1996) in a good solvent ($a_C \sim c^{3.5}$) than to that of κ-carrageenan helices (Chronakis et al., 2000) in 0.2M NaI ($a_C \sim c^{16}$) and to that of xanthan solutions (Launay et al., 1984) above the overlap concentration ($a_C \sim c^{7.4}$). The characteristic time $\tau_{G'=G''}$ and the characteristic strength $G_{G'=G''}$ at which *G′* and *G″* crossed over are also shown in Table 5.3.

Table 5.1 Horizontal and vertical shift factors, a_T, and b_T, of TSX solutions for a master curve obtained from time-temperature superposition.

2%			4%			8%			10%		
T/°C	a_T	b_T	T/°C	a_T	b_T	T/°C	a_T	b_T	T/°C	a_T	b_T
9.7	1.7	1.1	20	1	1	10	1.6	1.0	10	1.6	1.0
20	1	1	30	0.66	0.93	20	1	1	20	1	1
29	0.69	0.96	40	0.46	0.87	30	0.66	0.94	30	0.65	1.0
40	0.43	0.97	50	0.34	0.81	40	0.45	0.90	40	0.43	1.0
51	0.26	0.85									

Table 5.2 The apparent activation energy of TSX solutions at various concentrations.

Conc. / wt%	E_a kJ/mol
2	33.7
2.5	32.2
3	31.3
3.5	31.7
4	28.4
8	30.7
10	31.4

Table 5.3 Horizontal and vertical shift factors, a_c, and b_c, for master curve and $G_{G'=G''}$ and $\tau_{G'=G''}$ at 20°C.

Conc. / wt%	a_c	b_c	$G_{G'=G''}$ / Pa	$\tau_{G'=G''}$ / s
1	1	1		
2	11.5	0.59		
3	35	0.32	107	0.168
4	78	0.23	152	0.367
5	110	0.11	316	0.532
8	380	0.055	649	1.72
10	700	0.027	1333	3.11

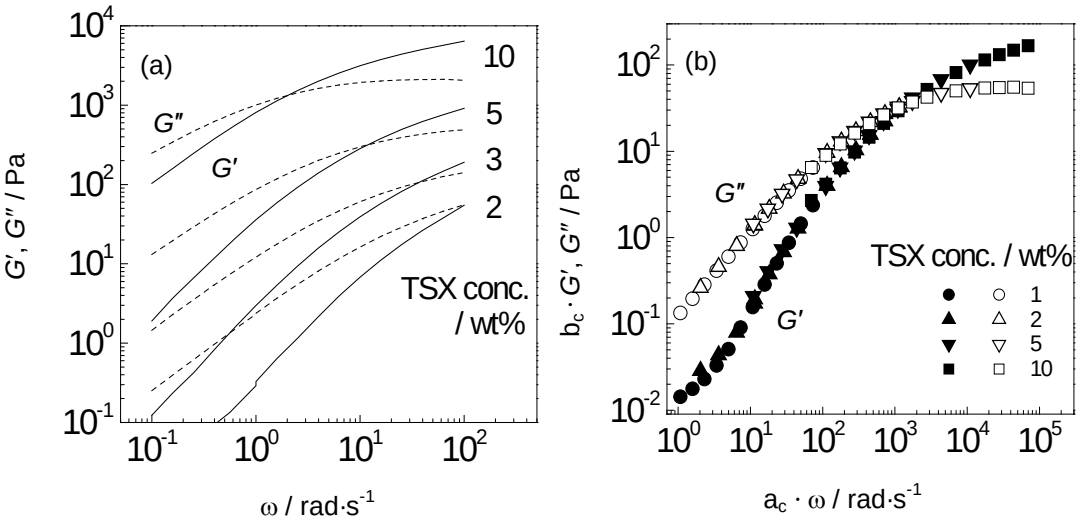

Figure 5.2 (a) Frequency dependence of the storage and loss shear moduli, G'(−) and G'' (┈), of TSX at various concentrations and (b) master curves of G' (closed) and G'' (open), of TSX in the concentration range from 1 to 10 wt% at 20°C. Reference concentration, 1 wt%. a_c, and b_c, horizontal and vertical shift factors, respectively.

Gelation of TSX in the presence of EGCG

Figure 5.3 shows frequency dependence of G' and G'' of 2 wt% TSX solutions with 0.1 wt% EGCG on cooling. Time-temperature superposition failed in obtaining a master curve for this system below 20°C, indicating that TSX chain nature changed with temperature. At higher temperatures, G'' was larger than G' at any frequencies, which was like TSX solutions in the absence of EGCG. With decreasing temperature, the 'dilute solution' type behavior changed into 'semi-dilute solution' type behavior and then into 'gel' type behavior where G' was larger than G'' at all experimental frequencies. This indicates that TSX formed a gel by addition of EGCG.

Fig. 5.4 (a) shows temperature dependence of G' and G'' of 2 wt % TSX with 0.1 wt % EGCG on cooling and on subsequent heating and (b) shows cooling and heating DSC curves. The TSX-EGCG gel was found to be thermoreversible. G' exceeded G'' around 20°C at 1 rad/s and then G' and G'' increased with decreasing temperature.

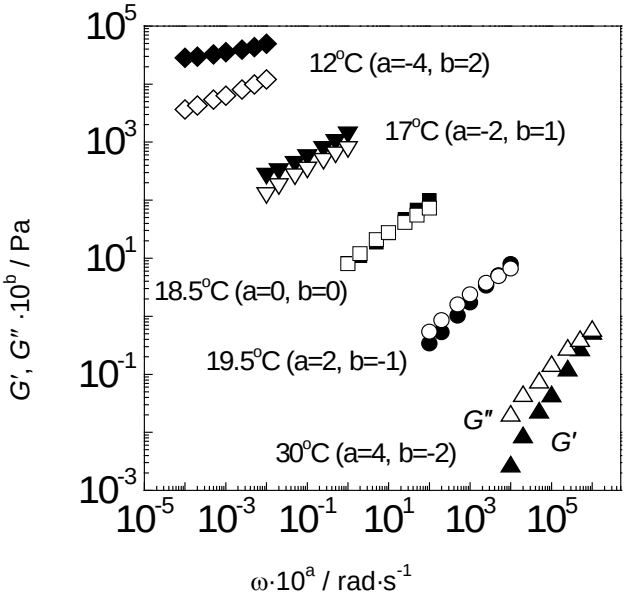

Figure 5.3 Frequency dependence of G' (closed) and G'' (open) of 2 wt% TSX with 0.1 wt% EGCG at various temperatures on cooling at 0.5°C/min. Data is shifted along the horizontal and vertical axes by shift factors 'a' and 'b' to avoid overlapping.

On subsequent heating, G' and G'' decreased steeply and G'' became larger than G' around 30°C. These temperature-induced rheological changes were attributed to the gelation and the subsequent gel-melting. DSC curves also supported the occurrence of the sol-gel transition. In cooling DSC curves, an exothermic peak appeared at almost the same temperature where G' and G'' increased steeply. An endothermic DSC peak appeared around the temperature where G' and G'' decreased steeply. Thermal hysteresis was observed in both rheological and DSC results.

Fig. 5.5 shows scanning rate dependence of DSC peak temperatures on cooling and on heating. The exothermic and endothermic peak temperatures at infinitely slow rate were estimated from Fig. 5.5 as 20.79°C and 28.39°C, respectively. Therefore thermal hysteresis observed in Fig. 5.4 was not due to the high rate of scanning. Thermoreversible sol-gel transition with thermal hysteresis was often seen in other gelling polysaccharides such as agarose and gellan (Clark and Ross-Murphy, 1987; Te

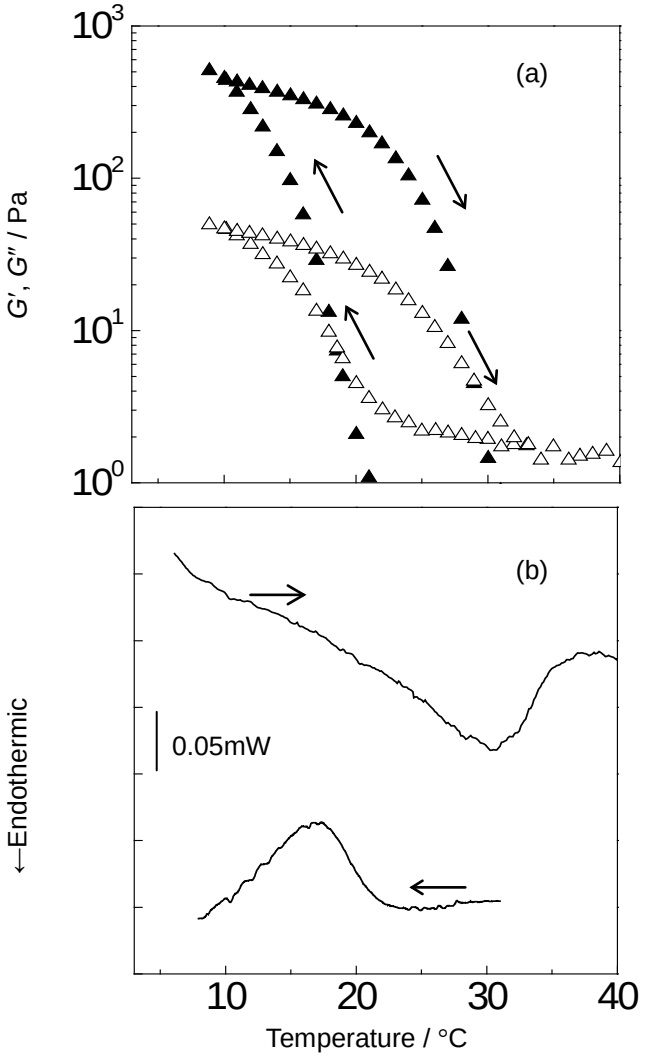

Figure 5.4 (a) Temperature dependence of G' (▲) and G'' (△) on cooling and on subsequent heating and (b) cooling and subsequent heating DSC curves of 2 wt% TSX with 0.1 wt% EGCG. Scanning rate, 0.5°C/min. Frequency, 1rad/s.

Nijenhuis, 1997). These gels are believed to be formed by a three-dimensional network where aggregates of gelling polysaccharides play a role of junction zones.

Effect of EGCG concentration on the sol-gel transition of TSX

Fig. 5.6 shows DSC curves of 1 wt % TSX containing EGCG of various concentrations. TSX alone did not show any peak whereas TSX in the presence of EGCG showed a single peak as observed in Fig. 5.4(a). The peak temperatures which

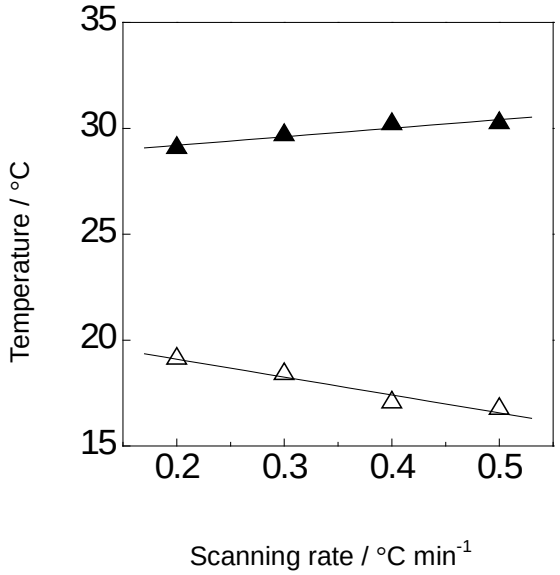

Figure 5.5 Scanning rate dependence of DSC peak temperatures on cooling (△) and on subsequent heating (▲), of 2 wt% TSX with 0.1 wt% EGCG.

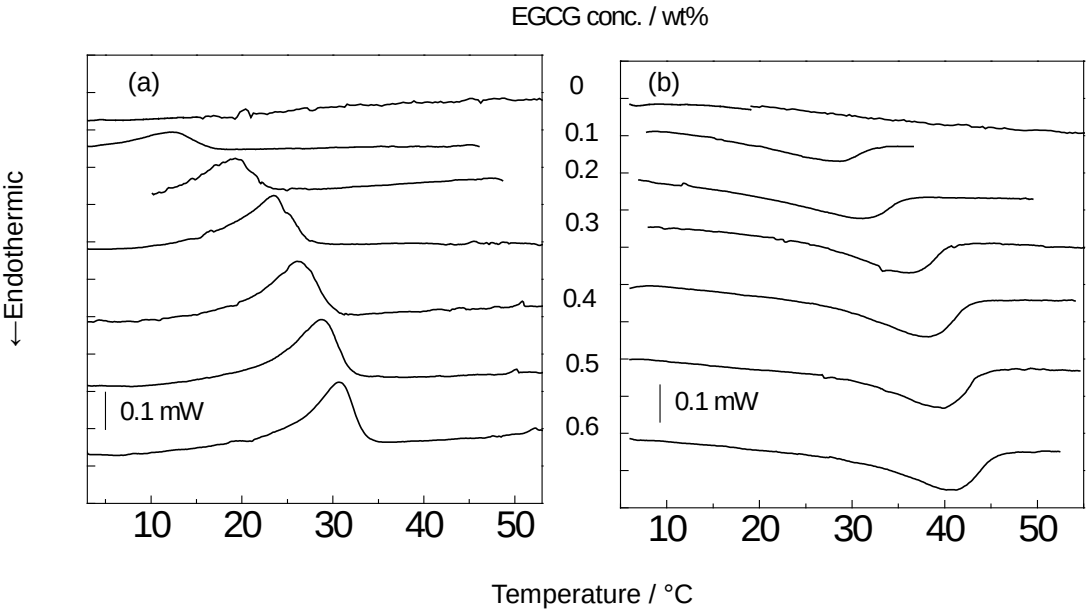

Figure 5.6 (a) Cooling and (b) subsequent heating DSC curves of 1 wt% TSX containing EGCG at various concentrations. Scanning rate, 0.5°C/min.

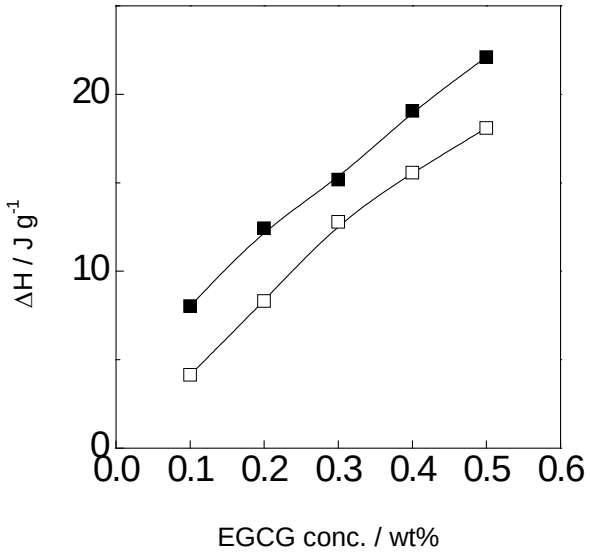

Figure 5.7 Endothermic (■) and exothermic (□) enthalpies, ΔH, of 1g TSX as a function of EGCG concentrations. Scanning rate, 0.5°C/min.

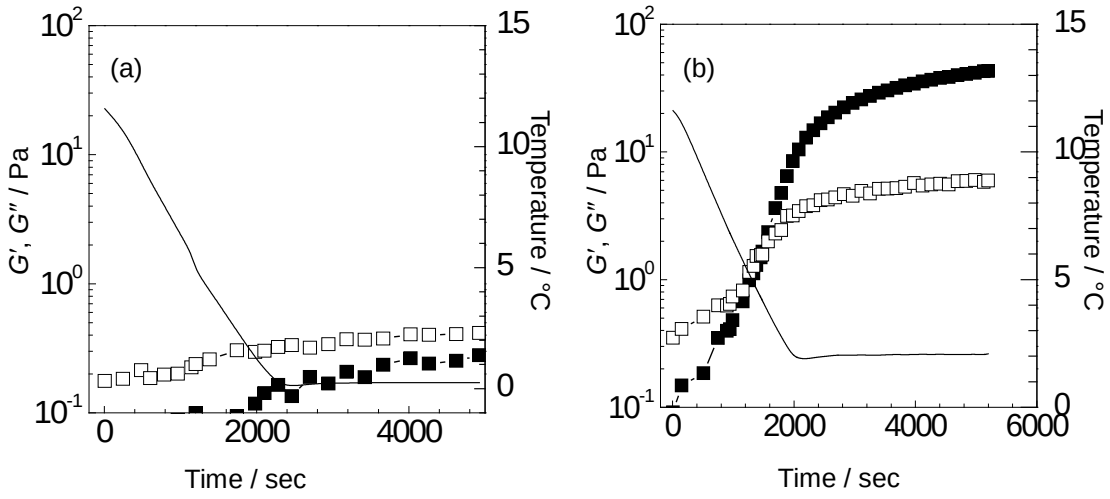

Figure 5.8 *G′* (■) and *G″* (□) of 1 wt% TSX solutions containing (a) 0.02 wt% or (b) 0.04 wt% EGCG at 1 rad/s. Solid line; temperature course.

were close to gelation and gel-melting temperatures in rheological measurements (data not shown) shifted to higher temperatures with increasing EGCG concentration. Fig. 5.7 shows changes in enthalpies ΔH of 1g TSX through the sol-gel transition as a function of EGCG concentration. ΔH increased in proportion to EGCG concentration.

Fig. 5.8 shows G' of TSX (1 wt%) in 0.02 or 0.04 wt% EGCG. When the added EGCG was 0.02 wt %, gelation did not occur above 0°C where G'' was larger than G' at 1 rad/s. In the presence of 0.04 wt % EGCG, G' exceeded G'' around 5 °C on cooling and G' increased to be the order of 10. When the added EGCG was above 0.15 wt %, G' became the order of 10^3 where frequency dependence of G' and G'' showed a 'true gel' type behavior (Nishinari, 1997): G' and G'' were almost independent of frequencies and tanδ was smaller than 0.1(data not shown). This indicates that TSX formed a three-dimensional network in the presence of EGCG.

Fig. 5.9 shows temperature dependence of G' of 1 wt% TSX at various EGCG concentrations on cooling. Gelation point, T_g, which was defined as the temperature at which G' increased steeply in the present study, shifted to higher temperatures with increasing EGCG concentrations. G' of the TSX gels at lower temperatures increased with increasing EGCG concentrations up to certain amount (Fig. 5.9(a)) and then decreased with increasing EGCG concentrations (Fig. 5.9(b)).

Fig. 5.10 shows the values of G' of 1 wt % TSX gels as a function of EGCG concentration at 10°C. As shown in Fig. 5.9, the values of the shear modulus of TSX gels were influenced strongly by EGCG concentration. G' increased first and then decreased dramatically with increasing EGCG concentration. Above 0.6 wt% EGCG macroscopic phase separation occurred. A liquid phase could be distinguished from a gel phase at 0.7 wt% or 0.8 wt% EGCG. This inhomogeneity induced large deviation of the value of G'. Precipitation occurred in 1 wt% EGCG on cooling around 40°C.

Fig. 5.11 shows changes in phase of 1 wt% TSX containing EGCG on cooling. The gelation point T_g and the cloud point T_c were plotted in Fig. 5.11. We referred to studies done by Wang et al. for determining Tc in which the phase behaviour was studied by visual observation for ethyl(hydroxyethyl)celluloses containing sodium dodecyl sulfate (Wang et al., 1997). Examples of appearance of TSX gel was shown in Fig. 5.11a. Macroscopic fluidity and appearance changed around Tg, and Tc, respectively. With increasing EGCG concentration, a transparent gel changed into a

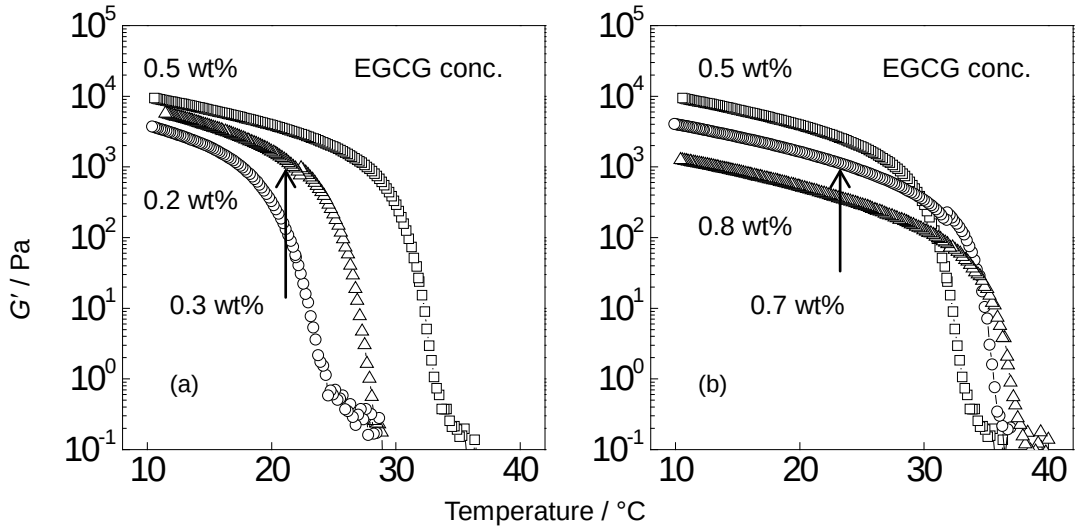

Figure 5.9 Temperature dependence of G' of 1 wt% TSX containing EGCG at various concentrations on cooling at 0.5°C/min and 1rad/s.

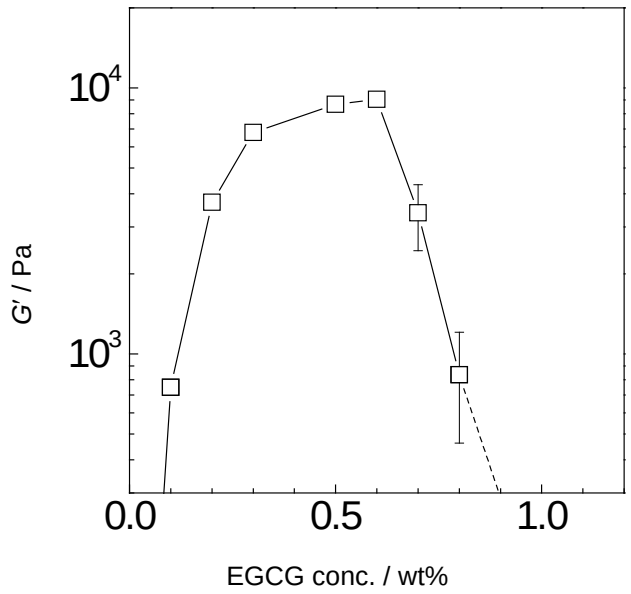

Figure 5.10 G' of 1 wt% TSX gels as a function of EGCG concentration at 10°C and 1rad/s. The error bars represent standard deviations.

translucent gel and into an opaque gel at fixed temperatures. Further addition of EGCG induced phase separation around Tc.

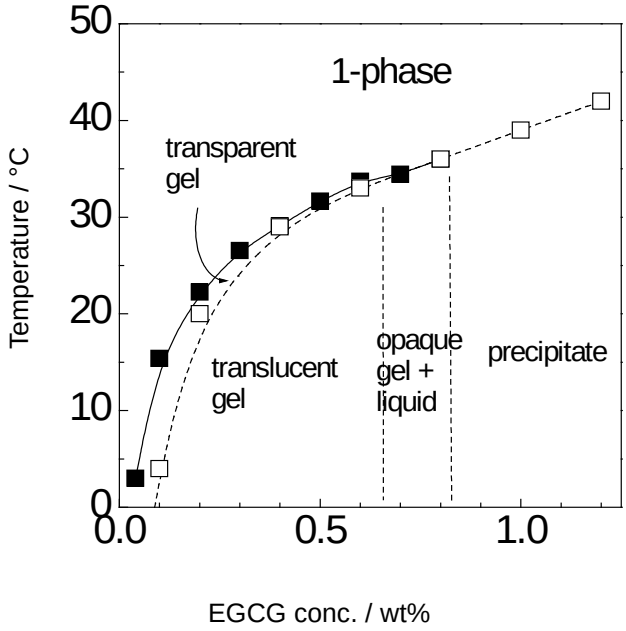

Figure 5.11 Changes in phases of 1 wt% TSX containing EGCG on cooling. ■; gelation point determined by rheology, □; cloud point determined by visual observation.

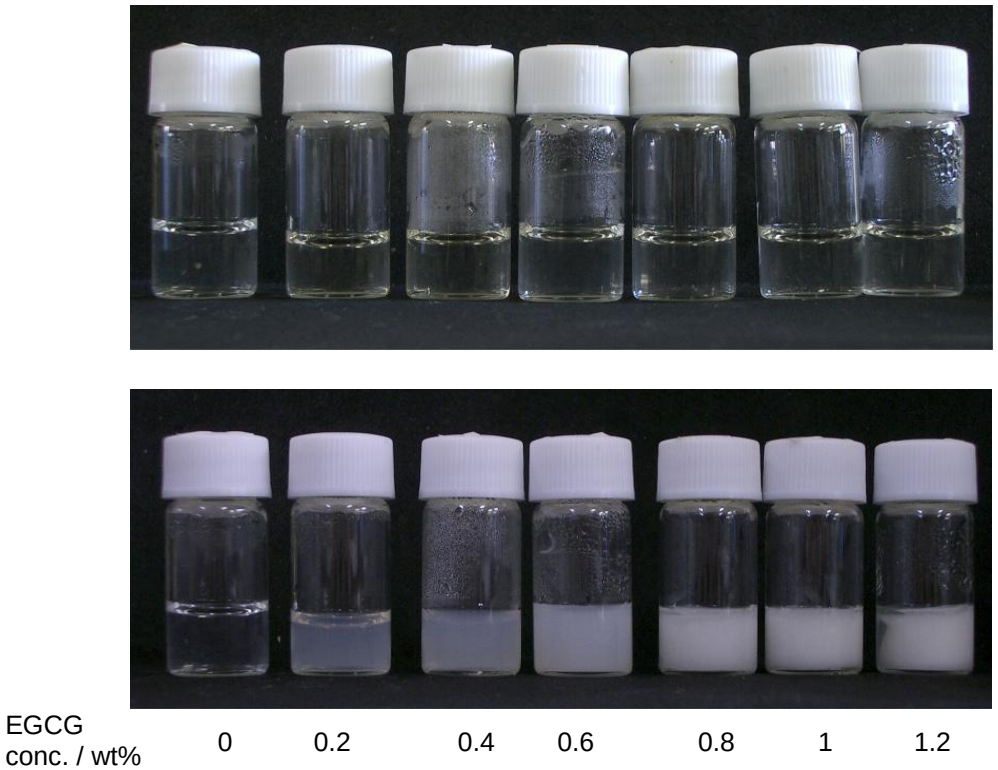

Figure 5.11a Appearance of 1 wt% TSX solutions containing EGCG with various concentrations.

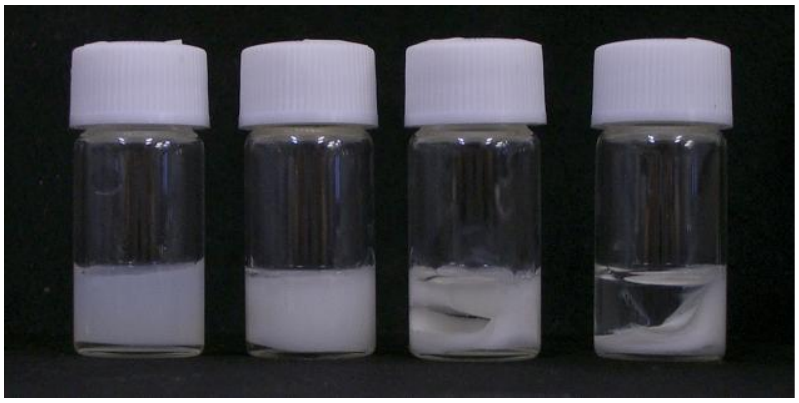

Figure 5.11b Appearance of 1 wt% TSX solutions containing EGCG with various concentrations after centrifugation.

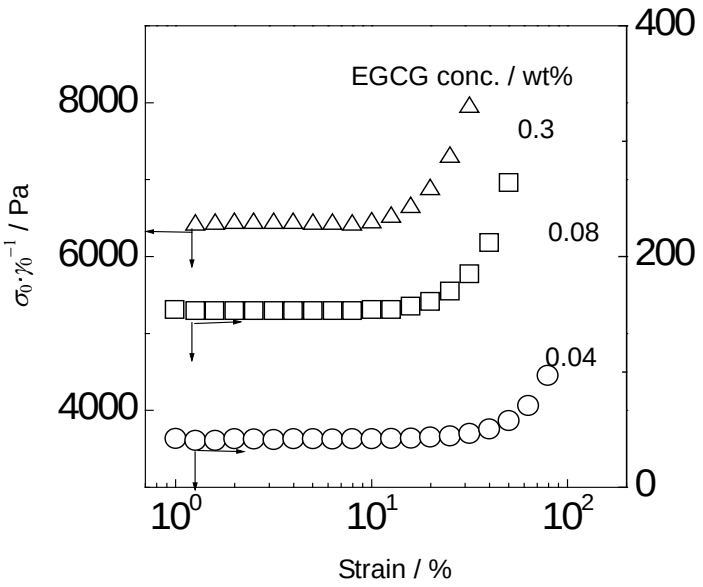

Figure 5.12 Strain dependence of the ratio of stress to strain of 1 wt % TSX containing EGCG at various concentrations. Frequency; 1 rad/s, Temperature; 10°C in 0.3 wt% or 0.08 wt% and 2°C in 0.04 wt%.

In the region where translucent gels were obtained, strain dependence of the rigidity was studied. Fig. 5.12 shows strain dependence of the ratio of stress to strain of 1 wt % TSX containing EGCG at various concentrations. In the linear viscoelastic region, the following relation is given;

$$\sigma_0/\gamma_0 = |G^*| = (G'^2+G''^2)^{0.5}$$

where σ_0 and γ_0 are the amplitude of the stress and strain, respectively, and G^* is the complex shear modulus. At lower strain σ_0/γ_0 corresponds to $|G^*|$ where σ_0/γ_0 is independent of the strain. The linear viscoelastic range of gels where σ_0/γ_0 is independent of the strain narrowed as EGCG concentration increased. Above the strain in the linear viscoelastic region, a strain-hardening phenomenon, an increase in σ_0/γ_0 with increasing strain, was observed.

Rheological and DSC results provided the evidence for the thermoreversible gelation of TSX in the presence of EGCG although TSX alone maintained sol state at the experimental conditions. Addition of a small amount of EGCG induced the cold-setting gelation of 1 wt% TSX with high shear modulus and thermal hysteresis.

TSX forms a gel by addition of large amount of sugars or alcohols. In that case, more than 20 wt % of such substances is necessary (Glicksman, 1986; Nishinari, et al., 2000). On the other hand, only a small amount of EGCG, e.g. 0.04 wt% of EGCG was required to induce the gelation of TSX in the present study. This difference might be related to indirect or direct interaction of TSX with these substances. EGCG probably interacted with TSX directly, through association with TSX, to form a network. NMR results also suggested that EGCG is bound to TSX, leading to gel network. Two-dimensional nuclear Overhauser effect spectroscopy (2D NOESY) is useful to study the intermolecuar interactions (Kögler, and Mirau, 1992) in which intermolecular cross peaks are only observed for protons separated by less than 5 Å. Fig. 5.13 shows NOESY spectra of TSX-EGCG mixtures in D_2O. 0.5 wt% TSX with 0.2 wt% EGCG

formed a gel in D_2O around 25°C on cooling and returned to a sol around 45°C on heating according to DSC results (data not shown). The mixtures at 50°C were compared with those at 35°C after gelation to compare a sol (50°C) with a gel (35°C). Each signal was assigned based on published data (York et al., 1993; Davis et al., 1996; Valcic et al., 1999; Inoue et al., 2002). The A-ring proton signal in EGCG (Fig. 1) was not observed as a result of deuteriation according to reports by Inoue et al (2002). It was found that intermolecular cross peaks appeared between xyloglucan (δ= 3.5-4.0 ppm) and EGCG (δ= 6.61 and δ= 7.00 ppm) in the gel state at 1.0s mixing time (Fig. 5.13(b)). In contrast, the intermolecular cross peaks were not observed in a sol state (Fig. 5.13 (a)). These indicate that EGCG was close to TSX at the distance less than 5 Å under gelling condition. Cross peaks also appeared between C-ring (δ= 2.8-3.2, 5.15 and 5.62 ppm) and D- (δ= 7.00 ppm) ring of EGCG in the gel. These peaks would appear if an assembly of EGCG exists in the gel. The detailed study on the EGCG structure in the gel will be done in the future. The build-up rate of the NOE of the intermolecular cross-peaks was lower than that of the intramolecular ones, as shown in Fig. 5.13(b) and (c). The different build-up rate was induced by a different mobility (hence different correlation time) and/or by the spin diffusion. In either event a new cross-relaxation path is formed across different 2 molecules in the gel state. This supports that EGCG is directly contact with TSX in the gel state.

If TSX combined with EGCG covalently, the resultant gel should be thermoirreversible. Thermoreversible gel formation suggests that network was formed by noncovalent bond like hydrogen bond and hydrophobic interaction. We think that hydrogen bonding played a crucial role in the gelation judging from the cold-setting gelation, the exothermic reaction during gelation, and intermolecular cross peaks between D or B rings of EGCG and TSX in ^1H-^1H NOESY spectra since each D or B ring has three OH group, the donor of the hydrogen bond, as shown in Figure 5.1 and it is potentially possible to make a hydrogen bond against the hydrogen bond acceptor in the xyloglucan. However at the present stage it is safe to say that EGCG associated

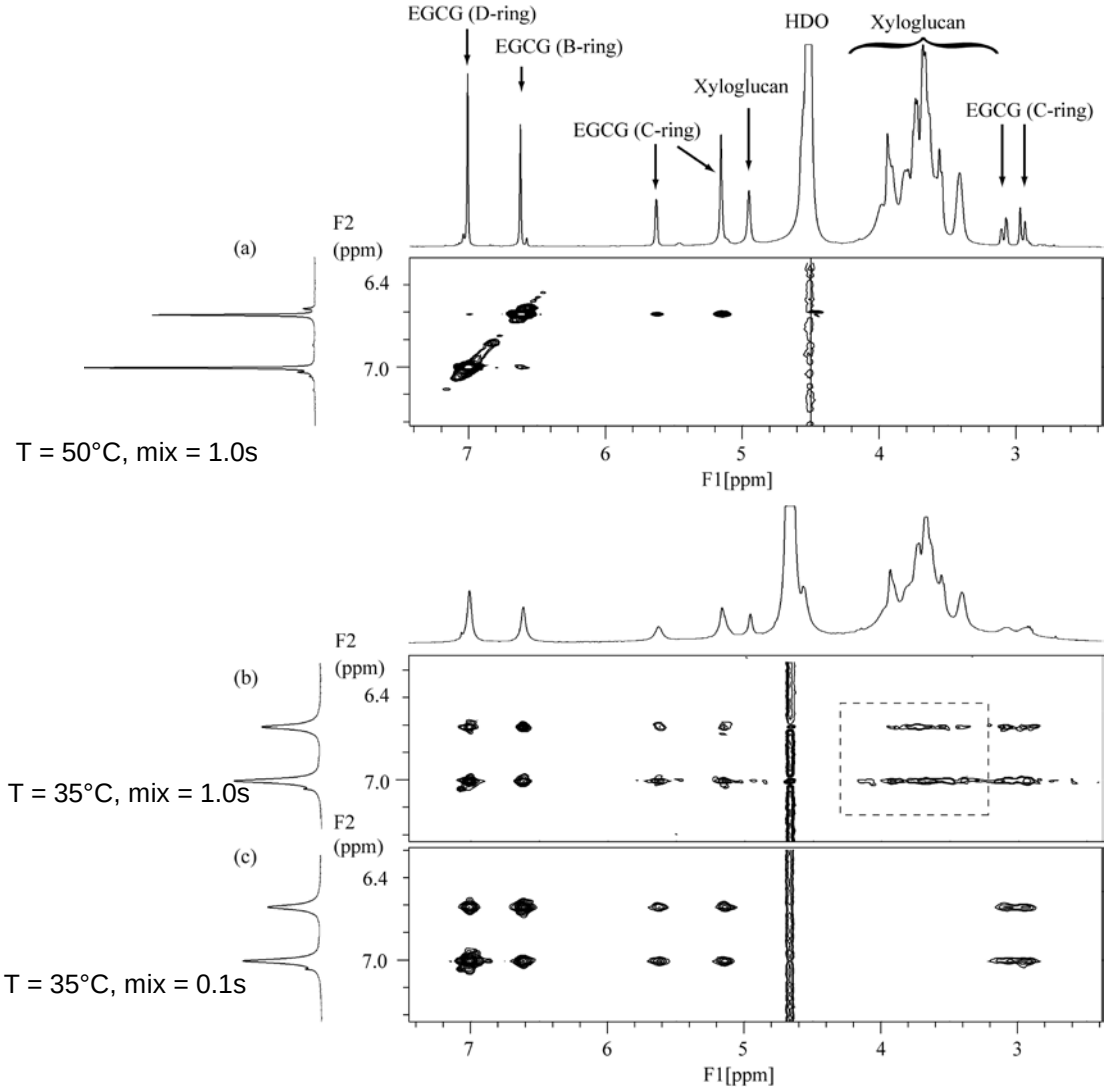

Figure 5.13 ^{1}H 1D spectra and ^{1}H-^{1}H NOESY spectra of 0.5 wt% TSX with 0.2 wt% EGCG in D_2O at 35 and 50°C. Intermolecular cross-peaks observed in Fig.(b) are highlighted in a box (broken line). The sign of all the peaks in Fig.(a) is plus except for the diagonal peaks (minus), and that in Fig. (b) and (c) is minus and an artifact was observed near the peak assigned to HDO (plus), and is induced by the large intensity of the HDO signal.

with TSX through noncovalent bond to form a gel.

Based on this interpretation about the interaction of TSX and EGCG, a possible gelation mechanism of TSX/EGCG system can be proposed as follows; EGCG was

bound to TSX chains to bridge different TSX chains. The binding sites acted as a junction zone. As a result, the shear modulus of the gels depended on EGCG concentration strongly. Enthalpy change for this transition was attributed to the energy of binding of EGCG to TSX. Thermal hysteresis suggests that TSX and EGCG formed junction zones which consist of TSX aggregates.

Strain dependence of the rigidity of the gels at various EGCG concentrations in Fig. 5.12 would also be interpreted as follows; the number of junction zones increased with increasing EGCG concentration and as a result TSX chains became less extendible, which narrowed the linear viscoelastic region. The strain-hardening effect, the increase of σ_0/γ_0 at higher strain, was recently observed in schizophyllan network cross-linked by Borax (Fang et al., 2004). It was concluded that the deformation has been approaching the limiting extensibility of the schizophyllan chains at the region where the strain-hardening effect was observed. TSX chains also might have been reaching the limiting extensibility at the region where the strain-hardening effect was observed.

The sol-gel transition temperatures and DSC peak temperatures shifted to higher temperatures with increasing EGCG concentration. This suggests that a formation of TSX aggregates was promoted with increasing EGCG concentration. This also explains the increase of the transition enthalpy change ΔH in proportion to EGCG concentration. The shear modulus of TSX gels increased with increasing EGCG concentration up to a certain value and then decreased by addition of higher amount of EGCG. Precipitation occurred by addition of excessive amount of EGCG. Addition of excessive amount of EGCG might induce further aggregation which forms water-insoluble substances instead of gel network. Appearance of TSX gels was related to the change in the shear modulus as a function of EGCG concentration: translucent gels were obtained below 0.6 wt% EGCG, above which opaque gels were obtained.

5.1.4 Conclusion

Gelation of TSX in the presence of EGCG was confirmed by rheology and DSC although TSX alone showed a sol-type behavior in the experimental conditions. A formation of gels with thermal hysteresis on gel setting and gel melting suggested a formation of junction zones consisting of TSX aggregates. A thermoreversibilty of the gel indicated the network formation through a noncovalent bond. EGCG was most likely bound to TSX chains for a gel network, which was detected as a DSC peak and NMR spectra (NOESY). This gelation is expected to be useful for designing foods with new texture and specific functionality.

6

Gelation and gel properties of xyloglucan by addition of macromolecules in foods

6.1 GELATION OF TAMARIND SEED XYLOGLUCAN BY MIXING WITH GELLAN

6.1.1 Introduction

Synergistic interaction of helix-forming polysaccharides and 1,4-β-D mannans was reported about 30 years ago (Rocks, 1971) and since then the interaction has been studied extensively (Morris, 1995a; Morris 1995b) not only from scientific interest in the interaction of different polymers but also from the viewpoint of industrial application of such polysaccharides as a texture modifier at lower costs and with a new texture. A molecular model of the interaction of agarose or κ-carrageenan and galacto- or gluco- mannans was proposed by Dea et al. first (1972). In their model, helices of the algal polysaccharides bind unsubstituted region of the mannan chains and substituted region exists in the interconnecting regions to form a three-dimensional network. On the other hand, Cairns et al. (1987) concluded that there is no specific interaction between the algal polysaccharides and galacto- or gluco- mannans from X-ray diffraction data. Only in the case of xanthan and mannan mixtures, X-ray diffraction data suggested synergistic interaction and a “sandwich” model was proposed in which cellulose-like backbone of xanthan forms two-fold helix instead of five-fold

helix and sandwich mannan chains. Another model has been proposed by Kohyama et al. (1993) to explain rheological change of the algal polysaccharide solutions by the addition of glucomannans. In this model, it was suggested that there were two kinds of junction zones: carrageenan alone and carrageenan-KGM, and the latter junction zone is not heat resistant but contribute to the elasticity. Which model is the most appropriate is still in debate. One of the reasons for difficulty in development of the molecular model is that there are only a few mixtures which show the synergistic interaction. Previously a mixture of gellan and konjac glucomannan was studied and only a weak interaction was observed (Nishinari et al., 1996c; Miyoshi et al., 1996b). In the present study, mixture of TSX and gellan gum was investigated. According to a model proposed by Dea et al. (1972), it is expected that TSX and gellan gum interact synergistically. Since sodium salt form gellan (Na-G) does not form a gel at a low concentration, synergism can be studied by observing whether mixtures of TSX and Na-G form a gel under non-gelling conditions of individual polysaccharide.

6.1.2 Experimental

Tamarind seed xyloglucan (TSX) was the same as that used in Chapter 5. Sodium salt form of gellan gum (Na-G) was supplied from San Ei Gen FFI Ltd., Japan and was used without further purification. The content of Na, K, Ca, and Mg in the Na-G was determined by ICP as 2.990%, 0.026%, 0.030%, and 0.002%, respectively. TSX and Na-G were dispersed in distilled water separately to be the concentration of 1 wt % and stirred at 20±2°C overnight. The samples were heated to 80°C for 1 hour and 90°C for 10min and then were mixed at various ratios. The mixtures were kept above 60°C before measurements.

The storage and loss shear moduli, G' and G'' were measured using a stress-controlled rheometer, Rheostress1 from Haake Ltd., Germany. About 6g of the sample solution was poured into a double-gap cylinder geometry (diameter of the cup = 43.4mm; outer gap = 0.3mm; inner gap = 0.25mm; height = 55mm) at 60°C and then

immediately covered with silicone oil to prevent the evaporation of water. Before measurements of temperature dependence and frequency dependence of G' and G'', strain dependence of G' and G'' was examined to determine a linear viscoelastic regime. Multi-wave was applied to obtain G' and G'' at various frequencies during sol-gel transition for the mixtures. Since 1.26 rad/s was a fundamental frequency in multi-wave mode measurements with duration time less than 10 seconds, temperature change during the time obtaining data on cooling and on heating at 0.5°C/min is expected to be almost negligible. The temperature was controlled by a Haake circulator DC30-K10 (Haake, Germany).

Differential scanning calorimetry (DSC) was performed using a micro DSC-III calorimeter, Setaram Ltd., France. Approximately 800mg of the sample solution and the equal amount of distilled water as a reference were put into each DSC pan and then sealed hermetically. Cooling and heating DSC curves were obtained in the temperature range from 5 to 100°C at 0.5°C/min.

Circular dichroism (CD) measurements were carried out with a JASCO-820A spectropolarimeter, Japan Spectroscopic Co. Ltd., Japan using a rectangular cell (2×10×40mm) in which the optical path length was 2mm. Temperature was controlled by a Peltier element (RTC9423L type, Japan Spectroscopic Co. Ltd., Japan). The molecular ellipticity of the samples was measured as spectra in the wavelength range from 190 to 250nm at various temperatures.

6.1.3 Results and discussion

Figure 6.1 shows temperature dependence of the storage shear modulus G' and the loss shear modulus G'' of 1 wt % TSX and 1 wt % Na-G solutions. In the TSX solutions G'' was larger than G' in the experimental temperature range, indicating that TSX solutions remained in sol state in this temperature range. The value of G'' was in the range from 0.1 to 1 Pa and the value of G' was lower than 0.1 Pa at 1.26rad/s. In the Na-G solutions, G' and G'' increased steeply around 25°C on cooling and decreased

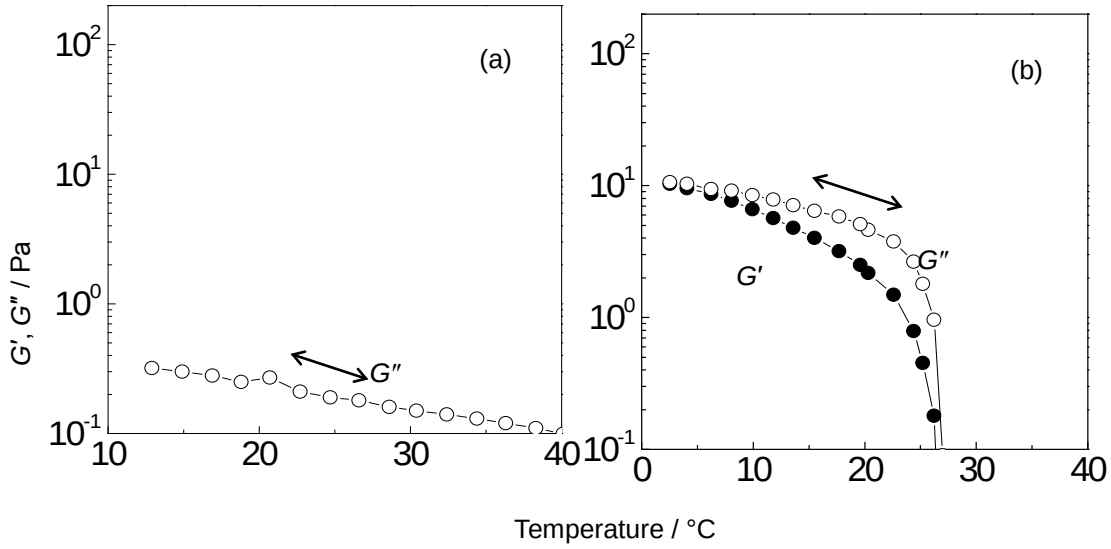

Figure 6.1. Temperature dependence of the storage and loss shear moduli, *G′* (●) and *G″*(○), of 1 wt % (a) TSX and (b) Na-G solutions at frequency of 1.26 rad/s and applied stress of 0.05 Pa. Cooling and heating rates; 0.5°C/min.

on heating without thermal hysteresis and *G″* was larger than *G′* at any temperature. The steep change of *G″* was attributed to a helix-coil transition of gellan molecules since it appeared in the temperature range at which DSC peak and a steep change in the ellipticity of CD measurements were observed (Matsukawa et al., 1999; Miyoshi and Nishinari, 1999b). Helix formation did not induce gel formation in 1 wt % Na-G solution in the present study. It could be considered that gel formation of the Na-G does not occur below 1 wt% since the number of helices and aggregates is not enough to form a percolated network as suggested previously (Miyoshi and Nishinari, 1999b).

Figure 6.2 shows temperature dependence of *G′* and *G″* of 1 wt % mixtures of TSX and Na-G. Results suggested that gel formation occurred by mixing TSX and Na-G at this concentration (1 wt %). On cooling, *G′* and *G″* were smaller than 0.1 Pa first and then increased steeply around 25°C at which *G′* exceeded *G″*. On heating *G′* and *G″* decreased gradually and then decreased steeply around 30°C. Thermal hysteresis was recognized on cooling and on heating in these mixtures even when the scan rate

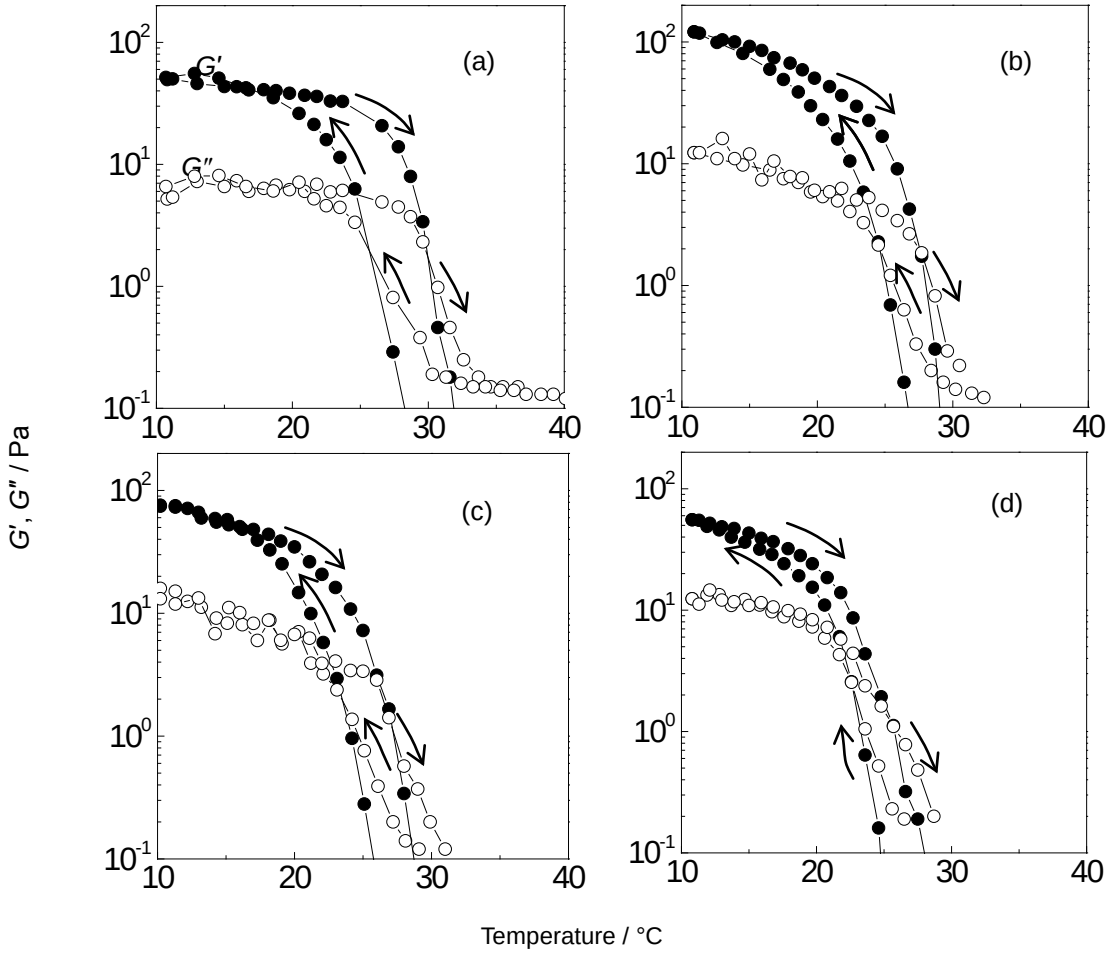

Figure 6.2 Temperature dependence of G' (●) and G'' (○), of 1 wt % mixtures on cooling and on subsequent heating at 1.26 rad/s and applied stress of 0.05Pa. TSX content; (a) 0.9, (b) 0.6, (c) 0.5 and (d) 0.4. Cooling and heating rates; 0.5°C/min.

was as low as 0.1°C/min (data not shown). In the case of agarose gels, it is considered that the thermal hysteresis is due to thermally stabilized network by aggregation between helices and such thermal hysteresis has often been observed in true gels (Clark and Ross-Murphy, 1987; Te Nijenhuis, 1997). Thus the experimental findings that G' became larger than G'' and that the thermal hysteresis was observed suggest that the gel formation occurred in the mixtures although each polysaccharide alone did not form a gel below 1 wt %.

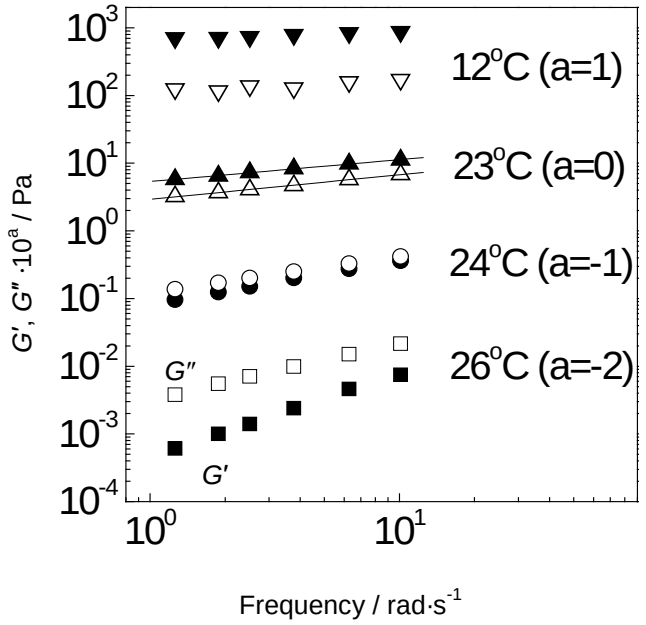

Figure 6.3 Frequency dependence of G' (closed) and G'' (open) obtained by multi-wave measurements of 1 wt % mixtures (TSX:Na-G = 5:5) at various temperatures. Data is shifted along the vertical axes by shift factor 'a' to avoid overlapping.

Figure 6.3 shows the frequency dependence of G' and G'' of 1 wt % mixtures (TSX:Na-G = 5:5) at various temperatures on cooling and Figure 6.4 shows the mechanical loss tangent tanδ of the mixtures at various frequencies on cooling. G' and G'' showed the same frequency dependence and thus tanδ (= G''/G') was independent of frequency at a certain temperature, above and below which the mixture behaved like viscoelastic fluids and viscoelastic solids, respectively. Thus the point at which a power law was obtained could be regarded as a gelation point. According to Winter-Chambon criteria (Winter and Chambon, 1986; Chambon and Winter, 1987), at critical gel point, G' and G'' show the same power laws in entire frequency range and thus n obtained from equation (1) would agree with n obtained from equation (2). The value of n_1 was obtained from the slope of frequency dependence of G' and G'' in equation (1) and n_2 was estimated from the value of tanδ in equation (2) at the point of

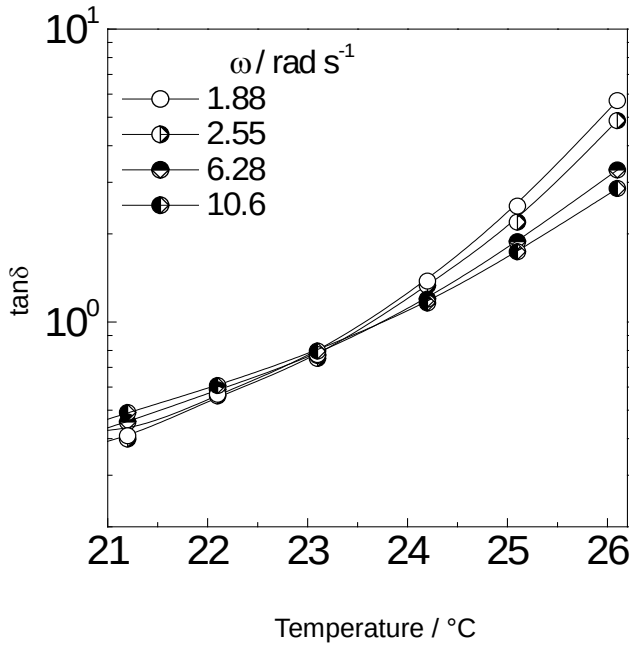

Figure 6.4 Temperature dependence of mechanical loss tangent, tanδ, of 1 wt % mixtures (TSX:Na-G = 5:5) at various frequencies on cooling at 0.5°C/min.

the same frequency dependence of G' and G''. The values of n_1 and n_2 are almost the same, $n_1 = n_2 = 0.42$. This indicates that a critical gel could be obtained in the mixture. The critical gel would possess a self-similar structure and such a structure can be formed when TSX and Na-G bind together to form a percolated network.

The gelation point could be determined by the Winter-Chambon criteria in other mixtures as well as mixtures with TSX content of 0.5. This was summarized in Table 6.1. The values of n_1 and n_2 ranged from 0.31 to 0.42 and are almost the same as the values of iota carrageenan gels (0.32-0.43) as reported by Hossain et al., (1997). Goycoolea et al. (2001) reported that a critical gel could be obtained in the mixture of galactomannan and deacylated xanthan in the ratio of 1:1, 4:1, and 1:1 with 1% dextran where tanδ at various frequencies showed the same value at a certain temperature.

Though they did not indicate the values of n explicitly, these values may be estimated as 0.47, 0.34, and 0.39, respectively, judging from the temperature dependence of tanδ at

Table 6.1 Temperatures at which power law was obtained on cooling and exponent n_1 and n_2 obtained from equation (1) and (2), respectively, of 1 wt % TSX and Na-G mixtures.

TSX content	Temp. / ℃	n_1	n_2
0.4	21	0.31	0.31
0.5	23	0.42	0.42
0.6	23	0.34	0.33
0.7	25	0.40	0.41

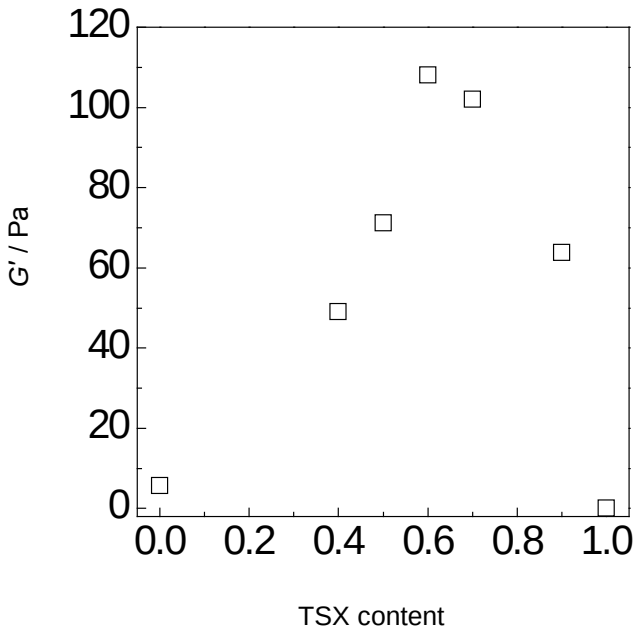

Figure 6.5. *G′* of 1 wt % mixtures as a function of TSX content at 12°C and 1.26 rad/s.

various frequencies for the galactomannan-deacylated xanthan mixtures (Goycoolea et al., 2001).

As expected, such critical point could not be obtained in the TSX alone and the Na-G alone at 1 wt % (data not shown). Hence it was suggested that synergistic interaction of TSX and Na-G induced gel formation. Figure 6.5 shows *G′* of 1wt% mixtures as a

function of TSX content. It is clear that synergistic interaction occurred in TSX and Na-G mixtures.

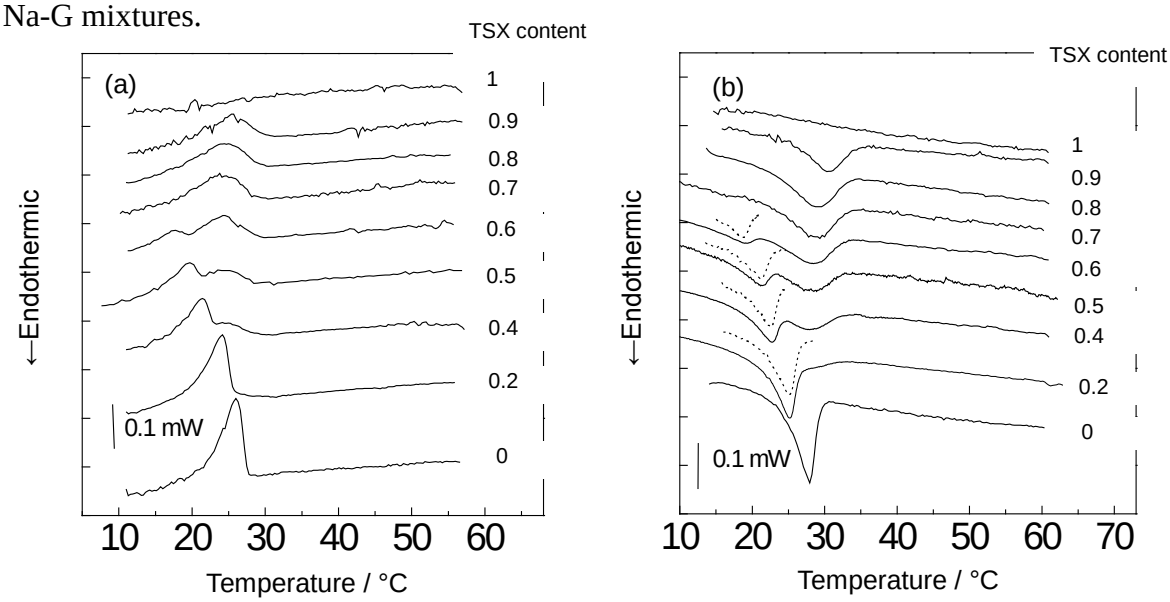

Figure 6.6 (a) Cooling and (b) heating DSC curves of 1 wt % mixtures (solid line) at various content of TSX and solutions of Na-G alone (dotted line) at various concentrations.

Figure 6.6 shows cooling and heating DSC curves for 1 wt % mixtures. DSC curves of 1 wt % TSX and 1 wt % Na-G were also shown. No peak for the TSX was observed and single peak appeared for the Na-G around 25°C, which is attributed to helix-coil transition of gellan. In the mixture, two peaks appeared when the content of TSX and that of Na-G were almost equal. The lower-temperature peak (~27°C for 1 % gellan alone) shifted to lower temperatures with decreasing concentration of gellan and this should be attributed to the conformational change in gellan. With decreasing Na-G content the lower-temperature peak became too small to be detected and the higher-temperature peak was observed in the temperature range from 25 to 30°C. We could not detect a peak of 0.1 wt % Na-G solution because of too low concentration to detect with negligible noise whereas 1 wt % mixture at the Na-G content of 0.1 showed a peak clearly. This suggests that the peak that appeared at higher temperatures might

be induced by the interaction of TSX and Na-G. The experimental findings that the junction zone formation induced by the interaction between gellan and xyloglucan appeared as a higher- temperature peak than the lower-temperature peak induced by the helix formation of gellan do not necessarily mean that the junction zones consisting of two polysaccharides are formed by disordered (coil form) gellan and xyloglucan because we cannot exclude the possibility that the coil-helix transition of gellan shifted to higher temperatures in the presence of xyloglucan.

Figure 6.7 shows endothermic peak temperatures of 1 wt % mixtures as a function of Na-G concentration. Endothermic peak temperatures of Na-G solutions at equal concentration of Na-G in the mixtures were also shown for comparison. It was found that Na-G alone showed DSC peak around the temperatures where the lower-temperature peak appeared in the mixtures. The lower-temperature peaks became more pronounced with increasing Na-G content and the shapes of the peaks were similar to those of the peaks for Na-G alone. These suggest that the lower-temperature peaks are attributed to helix-coil transition of Na-G and that the higher-temperature peaks stem from interaction of TSX and Na-G.

Circular dichroism (CD) results also supported that a higher-temperature DSC peak is due to the interaction of TSX and Na-G. CD spectra of the mixture could not be superposed on that of TSX or Na-G below 30°C.

Figure 6.8 (a) shows CD spectra of 0.5 wt % TSX solutions. Since TSX does not have chromophore that absorbs the light in the wavelength range from 200 to 250 nm, no peak was observed in this wavelength range. CD spectra were almost the same at 10 and 60°C and the ellipticity at 202nm was independent of temperature (Figure 6.8 (b)).

Figure 6.9 (a) shows CD spectra of 0.5 wt % Na-G solutions. Single peak appeared around 200 nm, which is due to carboxyl group in a repeating unit of gellan that absorbs the light around 200nm. Figure 6.9 (b) shows the ellipticity at 202nm as a function of temperature. The ellipticity at 202 nm shifted from positive to negative on cooling and

from negative to positive on heating around 20°C at which DSC peak appeared. The observed change in the ellipticity reflects the conformational change of gellan, i.e. the helix-coil transition (Matsukawa et al., 1999; Tanaka et al., 1996; Crescenzi et al., 1986).

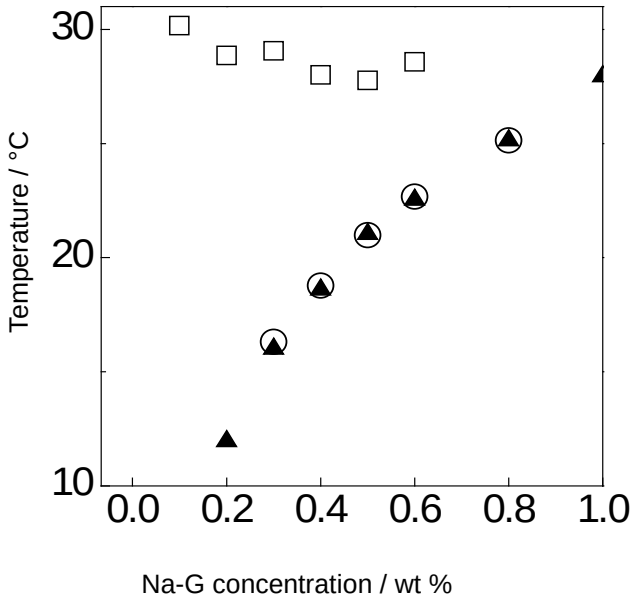

Figure 6.7 Endothermic peak temperatures (higher; □, lower; ○) of 1 wt % mixtures as a function of Na-G concentration and endothermic peak temperatures of solutions of Na-G alone (▲) at various concentrations in heating DSC curves.

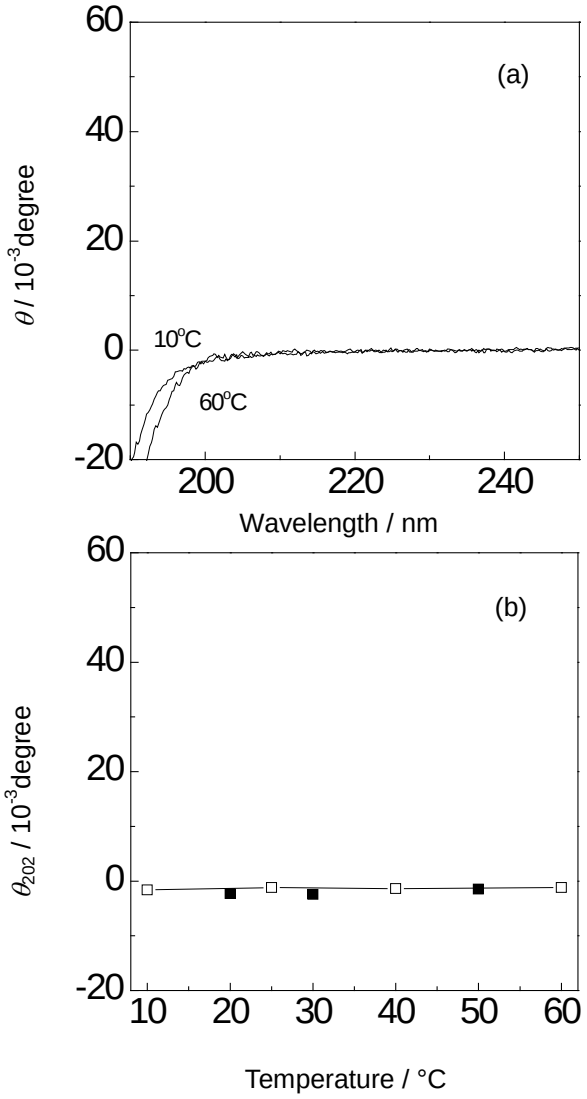

Figure 6.8 (a) The ellipticity, θ, of 0.5 wt % TSX solutions in the wavelength range from 190 to 250 nm at 10°C and 60°C and (b) the ellipticity at 202 nm, θ_{202}, on cooling (□) and on heating (■) at scan rate of ~1°C/min.

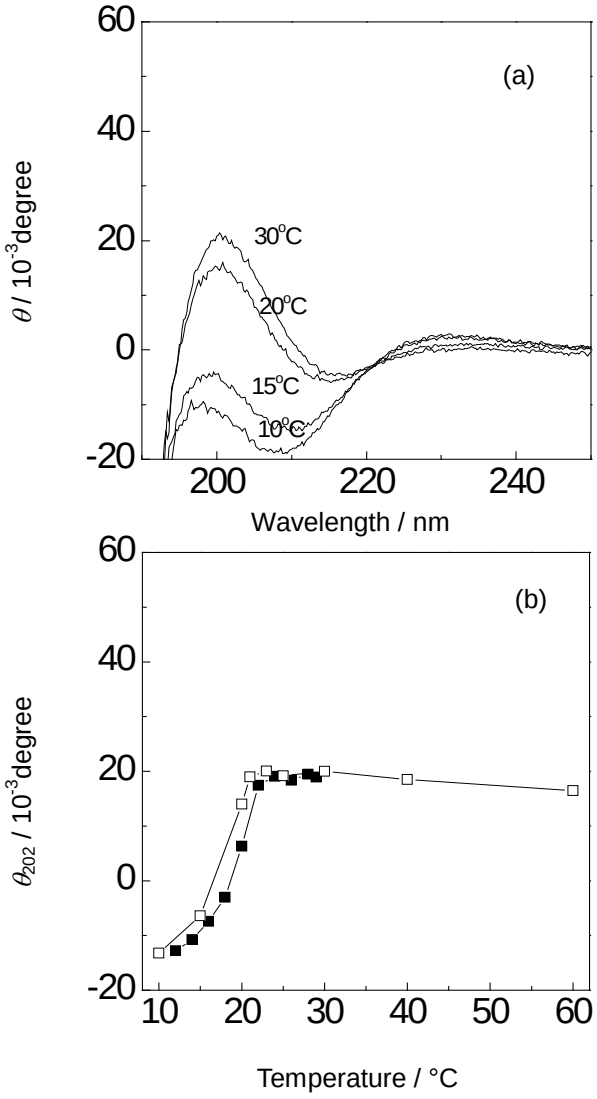

Figure 6.9 (a) The ellipticity, θ, of 0.5 wt % Na-G solutions in the wavelength range from 190 to 250 nm at different temperatures and (b) the ellipticity at 202 nm, θ_{202}, on cooling (□) and on heating (■) at scan rate of ~1°C/min.

Figure 6.10(a) shows CD spectra of 1 wt % mixtures at TSX:Na-G of 5:5. Single peak appeared around 200 nm, which might stem from carboxyl groups of gellan in the mixtures. At high temperatures, at disordered state of gellan, the magnitude of the ellipticity at 202 nm was almost the same as that of Na-G alone as shown in Figure 6.10 (b). This indicates that molecular environment around carboxyl groups was not influenced by TSX molecules at higher temperatures. As shown in Figure 6.10 (b) the ellipticity at 202 nm increased steeply, which was not observed in Na-G alone, on cooling around 25 to 30°C at which the higher-temperature peak appeared in DSC curves (Figure 6). Then the ellipticity decreased below 25°C at which the lower-temperature peak appeared in DSC curves. The ellipticity traced a similar course on heating to that on cooling. It was suggested that the change in the ellipticity at higher temperature range was induced by the interaction of TSX and Na-G and the change at lower temperature range was induced by the helix-coil transition of gellan.

Figure 6.11 shows CD results of 1 wt % mixtures at TSX:Na-G of 7:3. Figure 6.12 shows CD results of 1 wt % mixtures at TSX:Na-G of 9:1. As shown in Figure 6.11 (b) and Figure 6.12 (b), the ellipticity at 202 nm increased steeply on cooling around 25 to 30°C at which the higher-temperature peak appeared in DSC curves (Figure 6.6). In DSC measurements, only the higher-temperature peak appeared in the mixutures containing higher amount of TSX. CD results showed only increase of the ellipticity at 202 nm in the mixutures containing higher amount of TSX. These results does not conflict with the DSC results.

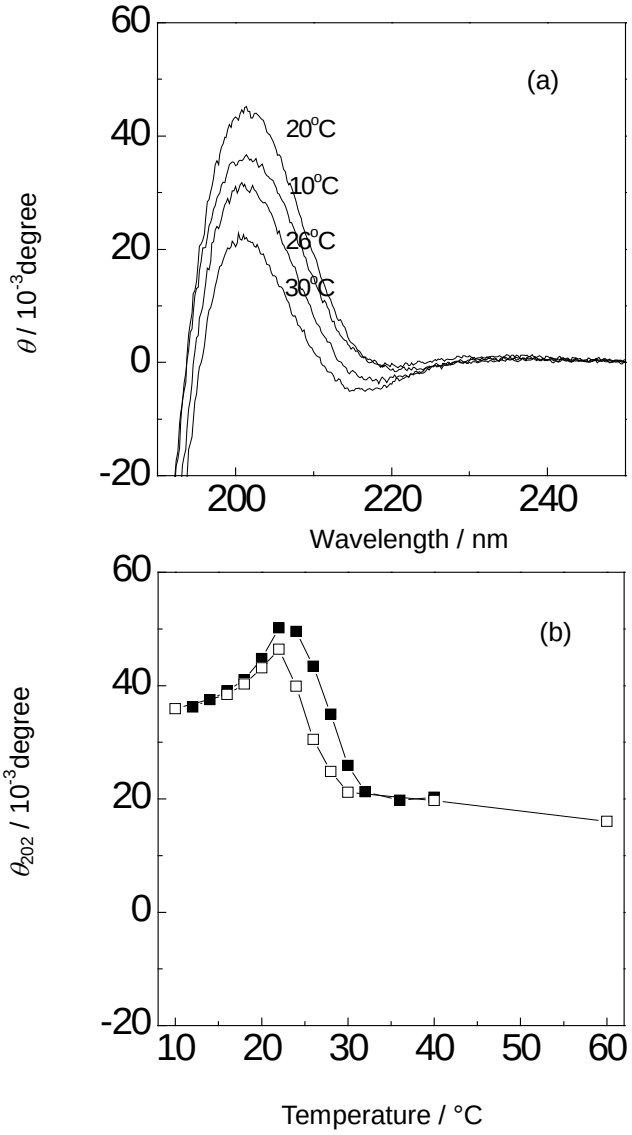

Figure 6.10 (a) the ellipticity, θ, of 1 wt % mixtures (TSX:Na-G = 5:5) in the wavelength range from 190 to 250 nm at different temperatures and (b) the ellipticity at 202 nm, θ_{202}, on cooling (□) and on heating (■) at scan rate of ~1°C/min.

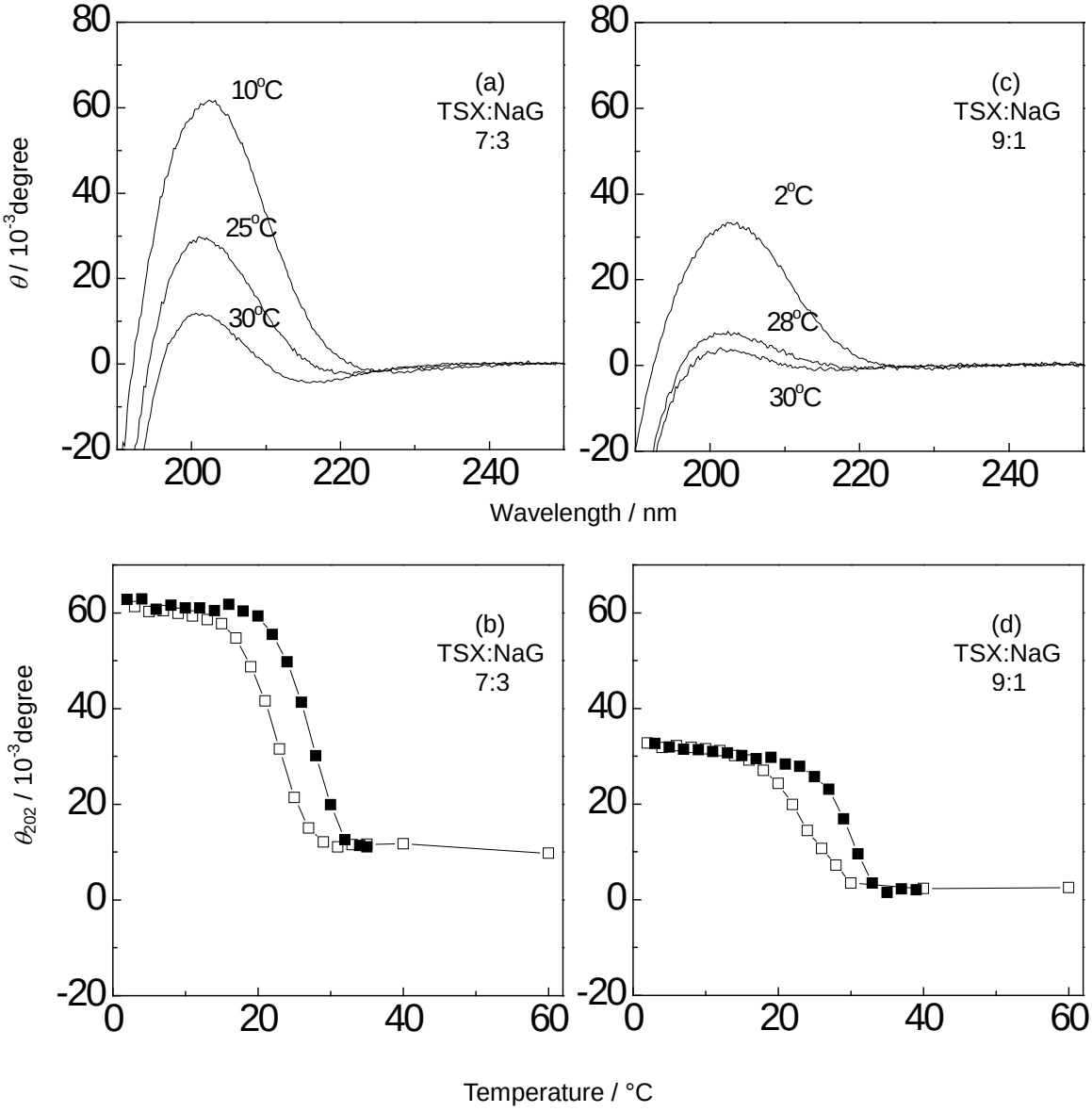

Figure 6.11 (a), (c) the ellipticity, θ, of 1 wt % mixtures in the wavelength range from 190 to 250 nm at different temperatures and (b), (d) the ellipticity at 202 nm, θ_{202}, of 1 wt % mixtures on cooling (□) and on heating (■) at scan rate of ~1°C/min.

In the mixture of Na-type κ-carrageenan/konjac glucomannan (total polysaccharide concentration 0.6%), as observed in the present study, two DSC peaks were observed (Williams et al., 1993): the lower temperature peak, which appeared only in mixtures in which the content of Na-type κ-carrageenan exceeded a certain limit, and shifted to higher temperatures with increasing κ-carrageenan content, was attributed to the κ-carrageenan alone and the higher temperature peak was concluded to be induced by the interaction between κ-carrageenan and konjac glucomannan. The higher-temperature peak induced by the interaction of these two polymers, shifted slightly to higher temperatures with increasing concentration of konjac glucomannan although konjac glucomannan alone did not show any peak. However, in the mixture of K-type κ-carrageenan/konjac glucomannan (Kohyama et al., 1996), although similar two DSC peaks were also observed, the higher-temperature peak, which was induced by the interaction of K-type κ-carrageenan and konjac glucomannan, shifted to higher temperatures with increasing concentration of K-type κ-carrageenan because the total concentration of the mixtures was fixed to 1.5%. The different behaviours of two mixtures, Na-type κ-carrageenan/konjac glucomannan and K-type κ-carrageenan/konjac glucomannan, should be studied further in the near future.

In the present mixture of Na-G/TSX, the helix-coil transition temperature of gellan shifted to lower temperatures remarkably with decreasing the Na-G content whereas the peak stemming from interaction of Na-G and TSX shifted to higher temperatures slightly with decreasing the content of Na-G. This behaviour of TSX/Na-G mixtures resembles that of the mixture of Na-type κ-carrageenan/konjac glucomannan (Williams et al., 1993).

Synergistic interaction of helix-forming polysaccharides and galactomannans, which results in the increase of viscosity and elastic modulus, depends on galactose content in galactomannans. It has been proposed that “smooth” region where galactose is absent interacts with helix-forming polysaccharides (Dea et al., 1972). Galactose in TSX also plays an important role for its solution properties. Yamanaka et al. (1999) reported

that partial removal of galatcose promoted lateral aggregation and TSX treated in this way formed a strong gel confirming the previous findings (Shirakawa et al., 1998). TSX seems to form aggregates in the solution, which makes it difficult to determine molecular weight (Lang and Burchard, 1993). Thus it was considered that even in sol state, smooth (galactose free) regions tend to aggregate. We suggest that galactose free region of TSX interacts with helical gellan to form a three-dimensional network in the mixture of TSX and Na-G.

As shown in Fig. 6.2, the degree of thermal hysteresis increased with increasing TSX content. The gelation temperature shifted to higher temperatures with increasing TSX content (Fig. 6.2 and Table 6.1). This indicates that the mixed gels became more heat-resistant with increasing TSX content. Agreement of the gelation temperature and DSC peak temperatures at which interaction of Na-G and TSX occurred indicates that a network formation is induced by an ordered structure formation by synergistic interaction.

6.1.4 Conclusion

Interaction of tamarind seed xyloglucan (TSX) and sodium form gellan (Na-G) was investigated by various techniques. Viscoelastic measurements revealed that gel formation occurred in the mixture of TSX and Na-G although individual polysaccharide did not form a gel at experimental concentrations. Gel formation occurred at a critical gel point where both equations $G' \sim G'' \sim \omega^n$ and $\tan\delta = \tan(n\pi/2)$ hold simultaneously. The appearance of the maximum G' as a function of TSX content provided clear evidence of a synergistic interaction of TSX and Na-G. The synergistic interaction of TSX and Na-G could be detected as a DSC peak that appeared at higher temperatures than a DSC peak arising from helix-coil transition of Na-G alone. The interaction could also be detected as a change in circular dichroism which was not observed in TSX alone and Na-G alone. We confirm that a mixture of TSX and Na-G is a new system

which shows a synergistic interaction between a 1, 4-β-D plant polysaccharide and a helix-forming polysaccharide, providing us a new type of texture modifier.

6.2 THE EFFECT OF SALT ON GELATION OF TAMARIND SEED XYLOGLUCAN/GELLAN MIXTURE

6.2.1 Introduction

In a previous study, it was found that mixing gellan and TSX formed a thermoreversible gel under non-gelling condition of individual polysaccharide and induced changes in DSC and circular dichroism (CD) which were not observed in TSX alone and Na-G alone. To further understand the mechanism involved, it is desirable to clarify the relation between helix formation of gellan and the synergistic interaction.

Addition of salts is a simple way to change the thermal stability of helices of polyelectrolyte gellan. In the present study, the synergistic interaction of TSX and Na-G in the presence of NaCl was investigated using viscoelastic measurements. DSC and CD measurements were also carried out to probe the conformational change of gellan.

6.2.2 Experimental

Sodium salt form of gellan gum (Na-G) and Tamarind seed xyloglucan (TSX) were the same as that used in Chapter 6.1. TSX and Na-G were dispersed in distilled water or NaCl solutions separately at a concentration of 0.1 wt % and stirred at 20±2°C overnight. The samples were heated to 80°C for 1 hour and 90°C for 10min and then were mixed at various ratios.

The storage and loss shear moduli, G' and G'', were measured using a stress-controlled rheometer, Rheostress1 from Haake Ltd., Germany. About 6g of the sample solution was poured into a double-gap cylinder geometry (diameter of the cup = 43.4mm; outer gap = 0.3mm; inner gap = 0.25mm; height = 55mm) at 60°C and then immediately covered with silicone oil to prevent the evaporation of water. Before measuring temperature dependence and frequency dependence of G' and G'', strain

dependence of G' and G'' was examined to determine a linear viscoelastic regime. The temperature was controlled by a Haake circulator DC30-K10 (Haake, Germany).

Circular dichroism (CD) measurements were carried out with a JASCO-820A spectropolarimeter, Japan Spectroscopic Co. Ltd., Japan using a rectangular cell which has an optical path length of 2 or 10mm. Temperature was controlled by a Peltier element (RTC9423L type, Japan Spectroscopic Co. Ltd., Japan). The molecular ellipticity of the samples was measured in the wavelength range from 190 to 250nm at various temperatures.

6.2.3 Results and discussion

Figure 6.12 shows cooling and subsequent heating DSC curves of 1 wt % mixtures (TSX:Na-G = 1:1) in the presence or absence of NaCl. DSC curves of 0.5 wt% Na-G solutions were also shown for comparison. In the absence of NaCl, two peaks appeared around 30ºC and around 25ºC. The higher-temperature peak and the lower-temperature peak were attributed to the synergistic interaction and the coil-to-helix transition, respectively, since the higher-temperature peak appeared only by mixing Na-G with TSX and the lower peak temperature agreed well with T_{ch} of 0.5 wt% Na-G. With increasing NaCl concentration, DSC peak arising from the normal helix-coil transition of gellan shifted to higher temperatures. On the other hand, DSC peak arising from the interaction of gellan and xyloglucan became unclear by addition of NaCl. In 25 or 50mM NaCl, significant differences were not observed in DSC curves between the mixture and Na-G alone. In the presence of NaCl, unlike the mixture of κ-carrageenan and KGM, the DSC peak arising from the interaction did not shifted to higher temperatures accompanying the DSC peak of the helix coil transition of gellan.

Fig. 6.13 shows cooling and subsequent heating DSC curves of 1 wt % mixtures (TSX:Na-G = 4:1). DSC curves of 0.2 wt% Na-G solutions were also shown for comparison. In this mixing ratio, a single peak appeared around 30°C in the absence

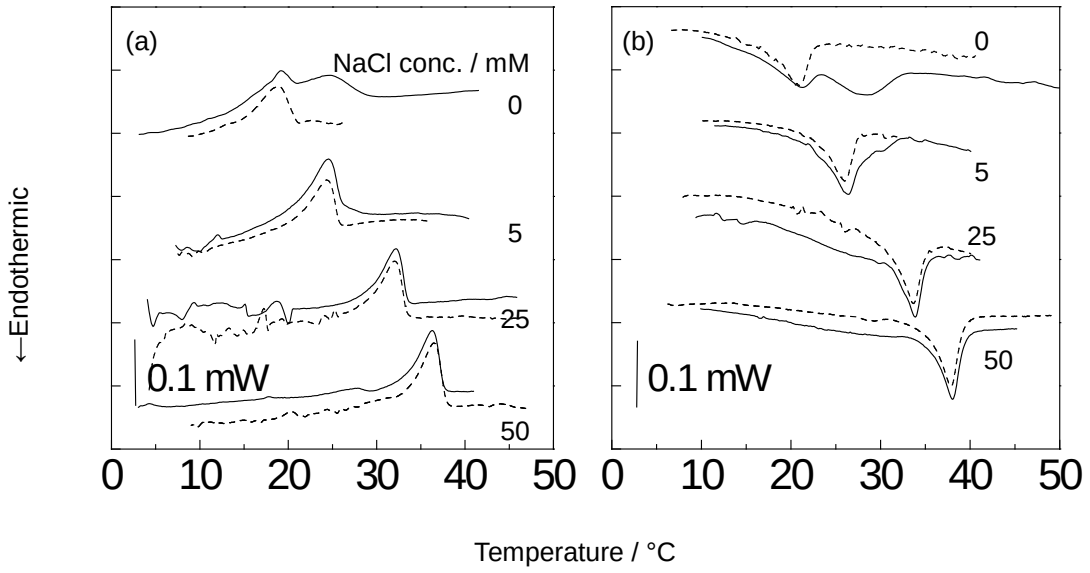

Figure 6.12 (a) Cooling and (b) subsequent heating DSC curves for 1 wt % mixtures (solid line, TSX:Na-G = 1:1) and 0.5 wt% Na-G solutions (dashed line) in presence/absence of NaCl at 0.5°C/min.

of NaCl and it was attributed to the synergistic interaction since the peak appeared only by mixing Na-G with TSX and Na-G alone or TSX alone did not show a DSC peak at this experimental condition. In 30mM NaCl, on cooling, a single peak appeared around 32°C in the mixture and the peak in Na-G solution also appeared at the same temperature. This peak in the mixture was considered to be due to the normal coil-to-helix transition of gellan. On subsequent heating, a broad peak and another peak appeared around 25°C and 35°C in the mixture. In Na-G solutions a single peak was observed around 35°C. Thus the peak observed around 35°C was attributed to helix-to-coil transition of gellan alone. This suggests that the peak around 25°C was due to the synergistic interaction. In the DSC results of κ-carrageenan and KGM system, DSC peak of the interaction was observed at slight higher temperatures than the coil-to-helix transition temperatures of κ-carrageenan at various KCl concentration (10-150 mM). DSC peaks stemming from the interaction shifted to higher

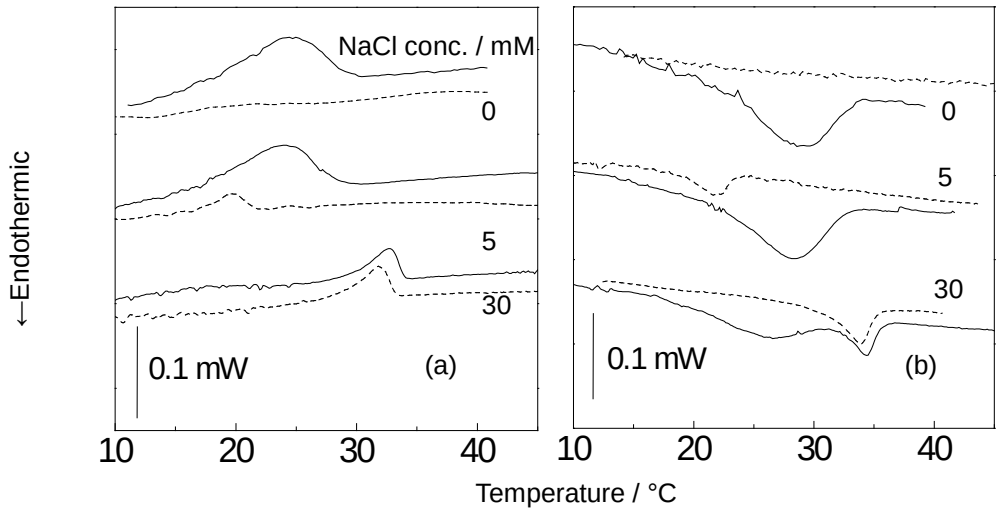

Figure 6.13 (a) Cooling and (b) subsequent heating DSC curves for 1 wt % mixtures (solid line, TSX:Na-G = 4:1) and 0.2 wt% Na-G solutions (dashed line) in presence/absence of NaCl at 0.5°C/min.

temperatures accompanying DSC peaks of the coil-to-helix transition of κ-carrageenan with increasing KCl concentration. This suggests that interacting mechanism involved is different between κ-carrageenan/KGM system and gellan/xyloglucan system. On the other hand, in xanthan/KGM mixtures, the interaction occurred at almost the same temperature irrespective of the presence of salt although thermal stability of xanthan helices was enhanced by the addition of salt (Annable et al., 1994). As shown in Fig.2, the interaction of gellan and xyloglucan seemed to occur at almost same temperature irrespective of the presence of salt. In terms of effect of salt on the interaction temperature, gellan/xyloglucan system is more similar to xanthan/KGM mixtures.

Fig. 6.14 shows temperature dependence of G'' and θ_{202} of 0.1 wt% mixture (Na-G:TSX = 1:1) and 0.05 wt% Na-G solution on cooling in the absence/presence of NaCl. In the absence of NaCl, Na-G alone maintained a disordered conformation at 0.05 wt%; G'' and θ_{202} of Na-G solutions did not show a significant change as a

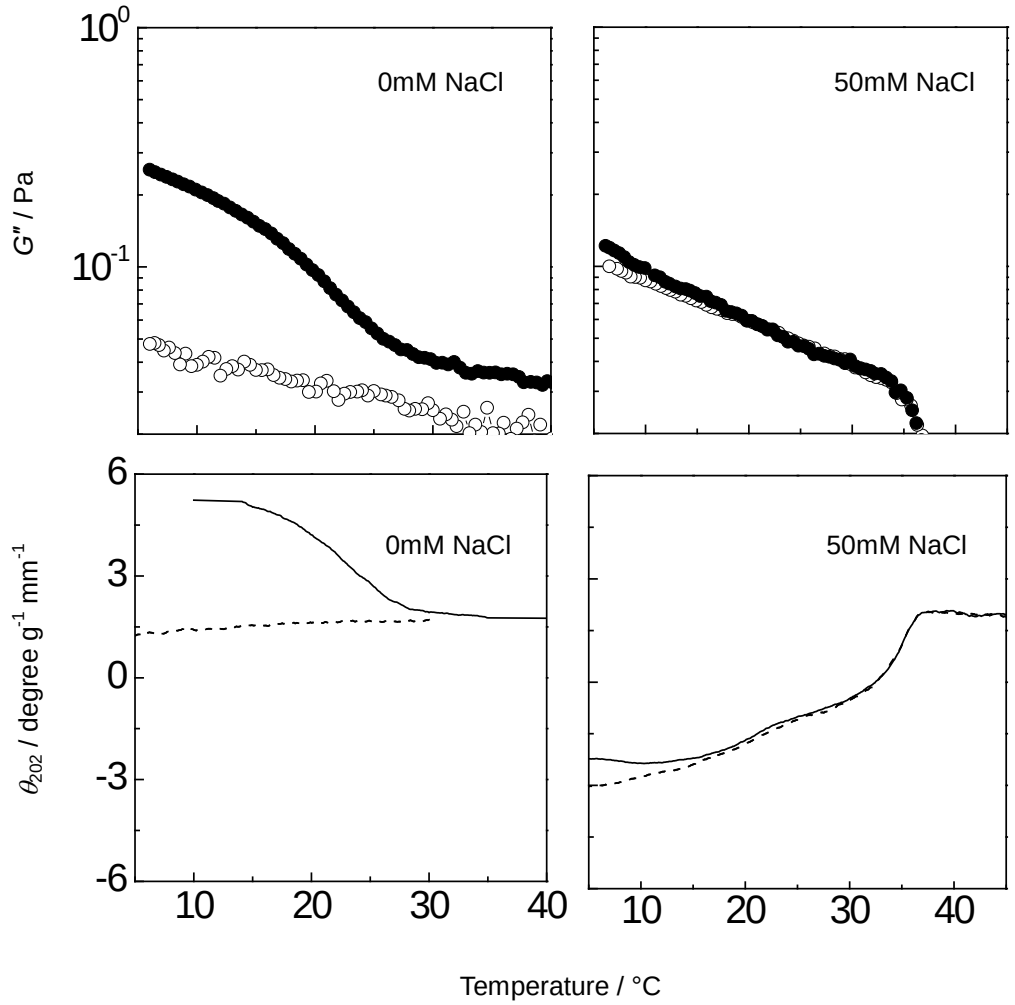

Figure 6.14 Temperature dependence of G'' of 0.1 wt% mixture (●, Na-G:TSX = 1:1) and 0.05 wt% Na-G solution (○) on cooling at various NaCl concentrations. Frequency 1.6Hz. Cooling rate, 0.5°C/min. Temperature dependence of θ_{202} of 0.1 wt% mixture (solid line, Na-G:TSX = 1:1) and 0.05 wt% Na-G solution (broken line) on cooling at various NaCl concentrations.

function of temperature above 0°C. In the mixture, G'' and θ_{202} increased steeply around 25°C on cooling, which was attributed to the synergistic interaction of Na-G and TSX.

In the presence of NaCl, G'' increased whereas θ_{202} decreased steeply at a certain temperature, indicating that a coil-to-helix transition occurred in gellan. It is believed that gellan molecules change from disordered chains to double helices on cooling at

sufficient amount of cations which will shield electrostatic repulsion of gellan (Miyoshi and Nishinari 1999). At the experimental condition in the present study, a sufficient amount of cations for the helix formation was provided by addition of NaCl. The coil-to-helix transition temperature, T_{ch}, shifts to higher temperatures with increasing NaCl concentrations in many reports and indicates that addition of salts enhances the thermal stability of gellan helices.

The decrease in θ_{202} on cooling has been reported in gellan systems whereas the increase in θ_{202} on cooling has not been reported in any of other gellan systems except the present mixture with TSX. Thus we regard the increase in θ_{202} on cooling as a result of conformational change of gellan induced by the interaction with TSX. From CD measurements, we distinguish the normal coil-to-helix transition of gellan indicated by a decrease in θ_{202} from the conformational change of gellan induced by the interaction with TSX indicated by an increase in θ_{202} on cooling.

CD results revealed that both the interaction with TSX and the coil-to-helix transition occurred in the mixture in 50mM NaCl as shown in Fig. 6.14. Around 35°C, the behavior of G'' and θ_{202} indicated that the coil-to-helix transition of gellan occurred. G'' and θ_{202} of the mixture were almost the same as those of Na-G alone above 20°C, below which G'' and θ_{202} became a little larger than those of the Na-G alone. This suggests that the interaction of gellan and TSX occurred below 20°C.

In the presence of 50mM NaCl, although Na-G seems to interact with TSX, the interaction was suppressed compared to the case without addition of NaCl. As shown in Fig. 6.14, G'' in 50mM NaCl was smaller than that in 0mM NaCl at lower temperatures. These indicated that the interaction of Na-G and TSX was prevented in the presence of 50mM NaCl.

The results above indicated that synergism reduced when the helix formation of gellan was enhanced by addition of NaCl. Further addition of NaCl promotes further helix formation and leads to gel network of gellan. It is expected that TSX will not improve the elastic modulus of gellan gels obtained by further addition of NaCl.

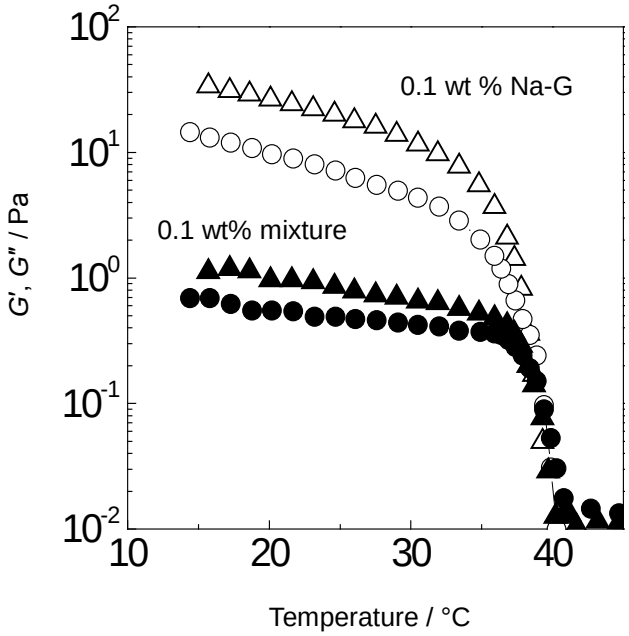

Figure 6.15 Temperature dependence of G' (open) and G'' (closed) of 0.1 wt % mixtures (TSX:Na-G = 1:1) and 0.1 wt % Na-G solutions in 80mM NaCl. Cooling rate, 0.5°C/min. Frequency, 1Hz.

Fig. 6.15 shows temperature dependence of G' and G'' of 0.1 wt% mixture (TSX:Na-G = 1:1) and 0.1 wt% Na-G in 80mM NaCl. G' and G'' increased steeply around 40°C below which G' and G'' showed a gel-type rheological behavior; G' and G'' was almost independent of frequencies from 0.1 to 100 rad/s maintaining $G' > G''$ (data not shown). This suggested that helix formation occurred around 40°C and at the same time three-dimensional network was obtained. As expected, the shear modulus and gelation temperature of gellan gels was not enhanced by the presence of TSX.

One possible reason why addition of salt prevented the synergistic interaction is that the tendency of self-association of gellan became stronger by the electrostatic shielding effect and aggregation of gellan proceeded consequently at the expense of formation of intermolecular binding between gellan and xyloglucan during the synergistic interaction. This interpretation was proposed before in the xanthan/konjac glucamannan (KGM) mixtures (Annable et al., 1994).

6.2.4 Conclusion

Synergistic interaction between gellan and TSX was studied in the addition of salts by rheology, DSC and CD. Gellan and TSX interacted at a certain temperature when the mixtures were cooled in the absence of salts. The interaction became less significant when the mixture was cooled in the presence of NaCl.

References

Ablett, S., Lillford, P. J., Baghdadi, A. M. A., and Derbyshire, W. (1978) Nuclear magnetic-resonance investigations of polysaccharide films, sols, and gels. 1. Agarose. *J.Colloid Interf. Sci.*, **67**, 355-377.

Amari, T., and Nakamura, M. (1978) Stress relaxation of aqueous gels of amylose, amylopectin, and their blends. *J. Soc. Rheol. Jpn.*, **6**, 28-31.

Annable, P., Williams, P. A., and Nishinari, K. (1994) Interaction in xanthan-glucomannan mixtures and the influence of electrolyte. *Macromolecules*, **27**, 4204-4211.

Aoki, Y., Li, L., and Kakiuchi, M. (1998) Rheological images of poly(vinyl chloride) gels. 6. Effect of temperature. *Macromolecules*, **31**, 8117-8123.

Aymard, P., Martin, D. R., Plucknett, K., Foster, T. J., Clark, A., and Norton, I. T. (2001) Influence on thermal history on the structural and mechanical properties of agarose gels. *Biopolymers*, **59**, 131-144.

Baird, J. K., Talashek, T. A., and Chang, H. (1992) Gellan gum: effect of composition on gel properties. In "*Gums and Stabilisers for the food Industry 6*", Edited. by Phillips, G. O., Williams, P. A., and Wedlock, D. J., IRL Press, Oxford, pp.479-487.

Baumgärtel, M., and Willenbacher, N. (1996) The relaxation of concentrated polymer solutions. *Rheol. Acta*, **35**, 168-185.

Blatz, P. J., Sharda, S. C., and Tschoegl, N. W. (1974) Strain energy function for rubberlike materials based on a generalized measure of strain. *Trans. Soc. Rheol.*, **18**, 145-161.

Bot, A., Amerogen, I., A., Groot, R. D., Hoekstra, N. L. and Agterof, G. M. (1996a) Large deformation rheology of gelatin gels. *Polymer Gels and Networks*, **4**, 189-227.

Bot, A., Groot, R. D. and Agterof, G. M. (1996b) Non-linear elasticity and rupture of gelatin gels. In "*Gums and stabilisers for the food inductry 8*" Edited by Phillips, G. O., Williams, P. A. and Wedlock, D. J., IRL Press, Oxford, pp. 117-126.

Cairns, P., Miles, M. J., Morris, V. J., and Brownsey, J. (1987) X-ray fibre-diffraction studies of synergistic binary polysaccharide gels. *Carbohydr. Res.*, **160**, 411-423.

Chambon, F., and Winter, H. H. (1987) Linear viscoelasticity at the gel point of a crosslinking PDMS with imbalanced stoichiometry. *J. Rheol.*, **31**, 683-697.

Chandrasekaran, R., Radha, A., and Thailambal, V. G. (1992) Roles of potassium ions, acetyl and L-glyceryl groups in native double helix: an X-ray study. *Carbohydr. Res.*,

224, 1-17.

Chandrasekaran, R., and Thailambal, V. G. (1990) The lnfluence of calcium ions, acetate and L-glycerate groups on the gellan double helix. *Carbohydr. Polym*., **12** 431-442.

Chen, Z., Zhu, Q. Y., Tsang, D., and Huang, Y. (2001) Degradation of green tea catechins in tea drinks. *J. Agric. Food Chem*., **49**, 477-482.

Chronakis, I. S., Doublier, J., and Piculell, L. (2000) Viscoelastic properties for kappa- and iota-carrageenan in aqueous NaI from the liquid-like to the solid-like behavior. *Int. J. Biol. Macromol*., **28**, 1-14.

Chronakis, I. S., Piculell, L., and Borgström, J. (1996) Rheology of kappa-carrageenan in mixtures of sodium and cesium iodide: two types of gels. *Carbohydr. Polym*., **31**, 215-225.

Clark, A. H., and Ross-Murphy, S. B. (1987) Agar. *Adv. Polym. Sci*., **83**, 122-125.

Crescenzi, V., and Dentini, M. (1988) Solution conformation of the polysaccharide gellan. In "*Gums and Stabilisers for the Food Industry 4*", Edited by Phillips, G. O., Williams, P. A. and Wedlock, D. J., Oxford. Univ. Press, Oxford, pp.63-69.

Crescenzi, V., Dentini, M., Coviello, T., and Rizzo, R., (1986) Comparative analysis of the behavior of gellan gum (S-60) and welan gum (S-130) in dilute aqueous solution. *Carbohydr. Res*., **149**, 425-432.

Davis, A. L., Cai, Y., Davies, A. P., and Lewis, J. R. (1996) ^{1}H and ^{13}C NMR assignments of some green tea polyphenols. *Magn. Reson. Chem*., **34**, 887-890.

Dea, I. C. M., McKinnon, A. A., and Rees, D. A. (1972) Tertiary and quaternary structure in aqueous polysaccharide systems which model cell wall cohesion: reversible changes in conformation and association of agarose, carrageenan and galactomannans. *J. Mol. Biol*., **68**, 153-172.

Djabourov, M., Leblond, J., and Papon, P. (1988) Gelation of aqueous gelatin solutions Ⅱ. Rheology of the sol-gel transition. *J. Phys. France*, **49**, 333-343.

Fang, Y., Takahashi, R., and Nishinari, K. (2004) A gel network constituted by rigid schizophyllan chains and nonpermanent cross-links. *Biomacromol*., **5**, 126-136.

Gidley, M. J., Lillford, P. J., Rowlands, D. W., Lang, P., Dentini, M., Crescenzi, V., Edwards, M., Fanutti, C., and Reid, J. S. G. (1991) Structure and solution properties of tamarind-seed polysaccharide. *Carbohydr. Res*., **214**, 299-314.

Glicksman, M. (1986) Tamarind seed gum. In "*Food Hydrocolloids*, Vol. III", Edited by Glicksman M., CRC Press, Florida, pp.191-202.

Goycoolea, F. M., Milas, M., and Rinaudo, M. (2001) Associative phenomena in galactomannan-deacylated xanthan systems. *Int. J. Biol. Macromol*., **29**, 181-192.

Grasdalen, H., and Smidsröd, O. (1981) Iodide-specific formation of κ-carrageenan single helices -I- 127NMR spectroscopic evidence for slective site binding of iodide anions in the ordered conformation. *Macromolecules*, **14**, 1842-1845.

Guenet, J..M. (1992) "*Thermoreversible gelation of polymers and biopolymers*",

Academic press, London.

Gunning, A. P., and Morris, V. J., (1990) Light scattering studies of tetramethyl ammonium gellan. *Int. J. Biol. Macromol*., **12**, 338-341.

Hatakeyama, T. and Quinn, F. X. (1994) "*Thermal Analysis*". John Wiley & Sons Ltd, England.

Hossain, K. S., Nemoto, N., and Nishinari, K. (1997) Dynamic viscoelasticity of iota carrageenan gelling system near sol-gel transition. *NIHON REOROJĪ GAKKAISHI,* **25**, 135-142.

Hsu, S., and Jamieson, A. M. (1993) Viscoelastic behavior at the thermal sol-gel transition of gelatin. *Polymer*, **34**, 2602-2608.

Ikeda, S., Morris, V. J., and Nishinari, K., (2001) Microstructure of aggregated and nonaggregated κ-carrageenan helices visualized by atomic force microscopy. *Biomacromol*., **2**, 1331-1337.

Ikeda, S., and Nishinari, K., (2001) "Weak gel"-type rheological properties of aqueous dispersions of nonaggregated κ-carrageenan helices. *J. Agric. Food Chem*., **49**, 4436-4441.

Ikeda,S., Nitta,Y., Kim, B. S., Temsiripong, T., Pongsawatmanit, R., and Nishinari, K. (2004) Single-phase mixed gels of xyloglucan and gellan. *Food Hydrocoll*. **18**, 669-675

Innden, T., and Yokawa, T. (1999) Practice of texture control. In "*Shin Shokkan Jiten*". Edited by Nishinari, K., Nakazawa, F., Katsuta, K., and Toda, J., Science forum, Tokyo, pp.304-307.

Inoue, M. B., Inoue, M., Fernando, Q., Valcic, S., and Timmermann, B. N. (2002) Potentiometric and ^{1}H NMR studies of complexation of Al^{3+} with (−)-epigallocatechin gallate, a major active constituent of green tea. *J. Inorg. Biochem.*, **88**, 7-13.

Jansson, P. E., Lindberg, B., and Sandford, P. A. (1983) Structural studies of gellan gum, an extracellular polysaccharide elaborated by *Pseudomonas elodea*. *Carbohydr. Res*., **124**, 135-139.

Katayama, M., and Katayama, Y. (1997) Dietary fiber. In "*Nutritional Physiology and Biochemistry*". Sangyo Book Ltd., Tokyo, pp.87-90.

Kennedy, D. O., Nishimura, S., Hasuma, T., Yano, Y., Otani, S., and Yuasa, I. (1998) Involvement of protein tyrosine phosphorylation in the effect of green tea polyphenols on Ehrlich ascites tumor cells in vitro. *Chemico-Biologcal Interactions*, **110**, 159-172.

Kohyama, K., Iida, H., and Nishinari, K. (1993) A mixed system composed of different molecular weights konjac glucomannan and kappa carageenan: large deformation and dynamic viscoelastic study. *Food Hydrocoll*. **7**, 213-226.

Kohyama, K., Sano, Y., and Nishinari, K. (1996) A mixed system composed of different

molecular weights konjac glucomannan and kappa-carrageenan. 2. Molecular weight dependence of viscoelasticity and thermal properties. *Food Hydrocoll.*, **10**, 229-238

Koike, A., Nemoto, N., Takahashi, M., and Osaki, K. (1994) Dynamic viscoelasticity of end-linking α,ω-dimethyl silyl poly(propylene oxide) solutions near the gel point. Polymer, **35**, 3005-3010.

Kuo, M. S., Mort, A. J., and Dell, A. (1986) Identification and location of L-glycerate, an unusual acyl substituent in gellan gum. *Carbohydr. Res.*, **156** 173-187.

Kögler, G., and Mirau, P. A. (1992) Two-dimensional NMR studies of intermolecular interactions in poly(vinyl chloride)/poly(methyl methacrylate) mixtures. *Macromolecules*, **25**, 598-604.

Lang, P., and Burchard, W. (1993) Structure and aggregation behavior oftamarind seed polysaccharide in aqueous solution. *Makromol. Chem.*, **194**, 3157-3166.

Lapasin, R., and Pricl, S. (1995) Industrial applications of polysaccharides. In "*Rheology of Industrial Polysaccharides*". Chapman & Hall, New York, pp.134-161.

Launay B., Cuvelier, G., and Martinez-Reyes, S. (1984) Xanthan gum in various solvent conditions: intrinsic viscosity and flow properties. In "*Gums and Stabilisers for the Food Industry 2*", Edited by Phillips, G. O., Williams, P. A., Wedlock, D. J., Pergamon Press, Oxford, pp.79-98.

Laye, P. G. (2002) Differential thermal analysis and differential scanning calorimery. In "*Principles of Thermal Analysis and Calorimetry"*, Edited by Haines, P. J., The Royal Sciety of Chemistry, Cambridge, pp.55-93

Luck G., Liao H., Murray, N. J., Grimmer, H. R., Warminski, E. E., Williamson, M. P., Lilley, T. H., and Haslam, E. (1994) Polyphenols, astringency and proline-rich proteins. *Phytochemistry,* **37**, 357-371.

Marlett, J. A., McBurney, M. I., and Slavin, J. L. (2002) Position of the American Dietetic Association: Health implication of dietary fiber. *J. Am. Diet. Assoc.*, **102**, 993-1000.

Matsukawa, S., Tang, Z., and Watanabe, T. (1999) Hydrogen-bonding behavior of gellan in solution during structural change observed by NMR and circular dichroism methods. *Prog. Colloid Polym. Sci*., **114**, 15-24.

Mazen, F., Milas, M., and Rinaudo, M. (1999) Conformational transition of native and modified gellan. *Int. J. Biol. Macromol*., **26** 109-118.

McEvoy, H., Ross-Murphy, S. B. and Clark, A. H. (1985) Large deformation and ultimate properties of biopolymer gels:1. Single biopolymer component systems. *Polymer*, **26**, 1483-1492.

Meyer, L. M. (1960) Determination of protein in foods. In "*Food Chemistry*", Reinhold publishing corporation, New York, pp. 129-131.

Michon, C., Cuvelier, G. Relkin, P., and Launay, B. (1997) Influence of thermal history on the stability of gelatin gels. *Int. J.Biol. Macromol*., **20**, 259-264.

Miyoshi, E. and Nishinari, K. (1999a) Effects of sugar on the sol-gel transition in gellan gum aqueous solutions. *Progr. Colloid Polym. Sci*., **114**, 83-91.

Miyoshi, E. and Nishinari, K. (1999b) Rheological and thermal properties near the sol-gel transition of gellan gum aqueous solutions. *Progr. Colloid Polym. Sci*., **114**, 68-82.

Miyoshi, E., Takaya T., and Nishinari, K. (1995a) Effects of salts on the gel-sol transition of gellan gum by differential scanning calorimetry and thermal scanning rheology. *Thermochim. Acta*., **267**, 269-287.

Miyoshi, E., Takaya, T., and Nishinari, K. (1995b) Gel-sol transition in gellan aqueous solutions. *Macromol. Symp*., **99**, 83-91.

Miyoshi, E., Takaya, T., and Nishinari, K. (1996a) Rheological and thermal studies of gel-sol transition in gellan gum aqueous solutions. *Carbohydr. Polym*., **30**, 109-119.

Miyoshi, E., Takaya, T., Williams, P. A., and Nishinari, K. (1996b) Effects of sodium chloride and calcium chloride on the interaction between gellan gum and konjac glucomannan. *J. Agric. Food Chem.*, **44**, 2486-2495.

Mohammed, Z. H., Hember, M. W. N., Richardson, R. K., and Morris, E. R. (1998) Kinetic and equilibrium processes in the formation and melting of agarose gels. *Carbohydr. Polym*. **36**, 15-26.

Moritaka, H., Fukuba, H., Kumeno, K., Nakahama, N., and Nishinari, K., (1991) Effect of monovalent and divalent cations on the rheological properties of gellan gels. *Food Hydrocoll.*, **4**, 495-507.

Moritaka, H., Nishinari, K., Taki, M., and Fukuba, H. (1995) Effects of pH, potassium chloride, and sodium chloride on the thermal and rheological properties of gellan gum gels. *J. Agric. Food. Chem*., **43**, 1685-1689.

Morris, E. R., Rees, D. A., Young, G., Walkinshaw, M. D., and Darke, A. (1977) Order-disorder transition for a bacterial polysaccharide in solution – role for polysaccharide conformation in recognition between xanthomonas pathogen and its plant host. *J. Mol. Biol.*, **110**, 1-16.

Morris, E. R. (1994) Chiroptical methods. In "*Physical techniques for the study of food biopolymers"* Edited by Ross-Murphy, S. B., Blackie Academic & Professional, London, pp.15-64

Morris, E. R. (1995a) Polysaccharide synergism – more questions than answers? In "*Biopolymer Mixtures*", Edited by Harding, S. E., Hill, S. E., Mitchell, J. R., Nottingham University Press, Nottingham, pp 247-288.

Morris, E. R., and Rees, D. A. (1980). Calorimetric and chiroptical evidence of aggregate-driven helix formaiton in carrageenan systems. *Carbohydr. Res*., **80**, 317-323.

Morris, E. R., Gothard, M. G. E., Hember, M. W. N., Manning, C. E., and Robinson, G. (1996). Conformational and rheological transitions of welan, rhamsan and acylated gellan. *Carbohydr. Polym.*, **30** 165-175.

Morris, V. J. (1995b) Synergistic interactions with galactomannans and glucomannans. In "*Biopolymer Mixtures*", Edited by Harding, S. E., Hill, S. E., Mitchell, J. R., Nottingham University Press, Nottingham, pp 289-314.

Muramoto, M., Omori, M., and Kato, H. (1999) Interaction between tea catechin and food constituents in the digestive system. *Journal of home economics of Japan*, **50**, 163-168.

Nagano, T. and Nishinari, K. (2001) Rheological studies on commercial egg white using creep and compression measurements. *Food Hydrocoll.*, , **15**, 415-421.

Nagano, T., Yano, Y., and Nishinari, K. (2003) Study on soybean curd using compression test and confocal laser scanning microscopy. *Journal of the Japanese society for food science and technology*, **50**, 344-349.

Nagano, T., and Nishinari, K. (2003) Effect of compression speed pn the stress-strain curves of spray-dried egg white gels. *Journal of home economics of Japan*, **54**, 257-262.

Nakamura, K., Harada, K., and Tanaka, Y. (1993) Viscoelastic properties of aqueous gellan solutions: the effects of concentration on gelation. *Food Hydrocoll.*, **7**, 435-447.

Namiki, K., Yamanaka, M., Tateyama, C., Igarashi, M., and Namiki, M. (1991) Platelet-aggregation inhibitory activity of tea extracts. *Journal of the Japanese society for food science and technology* **38**, 189-195.

Nishinari, K. (1996a) Properties of gellan gum. In "*Gums and Stabilisers for the Food Industry* 8", Edited. by Phillips, G. O., Williams, P. A. and Wedlock, D. J., IRL Press, Oxford, pp. 371-383.

Nishinari, K. (1997) Rheological and DSC study of sol-gel transition in aqueous dispersions of industrially important polymers and colloids. *Colloid Polym. Sci.*, **275**, 1093-1107.

Nishinari, K. (1996b) Introduction. *Carbohydr. Polym.*, **30**, 75-76.

Nishinari, K., Horiuchi, H., Ishida, K., Ikeda, K., Date, M., and Fukada, E. (1980) A new apparatus for rapid and easy measurement of dynamic viscoelasticity for gel-like foods. *Nippon Shokuhin Kogyo Gakkaishi*, **27**, 227-233.

Nishinari, K., Koide, S., and Ogino, K. (1985) On the temperature dependence of elasticity of thermo-reversible gels. *J. Phys. France*, **46**, 793-797.

Nishinari, K., Koide, S., Williams, P. A., and Phillips, G. O. (1990) A zipper model approach to the thermoreversible gel-sol transition. *J. Phys. France*, **51**, 1759-1768.

Nishinari, K., Nitta, Y., Miyoshi, E., Ikeda, S., and Takaya, T. (2002) Helix-coil transition in thermoreversible gels. In "*Gums and Stabilisers for the Food Industry*",

Edited. by Phillips, G. O., Williams, P. A. and Wedlock, D. J., IRL Press, Oxford, pp.85-94.

Nishinari, K., Miyoshi, E., Takaya, T., and Williams, P. A. (1996c) Rheological and DSC studies on the interaction between gellan gum and konjac glucomannan. *Carbohydr. Polym*., **30**, 193-207.

Nishinari, K., Yamatoya, K., and Shirakawa, M. (2000) Xyloglucan. In "*Handbook of Hydrocolloids*", Edited by Phillips, G. O., Williams, P. A., Woodhead Publishing, Cambridge, pp 247-267.

Norton, I. T., Goodall, D. M., Austen, K. R. J., Morris, E. R., and Rees, D. A. (1986) Dynamics of molecular organization in agarose sulphate. *Biopolymers*, **25**, 1009-1029.

Ogawa, E. (1993) Osmotic pressure measurements for gellan gum aqueous solutions. *Food Hydrocoll*., **7**, 397-405.

Ogawa, E. (1996) Influence of storage on the molecular weight of tetramethylammonium-type gellan gums. *Carbohydr. Polym*., **30**, 145-148.

Ogawa, E. (1999) Temperature dependence of the conformational properties of sodium-type gellan gum in aqueous solutions. *Prog. Colloid Polym. Sci*., **114**, 8-14.

Okamoto, T., Kubota, K., and Kuwahara, N. (1993) Light scattering study of gellan gum. *Food Hydrocoll.*, **7**, 363-371.

Oomoto, T., Uno, Y., and Asai, I. (1999) The latest technologies for the application of gellan gum. *Prog. Colloid Polym. Sci*. **114**, 123-126

O'Neill, M. A., Selvendran, R. R., and Morris, V. J. (1983) Structure of the acidic extracellular gelling polysaccharide produced by *Pseudomonas elodea*. *Carbohydr. Res*., **124**, 123-133.

Reid, J. S. G., Edwards, M. E., and Dea, I. C. M. (1988) Enzymatic modification of matural seed gum In "*Gums and Stabilisers for the food Industry* 6", Edited by Phillips, G. O., Williams, P. A., and Wedlock, D. J., IRL Press, Oxford, pp.391-398

Richardson, R. K and Goycoolea, F. M. (1994) Rheological measurement of κ-carragennan during gelation. *Carbohydr. Polym*., **24**, 223-225.

Rinaudo, M. and Milas, M. (2000). Gellan gum, a bacterial gelling polymer. In "*Novel Macromolecules in Food Systems*", Edited by Doxastakis, G. and Kiosseoglou, V., Elsevier Science, Amsterdam, pp. 239-263.

Robinson, G., Manning, C. E., and Morris, E. R. (1991) Conformation and physical properties of the bacterial polysaccharides gellan, wellan, and rhamsan. In "*Food Polymers, Gels and Colloids*", Edited by Dickinson, E., Royal Society of Chemistry, London, pp. 22-33.

Robinson, G., Morris, E. R. and Rees, D. A., (1980) Role of double helices in carrageenan gelation: the domain model. *J. Chem. Soc., Chem. Commun.*, 152-153.

Rocks, J. K. (1971) Xanthan gum. *Food Technology*, **25**,476-483.

Ross-Murphy, S. B. (1994) Rheological methods. In "*Physical techniques for the study of food biopolymers"* Edited by Ross-Murphy, S. B., Blackie Academic & Professional, London, pp.343-392.

Sanderson, G. R. (1990) Gellan gum. In "*Food Gels*", Edited by Harris, P., Elsevier Applied Science,. London and New York, pp. 201-232.

Shirakawa, M., Yamatoya, K., and Nishinari, K. (1998) Tailoring of xyloglucan properties using an enzyme. *Food Hydrocoll*., **12**, 25-28.

Siebert, K. J., Troukhanova, N. V., and Lynn, P. Y. (1996) Nature of polyphenol-protein interactions. *J. Agric. Food Chem*., **44**, 80-85.

Snoeren, T. H. M., and Payens, T. A. J. (1976) On the sol-gel transitions of kappa-carrageenan. *Biochimica et Biophysica Acta*, **437**, 264-272.

Stephen, A. M. (1991) Starch in human-nutrition – Introduction. *Can. J. Physiol. Pharmacol*., **69**, 54-55.

Sworn, G. (2000) Gellan gum. In "*Handbook of hydrocolloids*", Edited by Phillips, G. O. and Williams, P. A., Woodhead publishing Ltd, Cambridge, pp. 117-135.

Takahashi, M., Yokoyama, K., and Masuda, T. (1994) Dynamic viscoelasticity and critical exponents in sol-gel transition of an end-linking polymer. *J. Chem. Phys*., **101**, 798-804.

Takahashi, R., Akutu, M., Kuboka, K., and Nakamura, K. (1999) Characterization of gellan gum in aqueous NaCl solution. *Prog. Colloid Polym. Sci*., **114**, 1-7.

Tanaka, Y., Sakurai, M., and Nakamura, K. (1996) Ultrasonic velocity and circular dichroism in aqueous gellan solutions. *Food Hydrocoll*., **10**, 133-136.

Te Nijenhuis, K. (1981) Investigation into the ageing process in gels of gelatin/water systems by the measurement of their dynamic moduli. *Colloid Polym. Sci*., **259**, 522-535.

Te Nijenhuis, K. (1997) Viscoelastic properties of termareversible gels. *Adv. Polym. Sci*., **130**, 1-267

Te Nijenhuis, K., and Winter, H. H. (1989) Mechanical properties at the gel point of a crystallizing poly(vinyl chloride) solution. *Macromolecules*, **22**, 411-414.

Tinoco, J., Sauer, K., Wang, J. C., and Puglisi, J. D. (2002) In "*Physical Chemistry*" Prentice –Hall, New Jersey, pp.567-576.

Treloar, L. R. G. (1958) In "*The physics of rubber elasticity. Second edition*", Clarendon Press, Oxford, pp. 64-98.

Valcic, S., Muders, A., Jacobsen N. E., Liebler, D. C., and Timmermann, B. N. (1999) Antioxidant chemistry of green tea catechins. Identification of products of the reaction of (-)-epigallocatechin gallate with peroxyl radicals *Chem. Res. Toxicol*. **12**, 382-386.

Viebke, C., Piculell, L., and Nilsson, S., (1994) On the mechanism of helix-forming biopolymers. *Macromolecules*, **27**, 4160-4166.

Wang, L., Kim, D., and Lee, C. Y. (2000) Effects of heat processing and storage on flavanols and sensory qualities of green tea beverage. *J. Agric. Food Chem*., **48**, 4227-4232.

Wang, G., Lindell, K., and Olofsson, G. (1997) On the thermal gelling of ethyl(hydroxyethyl)cellulose and sodium dodecyl sulfate. Phase behavior and temperature scanning calorimetric response. *Macromolecules*, **30**, 105-112.

Watase, M., and Nishinari, K. (1993) Effect of potassium ions on the rheological and thermal properties of gellan gum gels. *Food Hydrocoll.*, **7**, 449-456.

Watase, M., and Nishinari, K. (1982) The rheological study of the interaction between alkali metal ions and kappa-carrageenan gels. *Colloid & Polym. Sci.*, **260**, 971-975.

Wientjes, R. H. W., and Duits, M. H. G., Jongschaap, R. J. J., and Mellema, J. (2000) Linear rheology of guar gum solutions. *Macromolecules*, **33**, 9594-9605.

Williams, P. A., and Phillips, G. O. (2000) Introduction to food hydrocolloids. In "*Handbook of hydrocolloids*", Edited by Phillips, G. O. and Williams, P. A., Woodhead publishing Ltd, Cambridge, pp.1-19.

Williams, P. A., Clegg, S. M., Langdon, M. J., Nishinari, K., and Piculell, L. (1993) Investigation of the gelation mechanism in κ-carrageenan/konjac mannan mixtures using differential scanning calorimetry and electron spin resonance spectroscopy. *Macromolecules*, **26**, 5441-5446.

Winter, H. H., and Chambon, F. (1986) Analysis of linear viscoelasticity of a crosslinking polymer at the gel point. *J. Rheol*., **30**, 367-382.

Wood, P. J. (1980) Specificity in the interaction of direct dyes with polysaccharides. *Carbohydr. Res*., **85**, 271-287.

Yamanaka, S., Yuguchi, Y., Urakawa, H., Kajiwara, K., Shirakawa, M., and Yamatoya, K. (2000) Gelation of tamarind seed polysaccharide xyloglucan in the presence of ethanol. *Food Hydrocoll*., **14**, 125-128.

Yamanaka, S., Yuguchi, Y., Urakawa, H., Kajiwara, K., Shirakawa, M., and Yamatoya, K. (1999) Gelation of enzymatically degraded xyloglucan extracted from tamarind seed. *SEN'I GAKKAISHI*, **55**, 528-532.

York, W. S., Harvey, L. K., Guillen, R., Albersheim, P., and Darvill, A. G. (1993) Structural analysis of tamarind seed xyloglucan oligosaccharides using β-galactosidase digestion and spectroscopic methods. *Carbohydr. Res*. **248**, 285-301.

Yoshimura, M., and Nishinari, K. (1999). Dynamic viscoelastic study on the gelation of konjakc glucomannan with different molecular weights. *Food Hydrocoll*., **13**, 227-233.

Young, R. J. (1981) Mechanical properties. In "*Introduction to Polymers*". Chapman and Hall, London, pp.211-321

Yuguchi, Y., Min, W., Kumagai, T., and Hirotsu, T. (2002) Gelation of xyloglucan by

addition of small molecules. In preprints of "*1st International Cellulose Conference*", pp. 148.

Zhang, H., Yoshimura, M., Nishinari, K., Williams, M. A. K., Foster, T. J., and Norton, I. T. (2001). Gelation behaviour of konjac glucomannan with different molecular weights. *Biopolymers*, **59**, 38-50.

Summary

The helix-coil transition of gellan in gels

Temperature dependence of the storage and loss Young's moduli and DSC peaks and change in the ellipticity showed that a conformational change occurred in gellan gels maintaining the shape of gels. On heating gellan gels showed a steep decrease in loss Young's modulus resulting in a steep decrease in mechanical loss tangent tanδ and an endothermic DSC peak and the decrease in the ellipticity around 202nm. On cooling, gellan gels showed a steep increase loss Young's modulus and tanδ, and an exothermic DSC peak and the increase in the ellipticity around 202nm. It was concluded that the thermoreversible helix-coil transition occurred in gellan gels.

The sol-gel transition of gellan affected by thermal history

Effect of cooling rate and storage temperature on the gelation of gellan was investigated. The storage Young's modulus and shear modulus of gellan gels decreased with increasing cooling rate or increasing storage temperature during gel formation. The gel melting temperature of gellan gels shifted to lower temperatures with increasing cooling rate or increasing storage temperature. This indicated that gelation of gellan is controlled by kinetics like gelation of gelatin and agarose. The change in the elastic modulus and gel melting temperature was considered to be due to change in the helix length of gellan and degree of kinetic trapping by network formation.

The effect of SDS on the gelation of gellan

The effect of addition of SDS on the sol-gel transition of gellan was investigated. Addition of smaller amount of SDS decreased the shear modulus of resultant gellan gels and addition of certain amount of SDS prevented the gel formation of gellan. DSC peaks and change in the ellipticity due to helix-coil transition of gellan shifted to higher

temperatures with increasing added SDS concentration. This indicated that helix formation of gellan was promoted by addition of SDS. The role of SDS on the gelaiton was thought to inhibit side-by-side aggregation of gellan helices to prevent network formation. In addition, SDS was thought to enhance helix formation of gellan by electric shielding effect of cation in SDS.

The effect of the immersion into salt solution on gel properties of gellan

The storage Young's modulus of gellan gels immersed in salt solutions increased with time during the immersion at room temperature. The increase of the storage Young's modulus by immersion could not be explained by the change in gellan concentration. The ellipticity showed that immersion induced helix formation in gellan gels. The gel melting temperature shifted to higher temperatures by the immersion, indicating that the lateral aggregation was enhanced by the immersion. It was suggested that during immersion cation penetrated into gellan gels and induced helix formation of disordered gellan in gels and promoted lateral aggregation of gellan helices.

The effect of sugars on gel properties of gellan

The large deformation test of gellan gels containing sugar showed that the stress-strain curve of gellan gels containing higher amount of sugar can be fitted well by BST equation $\sigma = 2/3(E/n)(\lambda^n - \lambda^{-2n})$, where σ is the true stress, E is the Young's modulus, n is the elasticity parameter, and λ is the stretch ratio. On the other hand, the stress-strain curve of gellan gels without sugar cannot be fitted by BST equation. This indicated that gel network changed to more rubber-like network by addition of higher amount of sugar.

Gelation of tamarind seed xyloglucan by addition of epigallocatechin gallate

The shear modulus of tamarind seed xyloglucan in the presence of epigallocatechin gellate increased significantly at a certain temperature on cooling. Frequency dependence of storage and loss shear moduli showed a gel like behaviour at lower temeprature. The shear modulus decreased on subsequent heating whereas tamarind seed xyloglucan alone did not change the shear modulus significantly with temperature.

This indicated that addition of epigallocatechin gallate induced thermoreversible gelation of tamarind seed xyloglucan. This sol-gel transition could be observed as an exothermic DSC peak on cooling and as an endothermic DSC peak on heating. Epigallocatechin gellate was thought to associate with chains of tamarind seed xyloglucan from NOESY study. It was suggested that binding of epigallocatechin gallate induced association of chains of tamarind seed xyloglucan, resulting in network formation. Further addition of epigallocatechin gallate induced precipitation, which was interpreted as further association among tamarind seed xyloglucan which caused phase separation due to poor solubility.

Gelation of tamarind seed xyloglucan by mixing with gellan

The storage shear modulus of mixture of tamarind seed xyloglucan and gellan gum increased steeply at certain temperature on cooling and decreased on subsequent heating. The mechanical spectra of the mixture showed a gel-like behaviour at lower temperatures under conditions where individual polysaccharides showed a sol-like behavior at any temperatures. This indicated that mixture formed a thermoreversible gel although tamarind seed xyloglucan or gellan gum alone does not form a gel at the experimental condition. At this condition, DSC peak and change in the ellipticity appeared, which was not expected in individual polysaccharide. This synergistic gelation of tamarind seed xyloglucan and gellan gum was regarded as new combination of synergism observed in β-plant polysaccharide and helix-forming polysaccharide.

The effect of salts on the gelation of tamarind seed xyloglucan/gellan mixture

The mixture of tamarind seed xyloglucan and gellan in the absence of salts showed the synergistic interaction at a certain temperature at which both the shear modulus and the ellipticity at 202nm increased significantly on cooling. When a certain amount of salts was added into the mixture, the resultant synergism of gellan and TSX reduced, which lowered the viscoelasticity and the ellipticity at 202nm of the mixture. DSC peak arising from interaction of tamarind seed xyloglucan and gellan disappeared in the presence of cerain amount of salts. Further addition of salts induced gelation of gellan

where the synersism in the shear modulus of the gels was not observed. These suggested that salts prevent the synergistic interaction of tamarind seed xyloglucan and gellan gum by promoting self-aggregation of gellan at the expence of interaction with tamarind seed xyloglucan.

Concluding remarks

As mentioned in the introduction, people require various kinds of texture modifier from the viewpoint of enjoying their food and managing their health. Industries also require many kinds of texture modifier to control the quality of products.

Creating novel texture modifier from existing food polysaccharides has the advantage of low cost production, compared with creating novel texture modifier from polysaccharides which have not been approved as food additives. Thus it is desirable to enlarge a possibility of existing food polysaccharides as a texture modifier.

There are a few food polysaccharides which have a gelling ability by themselves whereas there are a lot of non-gelling polysaccharides which are used as a thickener and stabilizer. The effective use of gelling food polysaccharides and finding the gelling condition of food polysaccharides used as a thickener and stabilizer have great importance for creation of various types of texture modifier. In addition, it is worthwhile to seek the combination of polysaccharides which can form a gel by synergistic effects, nevertheless it is rare for polysaccharides to show the synergistic interaction, because synergism will give us many advantages such as the increase of viscosity at very low concentration and the gelation under non-gelling condition of individual polysaccharide.

The present thesis includes basic knowledge about the gelation of food polysaccharide alone, the scientific evidence about the gelation induced by the interaction of a non-gelling food polysaccharide and a food component, and about the synergistic gelation of a novel combination of food polysaccharides. These are expected, in the future, to contribute to creation of texture modifiers which answer social and industrial requirements.

Acknowledgements

I appreciate my supervisor, Prof. Nishinari, for his enthusiastic and invaluable discussions throughout this work.

I would like to thank Prof. Yamaguchi and Prof. Yamamoto for their constructive and invaluable suggestions for this work.

So many people supported me during this work. This thesis would not have been possible without the tremendous assistance of them. I wish to express my sincere thanks to Mr. Takaya for his assistance, Dr. Miyoshi, Dr. Ikeda, and Mr. Fang for invaluable comments and discussions, Ms. Shirakawa and Dr. Yamatoya for supplying TSX samples and information about TSX, Dr. Oomoto and Dr. Asai for supplying gellan sample and information about gellan, Dr. Takemasa for his NMR measurements, Ms. Kim for her assistance in rheological and DSC measurements, Dr. Funami, Dr. Takahashi, Dr. Tanaka, Mr. Hiraiwa, Ms. Hayashi, and Mrs. Nakata for their kindness and encouragement.

Finally, I am grateful to my family who have been helpful in the development of this thesis.

March 2005, Osaka, Japan

List of publication

1. Helix-coil transition in gellan gum gels

   Y. Nitta, S. Ikeda, T. Takaya, and K. Nishinari

   Trans. Mat. Res. Soc. J, **26**, 621-624, (2001)

2. Helix-coil transition in thermoreversible gels

   K. Nishinari, Y. Nitta, E. Miyoshi, S. Ikeda, and T. Takaya

   Gums and Stabilisers for the Food Industory 11, Eds. Phillips GO and Williams PA, Royal Society of Chemistry Press, Cambridge, (2002) pp.85-94

3. Synergistic interaction of xyloglucan and Na-type gellan

   Y. Nitta, M. Shirakawa, and K. Nishinari

   Proceedings of *3rd International Symposium on Food Rheology and Structure* (2003) pp.181-184

4. Gel formation of K-gellan in the presence of SDS

   Y. Nitta, S. Ikeda, and K. Nishinari

   Trans. Mat. Res. Soc. J , **28**, 957-960 (2003)

5. Synergistic gel formation of xyloglucan/gellan mixture as studied by rheology, DSC and circular dichroism

   Y. Nitta, B.S. Kim, K. Nishinari, M. Shirakawa, K. Yamatoya, T. Oomoto, and I. Asai

   Biomacromolecules, **4**, 1654-1660 (2003)

6. Gellan gum (in Japanese)
   Y. Nitta and K. Nishinari
   FFI Journal, **208**, 930-934 (2003)

7. Gelation of xyloglucan by addition of epigallocatechin gallate as studied by rheology and differential scanning calorimetry
   Y. Nitta, Y. Fang, M. Takemasa and K. Nishinari
   Biomacromolecules, **5**, 1206-1213 (2004)

8. Gelation of gellan affected by thermal history
   Y. Nitta, and K. Nishinari
   In preparation

9. The effect of the immersion into salt solution on the gel properties of gellan
   Y. Nitta, S. Tanaka and K. Nishinari
   In preparation

10. The effect of sugar on the large deformation properties of gellan gels
    Y. Nitta, and K. Nishinari
    In preparation

11. The effect of salts on the gelation of mixtures of xyloglucan and gellan
    Y. Nitta, B.S. Kim and K. Nishinari
    In preparation